

# Supporting Information

## Enzymatic cyclization of dioxidosqualene to heterocyclic triterpenes

Hui Shan,<sup>†</sup> Michael J. R. Segura,<sup>¶</sup> William K. Wilson,<sup>†</sup>  
Silvia Lodeiro,<sup>¶</sup> and Seiichi P. T. Matsuda<sup>\*,†,¶</sup>

*Department of Chemistry and Department of Biochemistry and Cell Biology,  
Rice University, Houston, Texas 77005, USA*

### Contents

Full Citations for References 11 and 20a of Main Text.....	S1
Atom Numbering and Nomenclature.....	S2
Materials and Methods.....	S3
Preparation of (3 <i>S</i> ,22 <i>S</i> )-2,3:22,23-Dioxidosqualene .....	S4
Construction of Yeast Strain RXY6[JR1.16].....	S7
In Vitro Conversion of DOS to Oxacyclic Triterpenes by LUP1 .....	S7
In Vivo Production of Oxacyclic Triterpenes by LUP1 .....	S8
NMR Characterization of Compounds <b>A</b> , <b>B</b> , and <b>C</b> ( <b>9a</b> , <b>8</b> , and <b>9b</b> ) .....	S8
GC-MS Analysis of Compounds <b>A</b> , <b>B</b> , and <b>C</b> ( <b>9a</b> , <b>8</b> , and <b>9b</b> ) .....	S15
Structure Elucidation for Compounds <b>A</b> , <b>B</b> , and <b>C</b> ( <b>9a</b> , <b>8</b> , and <b>9b</b> ).....	S18
<sup>1</sup> H and <sup>13</sup> C NMR Assignments for Compounds <b>A</b> , <b>B</b> , and <b>C</b> ( <b>9a</b> , <b>8</b> , <b>9b</b> ) .....	S23
Literature Review: Lack of Evidence for 20 <i>R</i> -Epoxydammaranes .....	S24
Evidence for Traces of Diol <b>8</b> in a Published Lupanediol Spectrum.....	S27
Comparison of Observed and Predicted NMR Data for <b>8</b> .....	S28
Molecular Modeling: Formation of Oxonium Ions <b>10-12</b> from <b>5</b> .....	S30
Lack of C17 Epimerization in Oxacycle Formation from DOS .....	S37
Formation of Unsaturated Oxacyclic Triterpenes by LUP1 .....	S37
Possible Factors Affecting the Availability of DOS to LUP1 .....	S40
Predicted DOS Metabolites from Other Cyclases .....	S42
Reported DOS Metabolites .....	S43
Atomic Coordinates from B3LYP/6-31G* Geometry Optimizations .....	S45
References and Notes.....	S53

### Full Citation for References 11 and 20a of Main Text

#### Reference 11 of main text:

Gaussian 03, Revision C.02, Frisch, M. J.; Trucks, G. W.; Schlegel, H. B.; Scuseria, G. E.; Robb, M. A.; Cheeseman, J. R.; Montgomery, Jr., J. A.; Vreven, T.; Kudin, K. N.; Burant, J. C.; Millam, J. M.; Iyengar, S. S.; Tomasi, J.; Barone, V.; Mennucci, B.; Cossi, M.; Scalmani, G.; Rega, N.; Petersson, G. A.; Nakatsuji, H.; Hada, M.; Ehara, M.; Toyota, K.; Fukuda, R.;

Hasegawa, J.; Ishida, M.; Nakajima, T.; Honda, Y.; Kitao, O.; Nakai, H.; Klene, M.; Li, X.; Knox, J. E.; Hratchian, H. P.; Cross, J. B.; Bakken, V.; Adamo, C.; Jaramillo, J.; Gomperts, R.; Stratmann, R. E.; Yazyev, O.; Austin, A. J.; Cammi, R.; Pomelli, C.; Ochterski, J. W.; Ayala, P. Y.; Morokuma, K.; Voth, G. A.; Salvador, P.; Dannenberg, J. J.; Zakrzewski, V. G.; Dapprich, S.; Daniels, A. D.; Strain, M. C.; Farkas, O.; Malick, D. K.; Rabuck, A. D.; Raghavachari, K.; Foresman, J. B.; Ortiz, J. V.; Cui, Q.; Baboul, A. G.; Clifford, S.; Cioslowski, J.; Stefanov, B. B.; Liu, G.; Liashenko, A.; Piskorz, P.; Komaromi, I.; Martin, R. L.; Fox, D. J.; Keith, T.; Al-Laham, M. A.; Peng, C. Y.; Nanayakkara, A.; Challacombe, M.; Gill, P. M. W.; Johnson, B.; Chen, W.; Wong, M. W.; Gonzalez, C.; and Pople, J. A.; Gaussian, Inc., Wallingford CT, 2004. Revisions B.02, B.05, and C.01 were also used and, for the calculations described herein, should give results equivalent to those from revision C.02.

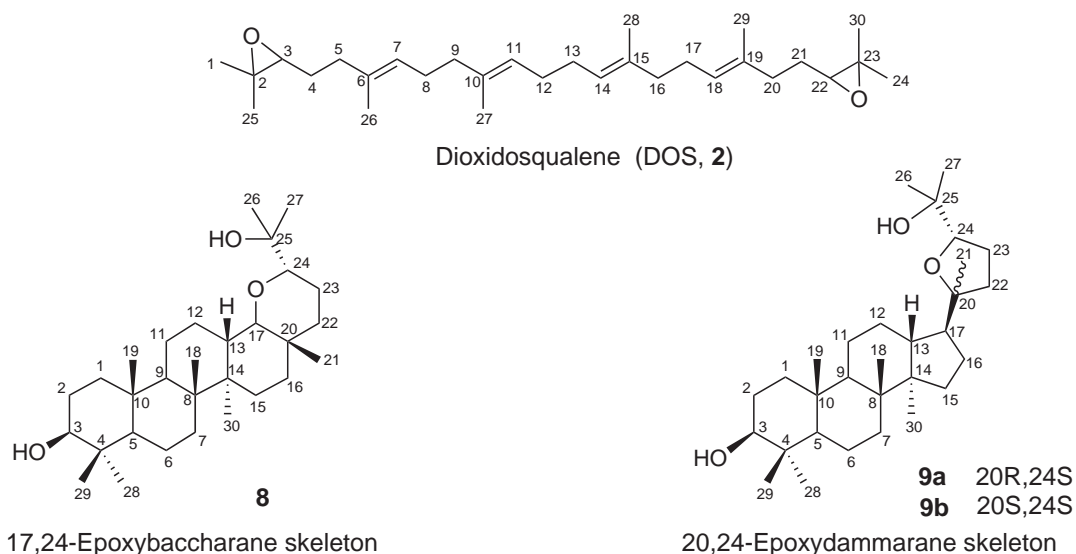
Reference 20a of main text:

Hwang, B. Y.; Su, B. N.; Chai, H.; Mi, Q.; Kardono, L. B.; Afriastini, J. J.; Riswan, S.; Santarsiero, B. D.; Mesecar, A. D.; Wild, R.; Fairchild, C. R.; Vite, G. D.; Rose, W. C.; Farnsworth, N. R.; Cordell, G. A.; Pezzuto, J. M.; Swanson, S. M.; Kinghorn, A. D. *J. Org. Chem.* **2004**, 69, 3350-3358. Erratum: *J. Org. Chem.* **2004**, 69, 6156-6156. The erratum states that the plant studied was *Aglaia foveolata* Pannell, not *Aglaia silvestris* (M Roemer).

## Atom Numbering and Nomenclature

The standard atom numbering for epoxydammaranes uses a modified sterol numbering system, similar to that of lanosterol except that position 18 corresponds to the C8 methyl (rather than the C13 methyl of lanosterol). This numbering scheme was also used in the sole report on 17,24-epoxybaccharanes (ref. 20a of the main text).

As shown below, we have used sterol numbering for oxacyclic triterpenes **8**, **9a**, **9b**, and mechanistic intermediates. However, standard squalene numbering was used 2,3-oxidosqualene and DOS.



Formal names for the oxacyclic triterpenes described herein are:

**8** (17*R*,20*R*,24*S*)-17-24-epoxybaccharane-3 $\beta$ ,25-diol

**9a** (17*S*,20*S*,24*R*)-20,24-epoxydammarane-3 $\beta$ ,25-diol

**9b** (17*S*,20*S*,24*S*)-20,24-epoxydammarane-3 $\beta$ ,25-diol

These compounds have the usual C17 stereochemistry for epoxydammaranes and epoxybaccharanes. The configurations at C5, C8, C9, C10, C13, C14, and C17 configuration are not normally specified unless there is deviation from the natural dammarane/baccharane stereochemistry.

The nomenclature for compounds **8**, **9a**, and **9b** is based on the longstanding practice of naming of oxygen bridges as epoxy substituents in steroids and other natural products. This practice is recognized in IUPAC names for steroids.<sup>1</sup> However, casual use of this nomenclature can generate confusion because there are also epoxydammaranes and epoxybaccharanes in which “epoxy” refers to an oxirane ring. Herein the terms “epoxydammarane” and “epoxybaccharane” refer only to 20,24-epoxydammaranes and 17,24 epoxybaccharanes.

## Materials and Methods

### *Materials*

Components of synthetic complete medium and TLC plates (from E. Merck) were obtained from Fisher Scientific (Pittsburgh, PA). Organic solvents and solid-phase extraction (SPE) SiO<sub>2</sub> cartridges (1000 mg, 50  $\mu$ m) were obtained from Honeywell Burdick & Jackson (Muskegon, MI). Heme (in the form of hemin) and ergosterol were from Sigma (St. Louis, MO). Bis(trimethylsilyl)trifluoroacetamide (BSTFA) was purchased from Aldrich Chemical Co. (Milwaukee, WI).

### *NMR and HPLC Instrumentation*

<sup>1</sup>H and <sup>13</sup>C NMR spectra were acquired on a Bruker Avance 500 spectrometer at 25 °C in relatively dilute CDCl<sub>3</sub> solution (<10 mM triterpene). Spectra were referenced to tetramethylsilane at 0 ppm for <sup>1</sup>H and to CDCl<sub>3</sub> at 77.00 ppm for <sup>13</sup>C NMR. 1D spectra shown in the figures were transformed with mild resolution enhancement (Gaussian apodization with line broadening (LB) of –0.8 Hz and GB of 0.08. Coupling constants were measured from strongly resolution-enhanced spectra (LB of –2 and GB of 0.4 or higher). Many of the fine couplings are visible only in resolution-enhanced spectra and not in the figures shown herein.

HPLC separation of enzymatic reaction products **9a** and **9b** was done using a Waters 515 pump with a Phenomenex Prodigy 5  $\mu$ m ODS (3) column (250  $\times$  21.2 mm i.d.). The mobile phase was methanol-water 9:1, and the detection of individual components was carried out off-line using TLC (developed with 1:1 MTBE/hexanes).

### *Derivatization for Gas Chromatography (GC)*

TMS derivatives were prepared by dissolving each sample in 100  $\mu$ L of BSTFA-pyridine (1:1) and held at room temperature for 1 h. The solution was then evaporated to dryness and the residue re-dissolved in toluene for GC-MS analysis. Experiments with longer TMS derivatization

times and injections of samples in BSTFA-pyridine (without evaporation of the reagent) were also conducted for comparison.

### GC-MS Conditions

GC-MS was performed on an Agilent 5973N Mass Selective Detector interfaced to an Agilent 6890N GC System equipped with an Rtx-35 capillary column (Restek, 30 m × 0.25 mm i.d., 0.10 μm film thickness). Unless otherwise indicated, samples were injected at 280 °C in a pulsed splitless mode keeping a pressure of 50 psi (3.45 bar) for 1 min. A constant column flow rate was maintained at 1 mL/min and the following temperature program was applied: initial 110 °C for 1 min, increased at 40 °C/min to 270 °C, then at 1 °C/min to 280 °C, held this temperature for 15 min. Ionization was done by electron-impact (EI) at 70 eV with an ion source temperature of 250 °C. The data acquisition was in full scan mode, performed in the mass range of 50–650 amu. Experiments using an Rtx-5 capillary column with the same temperature program or modified programs were carried out, but also failed to distinguish the mono-TMS ether derivatives of **9a** and **9b**.

### Preparation of (3*S*,22*S*)-2,3:22,23-Dioxidosqualene

(3*S*,22*S*)-2,3:22,23-Dioxidosqualene (DOS) was obtained as a byproduct of oxidosqualene cyclase mutants, similar to methods reported<sup>2</sup> previously using cyclase inhibitors or cyclase mutants. Recombinant yeast was grown to saturation in 1-L scale induction medium (1% yeast extract, 2% peptone, 2% galactose, 13 mg/L heme) at 30 °C with shaking. Centrifugation gave 21 g of cells, which were resuspended in two volumes of 100 mM sodium phosphate buffer pH 6.2, and lysed using an Emulsiflex-C5 homogenizer. Protein was precipitated by adding two volumes of ethanol, and the cell debris was removed by centrifugation. The ethanol was removed by rotary evaporation and the residual aqueous suspension was extracted with ethyl acetate. Concentration of the combined extracts *in vacuo* gave ~90 mg of crude extract (60:35:5 mixture of DOS, triacylglycerols, and other lipids by <sup>1</sup>H NMR analysis). A portion (~20 mg) of this residue was purified by silica gel column chromatography using gradients of ethyl ether/hexanes (5–10%) to give ~8 mg of 3*S*,22*S*-DOS (**2**): TLC (silica gel, 1:1 hexanes/ether) *R<sub>f</sub>* 0.75; GC-MS (split injection, 40:1 ratio; 260 °C isothermal), single TIC peak at *t<sub>R</sub>* 9.1 min (Figure S1a); <sup>1</sup>H NMR (CDCl<sub>3</sub>, 500 MHz): δ 5.164 (2H, t of sextet, 6.9, 1.4 Hz), 5.142 (2H, t of sextet, 6.9, 1.4 Hz), 2.702 (2H, t, 6.3 Hz), 2.18–2.04 (8H, m), 2.02–1.97 (8H, m), 1.619 (6H, dt, 1.4, 0.9 Hz), 1.602 (6H, d, 1.3 Hz), 1.70–1.57 (4H excluding methyls, m), 1.300 (6H, s), 1.258 (6H, s). The NMR spectrum (Figure S1b, panel A) showed ca. 10% triacylglycerol and <1% of other triterpenes and sterols.

Despite numerous synthetic and biochemical reports of DOS, we are unaware of published NMR data for DOS aside from spectra measured in very concentrated CDCl<sub>3</sub> solution.<sup>3</sup> Our <sup>1</sup>H NMR data for DOS were essentially identical to values for OS reported by Corey et al.,<sup>4</sup> apart from the expected lacked signals for the –CH=CMe<sub>2</sub> unit of OS (δ 5.09 (m) and 1.68 (s)). For additional authentication of the DOS sample, we compare in Figure S1b NMR spectra of (a) the biosynthetic DOS sample described above, (b) synthetic DOS used in a reported<sup>5</sup> incubation with recombinant yeast, and (c) synthetic OS. The synthetic OS was prepared by the method

described by Nadeau and Hanzlik.<sup>6</sup> Essentially the same method was used to obtain DOS (as a *dl* pair plus the *meso* isomer), which is the major byproduct in the preparation of OS.

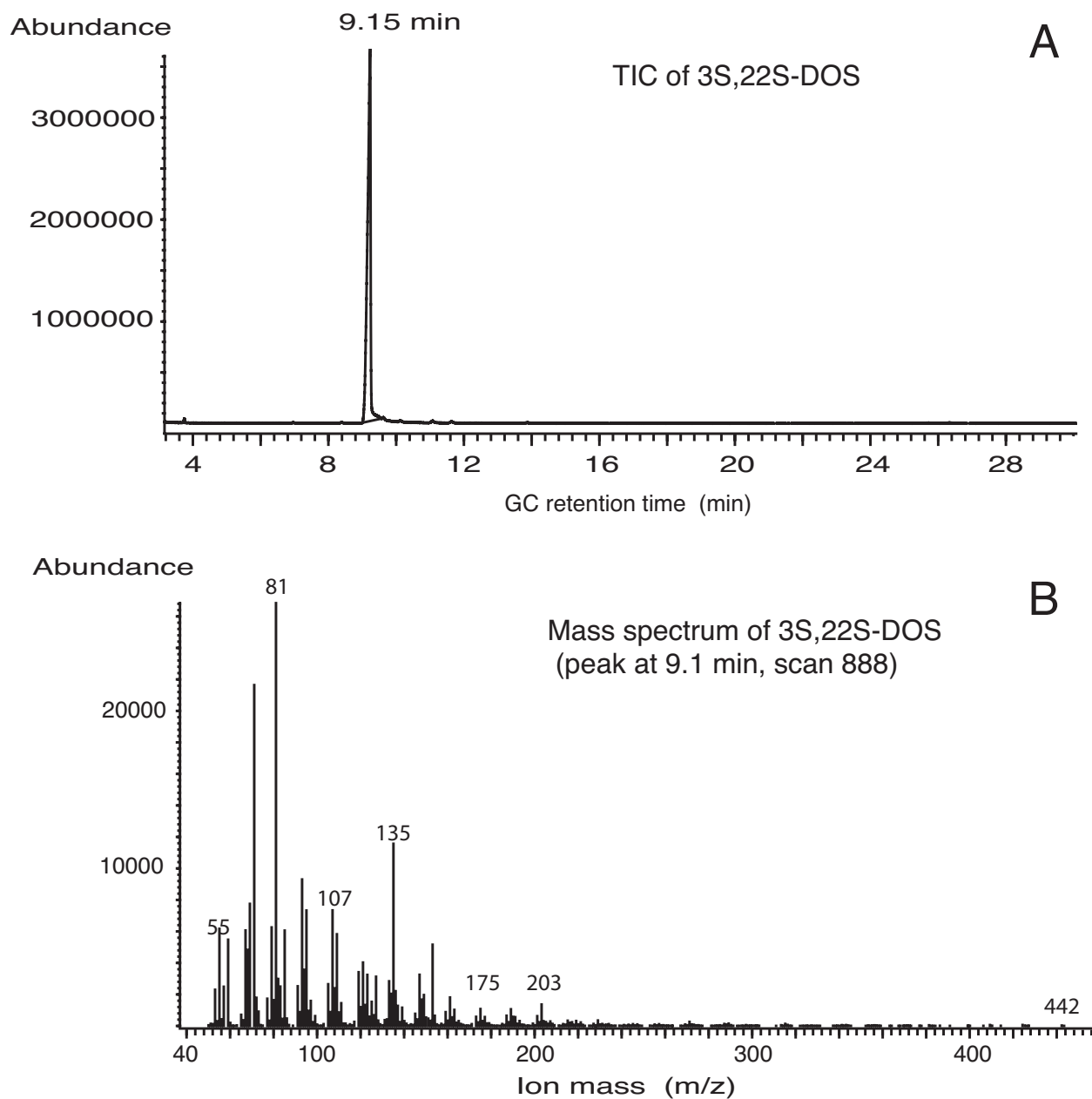


**Figure S1a.** GC-MS analysis of (3*S*,22*S*)-2,3:22,23-dioxidosqualene isolated by column chromatography. (A) Total ion chromatogram. (B) Mass spectrum. The ca. 10% impurity of triacylglycerols is insufficiently volatile to be observed under the GC-MS conditions.

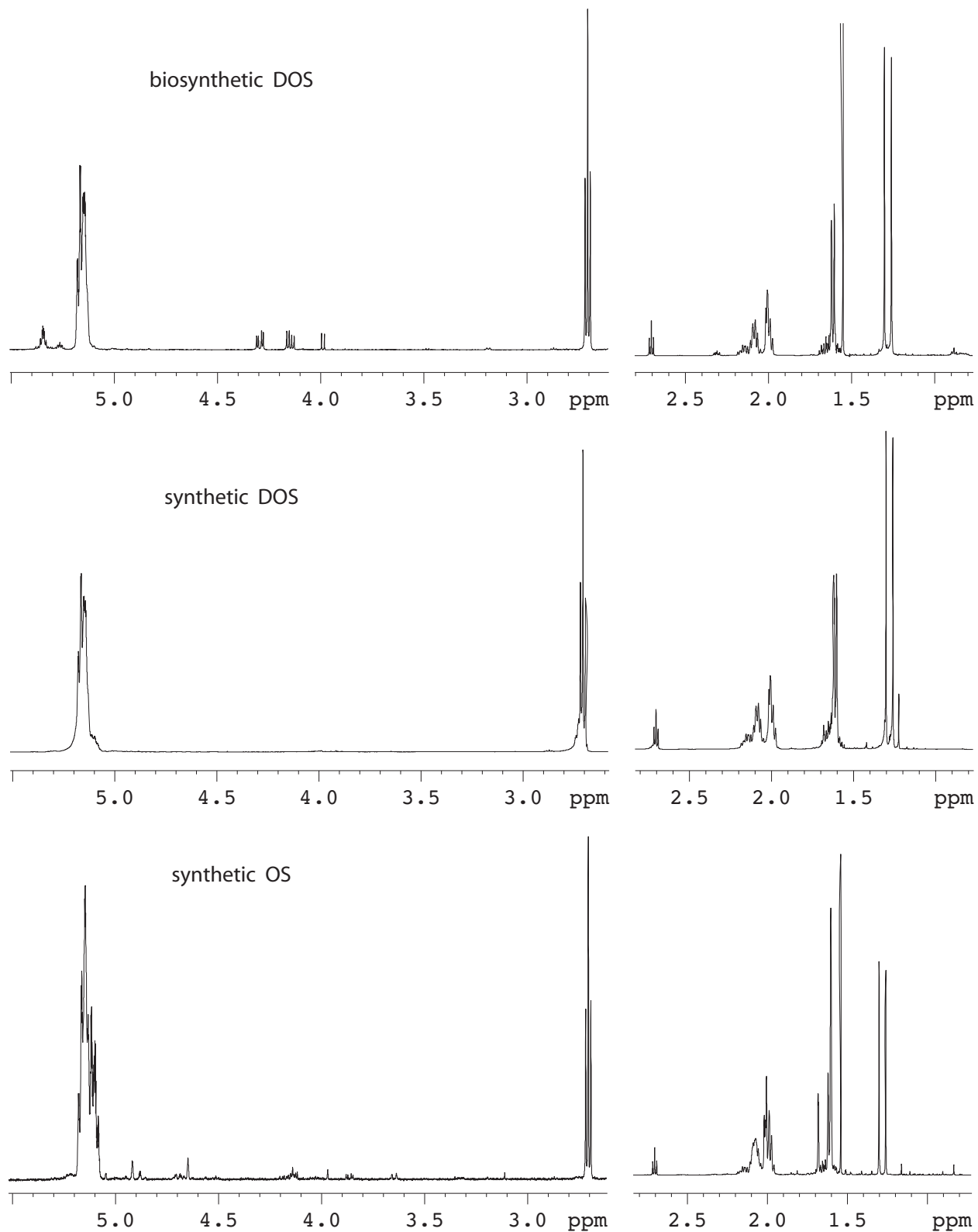


**Figure S1b.** 500 MHz <sup>1</sup>H NMR spectra of biosynthetic DOS, synthetic DOS, and synthetic OS. Methyl and CH-O signals differed among these three spectra by  $\leq 0.001$  ppm.

Evidence for the 3*S*,22*S* stereochemistry of the biosynthetically derived DOS is based on the known stereospecificity of squalene epoxidase. This enzyme produces only the 3*S* enantiomer of 2,3-oxidosqualene.<sup>7</sup> Squalene epoxidase can further convert OS to DOS by epoxidation of the remaining terminal olefin.<sup>8</sup> This second epoxidation should generate another *S* chiral center at C22,<sup>9</sup> and this expectation has been confirmed by incubation of biosynthetic 3*S*,22*S*-DOS with rat liver homogenate to generate (24*S*)-24,25-epoxycholesterol.<sup>10</sup> This pattern of stereospecific epoxidation has been confirmed in many eukaryotic systems and is presumed to operate in our recombinant yeast strain as well. Our isolation of only 24*S* metabolites from the DOS incubations (described below) supports this presumption.

### Construction of Yeast Strain RXY6[JR1.16]

The yeast lanosterol synthase/squalene epoxidase double mutant RXY6 (*MATa erg7::HIS3 erg1::KanMX4 hem1::TRP1 ura3-52 trp1-Δ63 leu2-3,112 his3-Δ200 ade2 Gal<sup>+</sup>*) was the expression host, whose construction has been described.<sup>11</sup> pJR1.16 is a URA3-marked 2μ (high copy) plasmid encoding *A. thaliana* lupeol synthase under galactose control. RXY6 was transformed with pJR1.16 using the lithium acetate method,<sup>12</sup> and transformants were selected on synthetic complete media plates containing 2% glucose lacking uracil<sup>13</sup> and supplemented with ergosterol (20 μg/mL in Tween 80 solution) and heme (13 μg/mL).<sup>14</sup>

### In Vitro conversion of DOS to Oxacyclic Triterpenes by LUP1

RXY6[JR1.16] yeast were cultured under conditions described previously.<sup>15</sup> A saturated culture of RXY6[JR1.16] (100 mL) was used to inoculate a 1-L culture of synthetic complete medium lacking uracil and supplemented with ergosterol and heme as previously described. The culture was grown to saturation at 30 °C with shaking; centrifugation yielded 12.6 g of yeast cells.

The cells were suspended in 25 mL sodium phosphate buffer (0.1 M, pH 6.2) and lysed in a French Press at 10,000 psi (700 bar). To this slurry was added 8 mg of DOS substrate (9:1 DOS:triacylglycerols) in 20 mg/mL Tween-80 solution. After 2-day incubation at room temperature, 100 mL of ethanol was added, followed by centrifugation. The supernatant was partially evaporated to remove the ethanol, followed by partitioning between water and diethyl ether. Evaporation of the combined organic extracts afforded 100 mg of crude material.

NMR analysis of the crude ether extract showed three triterpene products (designated as **A**, **B**, and **C**, in descending order of amount) along with the supplemented ergosterol. The product ratio for **A**, **B**, and **C** (**9a**, **8**, and **9c**) was estimated to be 4:3:2 by NMR. GC-MS analysis of the mono-TMS-derivatives showed two peaks in a 2:1 ratio corresponding to (**A** + **C**) vs. **B**, along with ergosterol.

The crude extract was chromatographed on a SPE silica gel cartridge and eluted with a stepwise gradient solution of MTBE/hexanes (5-15%). Sterols and triterpenes were eluted in the following order: traces of DOS; ergosterol (including minor amounts of analogs and triterpenes); compound **B** (**8**); compounds **A** and **C** (**9a** and **9b**); and ergosterol-5,8-endoperoxide. Compound **B** (ca. 1.5 mg, R<sub>f</sub> 0.31 in 1:1 MTBE/hexanes) was isolated, as well as a mixture of **A** and **C** (3 mg, R<sub>f</sub> 0.37 in 1:1 MTBE/hexanes). These fractions were then subjected to GC/MS and NMR

analysis. Co-eluting **A** and **C** were further separated into individual components by preparative ODS HPLC (elution with methanol/water 9:1), with off-line monitoring by TLC. The ergosterol fraction and fractions between ergosterol and compound **B** appeared to contain small amounts of unsaturated analogs of oxacyclic triterpenes (see below), but the amounts were insufficient for identification. No other cyclized triterpenes were found.

### In Vivo Production of Oxacyclic Triterpenes by LUP1

This experiment used the yeast strain SMY8 (*MATa erg7::HIS3 hem1::TRP1 ura3-52 trp1-Δ63 leu2-3,112 his3-Δ200 ade2 Gal<sup>+</sup>*), a lanosterol synthase mutant. Unlike RXY6, SMY8 generates OS and thus can produce triterpenes without exogenous addition of substrate. The construction of both SMY8 and SMY8[JR1.16] has been described.<sup>16</sup>

SMY8[JR1.16] was selected on SCD-Ura,H,E plates (synthetic complete medium lacking uracil, containing 2% glucose, 13 μg/mL heme, 20 μg/mL ergosterol).<sup>15</sup> Isolated colonies were used to inoculate SCD-Ura,H,E liquid cultures (2 × 10 mL); cultures were grown at 30 °C with shaking until saturation (~2 days). The 10-mL cultures were used to inoculate two 100 mL cultures with the same medium, which were allowed to grow to high cell density (~30 hours). The 100-mL cultures served as inoculum for two 1-L cultures, which were grown in induction medium with SCG-Ura,H,E, where galactose instead of dextrose was used as carbon source. The 1-L cultures were grown to saturation at 30 °C with shaking, and cells were harvested by centrifugation (4000 rpm, 15 min, 4 °C) to give a cell pellet of 19 g.

The cell pellet was subjected to saponification (in 12.5% KOH in 3:1 methanol/water), stirring under N<sub>2</sub> at 70 °C for 1.5 h. The nonsaponifiable lipids were extracted with MTBE and washed with water. NMR analysis of the crude MTBE extract showed traces of **A**, **B**, and **C** together with the major LUP1 triterpenes (lupeol and lupanediol) and supplemented ergosterol. The crude extract was then chromatographed on a SPE silica gel cartridge and eluted with a stepwise gradient solution of MTBE/hexanes (5-25%). Sterols and triterpenes were eluted in the following order: traces of OS; lupeol; ergosterol and analogs; lupanediol, together with compounds **A**, **B** and **C**. The amounts of **A**, **B**, and **C** (**9a**, **8**, and **9b**) relative to the major LUP1 products (lupeol and lupanediol) were estimated by <sup>1</sup>H NMR to be about 7%, 2%, and 2%, respectively.

### NMR characterization of Compounds **A**, **B**, and **C** (**9a**, **8**, and **9b**)

<sup>1</sup>H NMR spectra of **A**, **B** and **C** are shown in [Figure S2](#). <sup>13</sup>C NMR and DEPT spectra of **A**, **B**, and **C** are shown in [Figure S3](#).



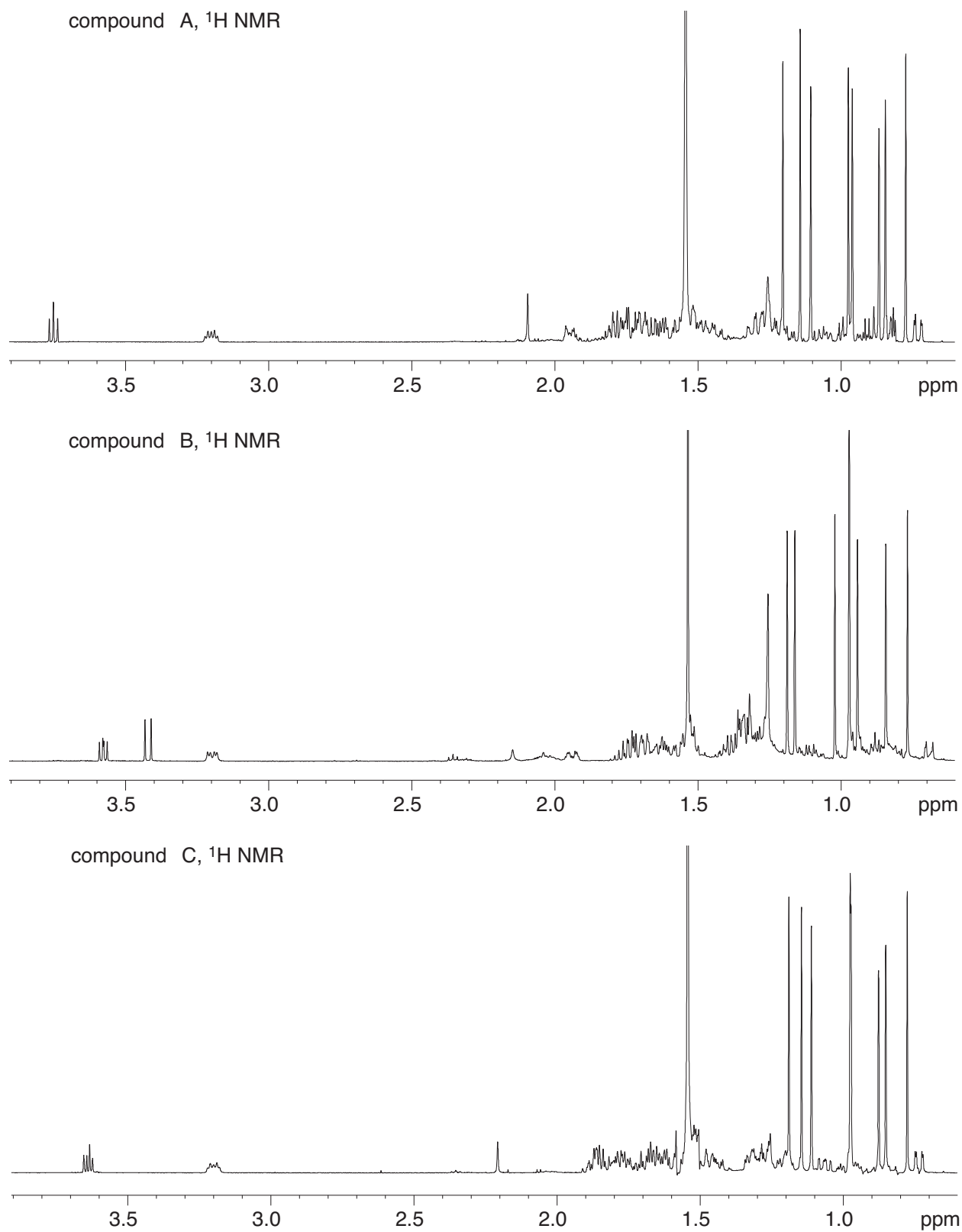


**Figure S2.**  $^1\text{H}$  NMR spectra of compounds **A**, **C** and **B** (**9a**, **9b**, and **8**).

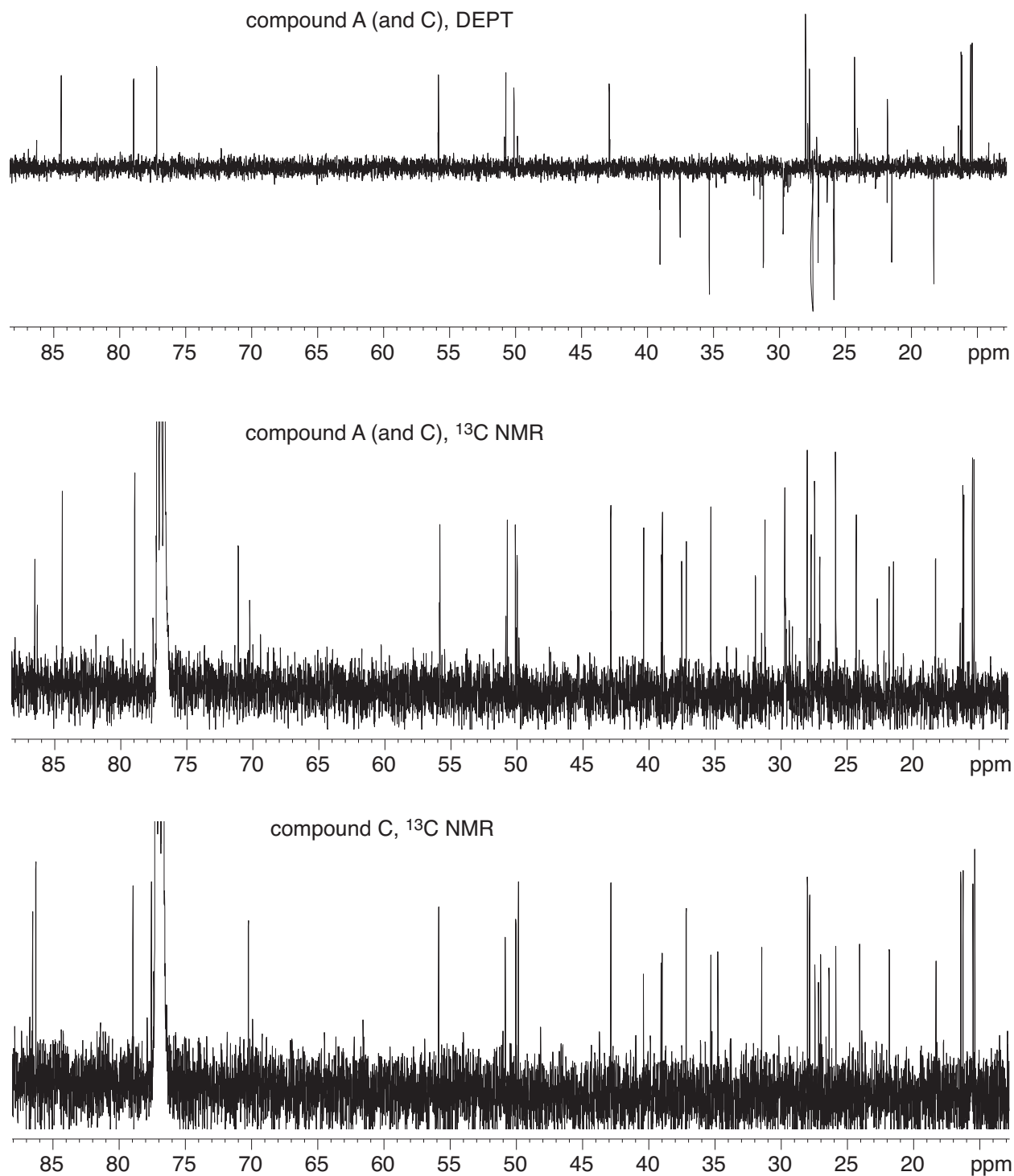


**Figure S3a.**  $^{13}\text{C}$  and DEPT spectra of **A** and **C** (compounds **9a** and **9b**).

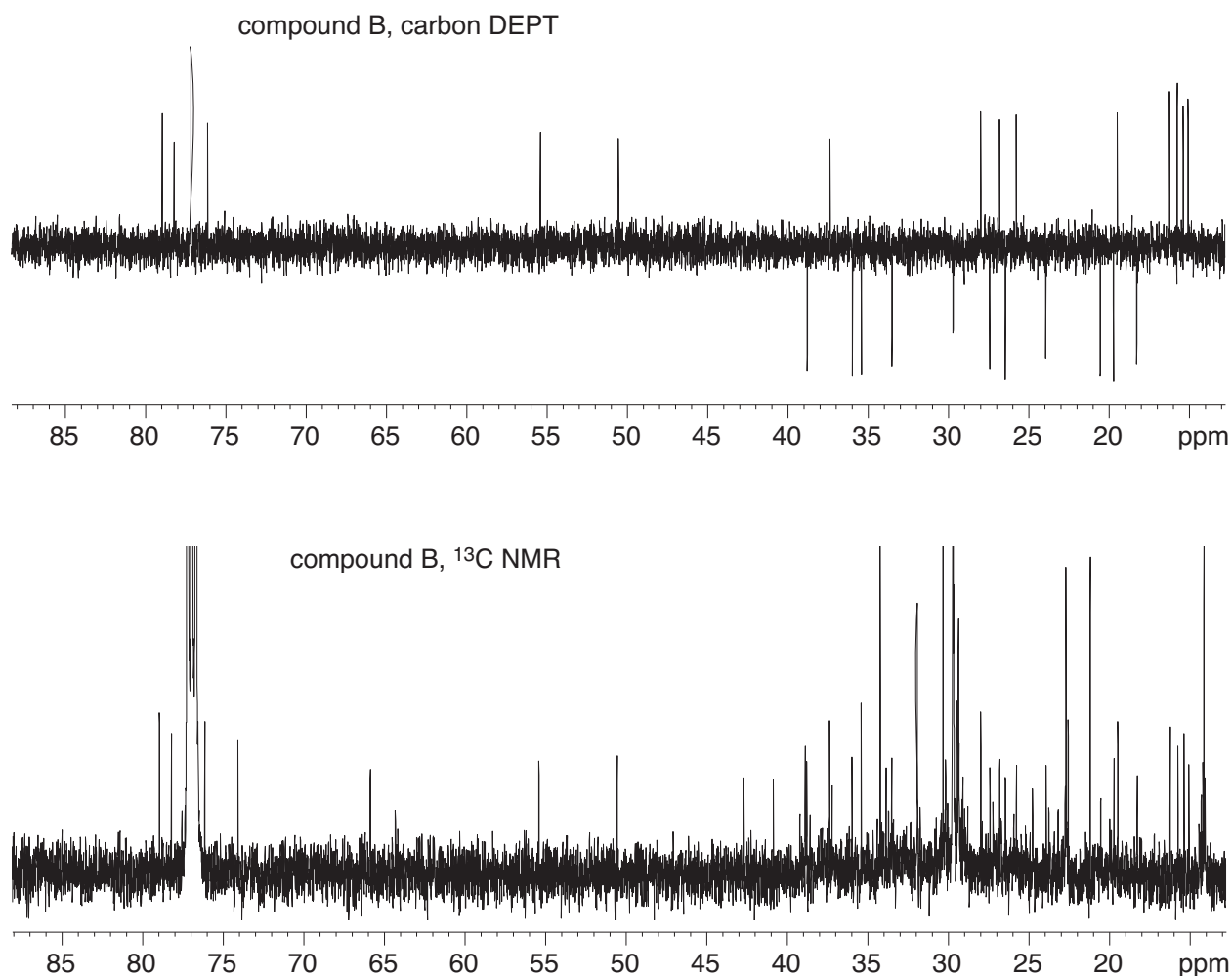


**Figure S3b.**  $^{13}\text{C}$  and DEPT spectra of **B** (compound **8**).

HMBC spectra of **A**, **B**, and **C** are shown in [Figure 4](#). Two of the downfield signals of **A** (C20 and C24) were folded and appear 70 ppm lower than their usual chemical shifts of  $\delta$  86.5 and 84.5. The  $f_1$  window for **C** was set even smaller to improve the  $^{13}\text{C}$  resolution, and folding affected the carbon signals beyond 50 ppm, namely C3, C5, C20, C24, and C25.

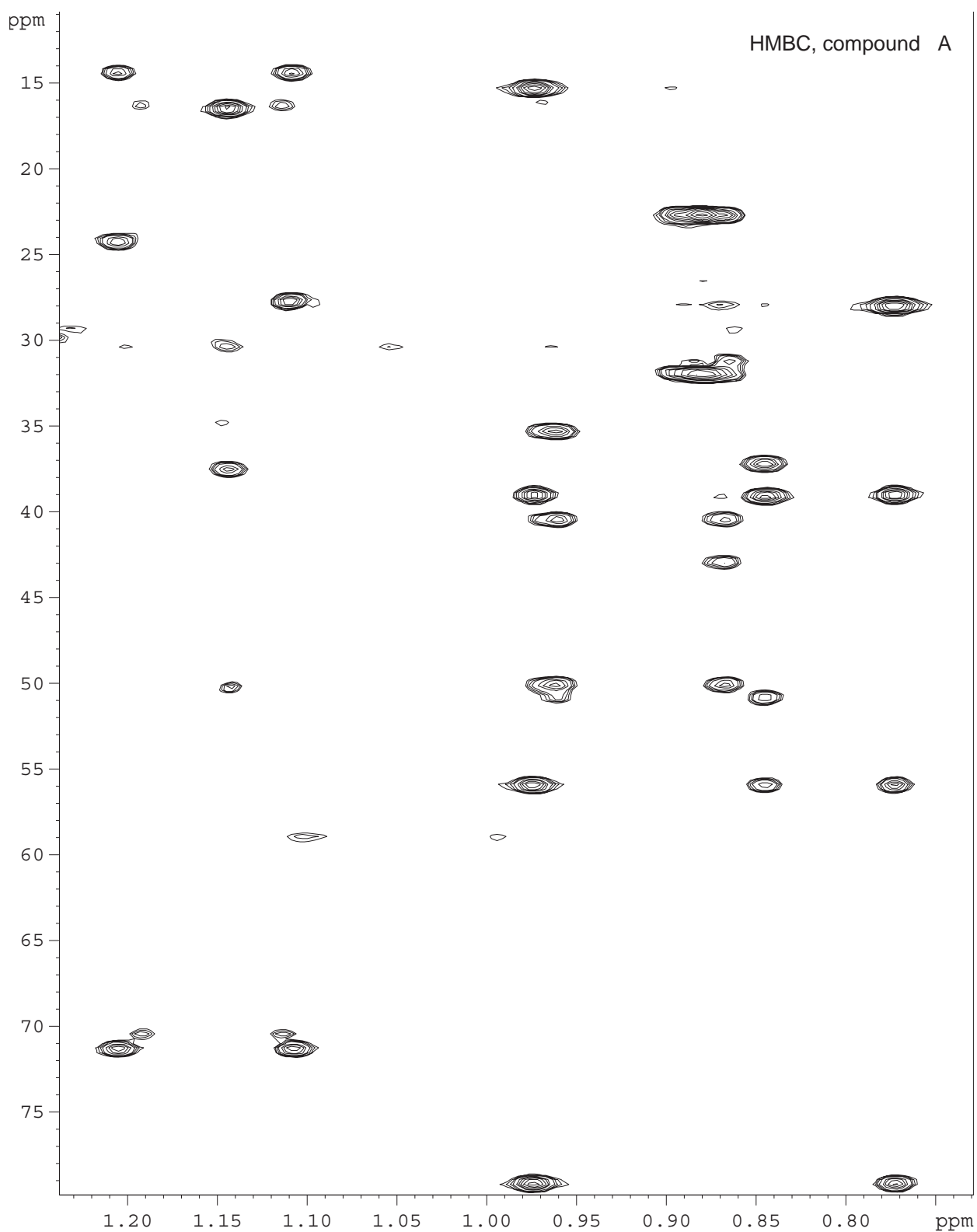


**Figure S4a.** HMBC spectrum of compound **A** (**9a**). The  $f_1$  spectral width was 70.0 ppm (10-80 ppm); 171  $t_1$  increments were collected.

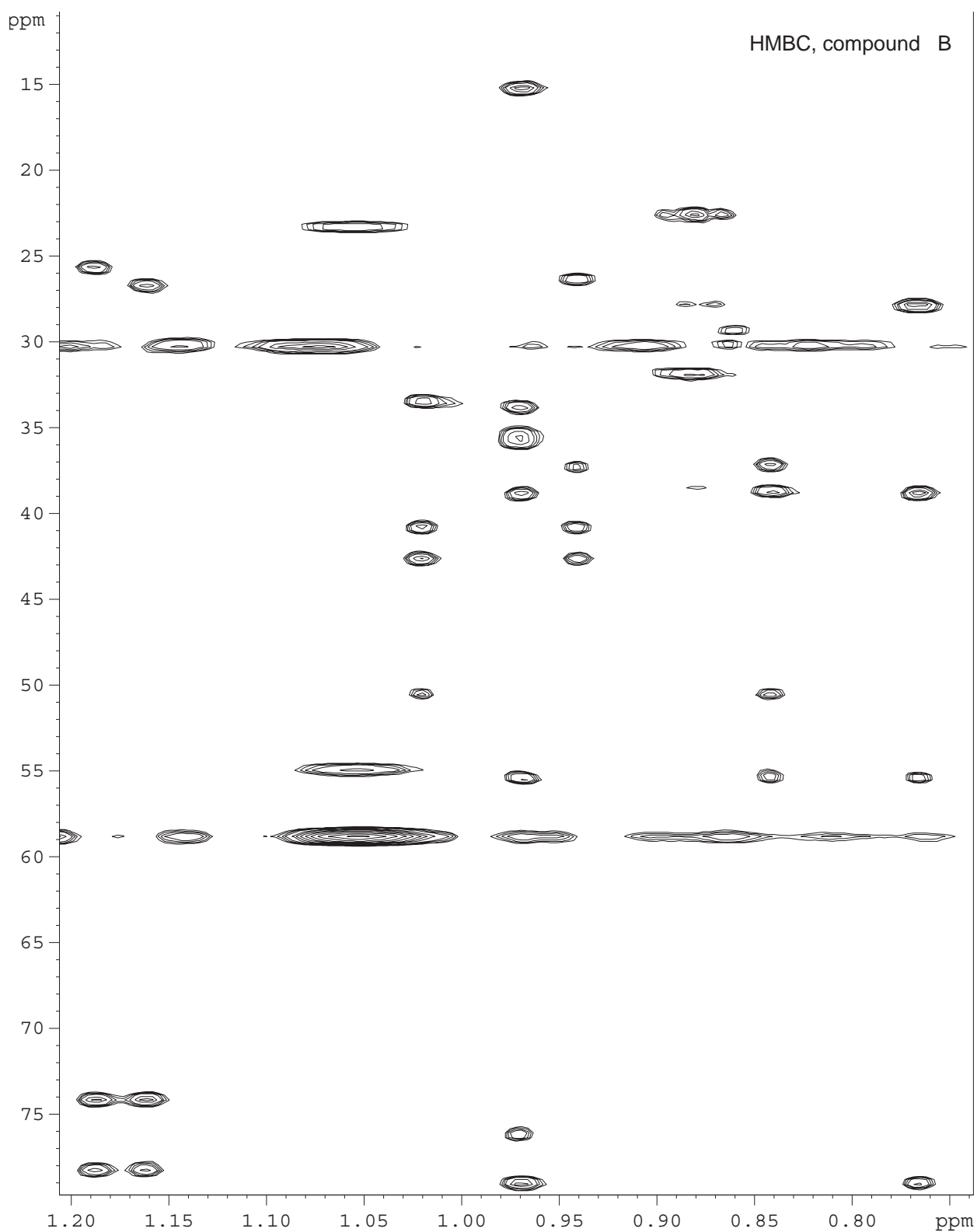


**Figure S4b.** HMBC spectrum of compound **B** (**8**). The  $f_1$  spectral width was 70.0 ppm (10-80 ppm); 184  $t_1$  increments were collected. The horizontal bands at 30 and 59 ppm are artefacts.

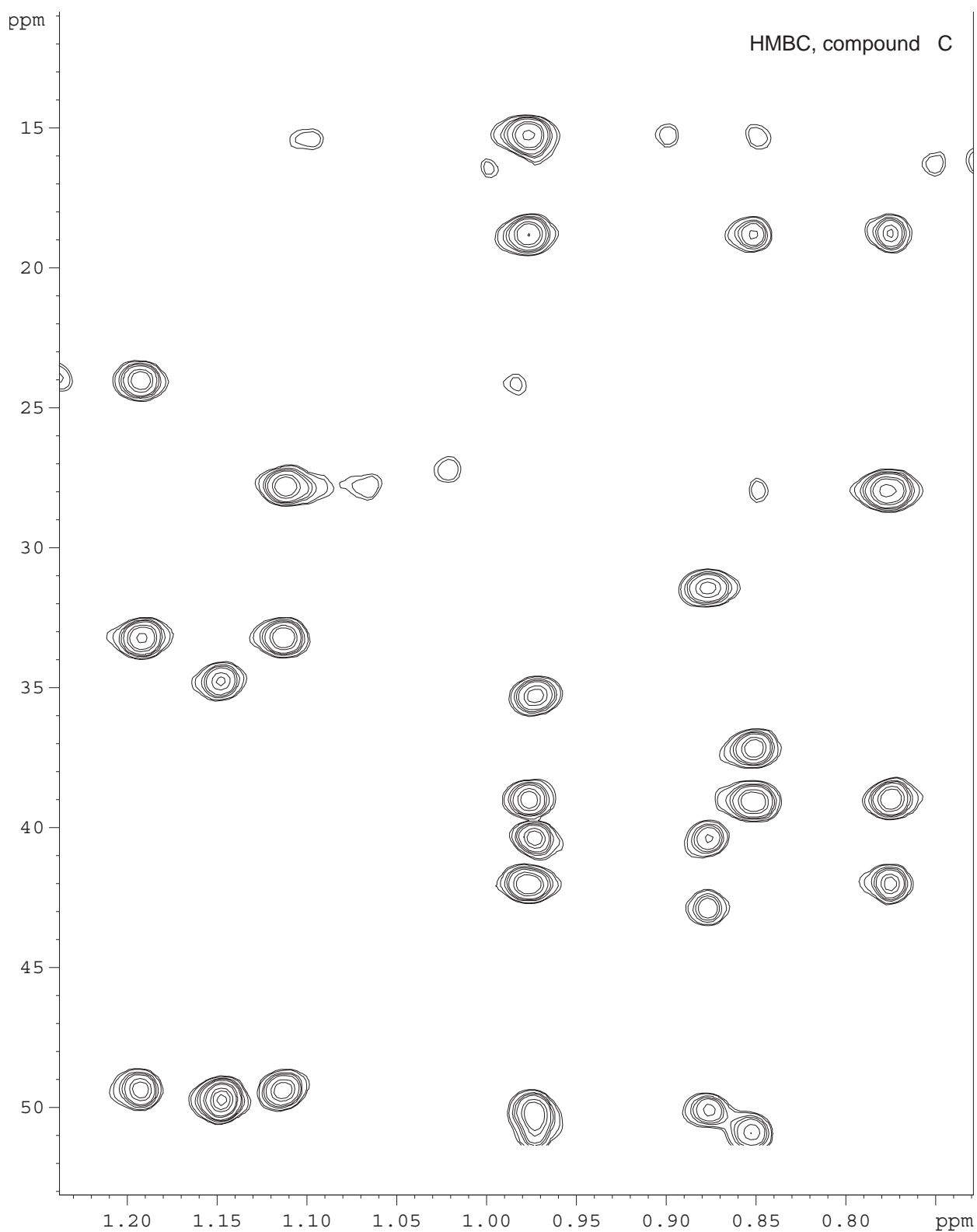


**Figure S4c.** HMBC spectrum of compound **C** (**9b**). The  $f_1$  spectral width was 37.0 ppm (15-52 ppm); 62  $t_1$  increments were collected.

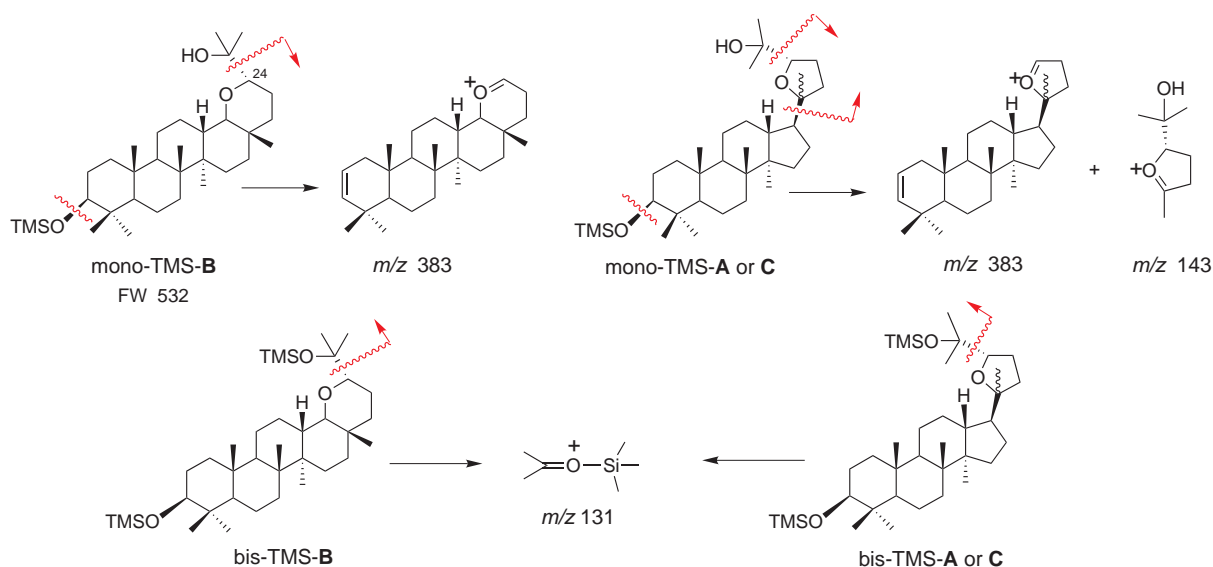
## GC-MS Analysis of Compounds A, B, and C (9a, 8, and 9b)

The diol samples were derivatized as TMS ethers. The mono-TMS ether, bis-TMS ether, or both could be formed depending on the derivatization and injection conditions.<sup>17</sup> When **A**, **B**, or **C** was injected in toluene after 1 h of TMS derivatization, mostly mono-TMS ether derivatives were observed. The GC retention times of the mono-TMS ether derivatives of **A**, **B** and **C** were 18.4, 23.4 and 18.4 min respectively. When the samples were injected in the BSTFA-pyridine reagent, multiple peaks were observed, including both mono- and bis-TMS ether derivatives. The GC retention times of the bis-TMS ether derivatives of **A**, **B** and **C** were 17.7, 21.6, and 18.0 min, respectively, i.e. slightly shorter than those of mono-TMS ethers.

Mass spectra of the mono-TMS ethers of **A** and **C** showed a base peak at  $m/z$  143 and small peaks at  $m/z$  191 and 383 (Figure S5).<sup>18</sup> The spectrum of the mono-TMS ether of **B** showed abundant ions at  $m/z$  191 and 383, a small peak at  $m/z$  473 (M-Me<sub>2</sub>COH), and essentially no signal at  $m/z$  143 (Figure S6). Spectra of the bis-TMS ethers were dominated by the base peak at  $m/z$  131, with minor peaks at  $m/z$  215 and 383 (**A** and **C**) or  $m/z$  191 and 383 (**B**).

Based on structures **9a**, **8**, and **9b** for **A**, **B**, and **C**, we suggest fragmentation mechanisms for several ions (Scheme S1). Among the mono-TMS ethers, the C24-C25 bond was preferentially cleaved in **B** to give  $m/z$  383, whereas in **A** and **C** cleavage occurred mainly at the C17-C20 bond to give  $m/z$  143. All three bis-TMS derivatives underwent C24-C25 bond cleavage with retention of positive charge on C25 ( $m/z$  131). Apart from the neutral loss of TMSOH at C3, the driving force for fragmentation was the stabilization of charge by oxygen, similar to the forces that generate the oxonium ion in the enzymatic mechanism.

GC-MS analysis of **A**, **B**, and **C** showed no identifiable molecular ions despite attempts to obtain milder fragmentation by decreasing the energy level of EI, the emission current, and/or the source temperature. However, assigning the  $m/z$  383 fragment ions as M – TMSOH – Me<sub>2</sub>COH led to a value of 532 for M<sup>+</sup>, corresponding to FW 460 for the underivatized diols. Together with <sup>13</sup>C NMR and DEPT results, this indicates a molecular formula of C<sub>30</sub>H<sub>52</sub>O<sub>3</sub> and thus requires five rings, given the absence of <sup>13</sup>C NMR signals for olefinic or carbonyl groups.



**Scheme S1.** Suggested mass spectral fragmentation of compounds **A**, **B**, and **C**.

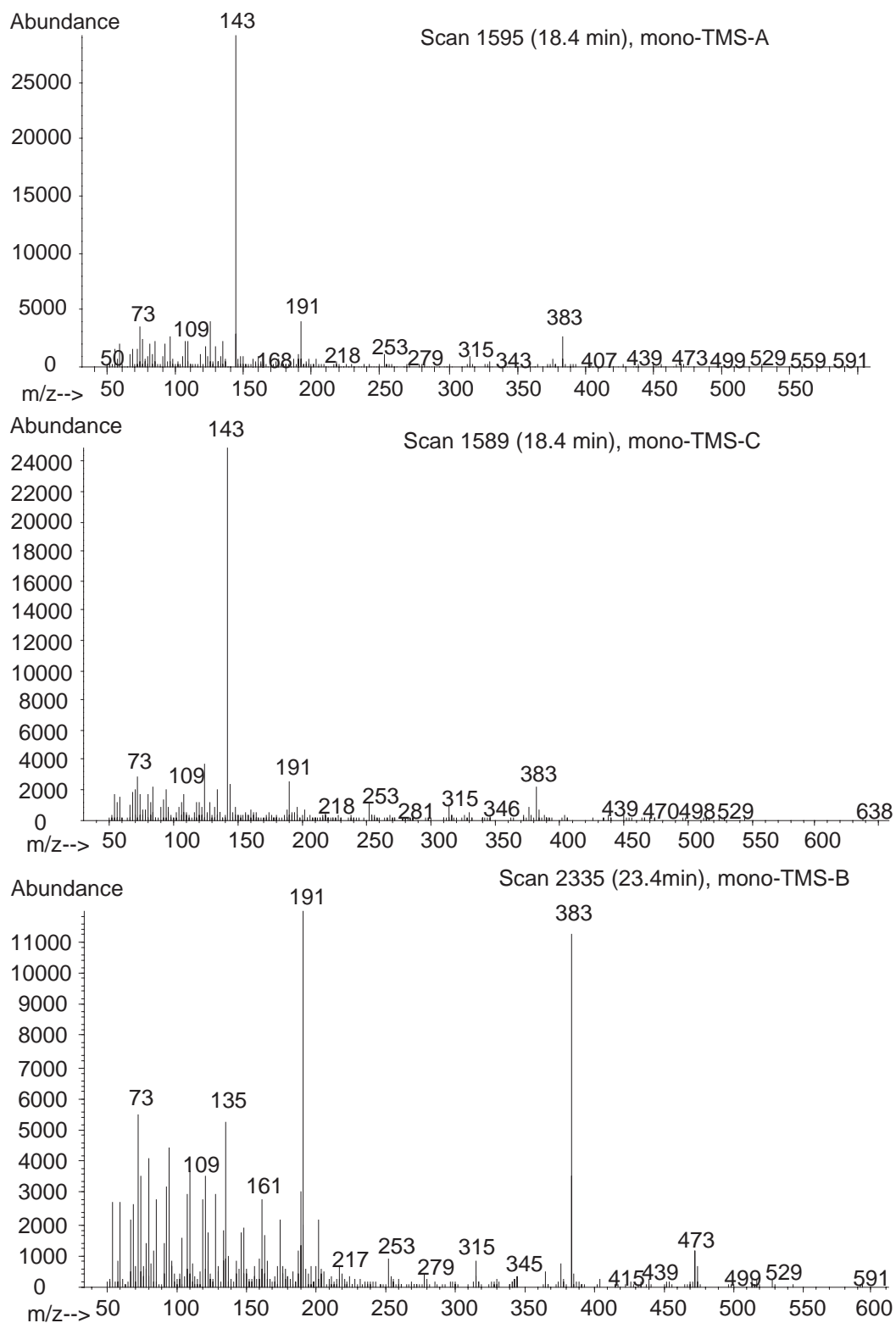


**Figure S5.** Mass spectra of the mono-TMS derivatives of compounds **A**, **C**, and **B** (**9a**, **9b**, and **8**).



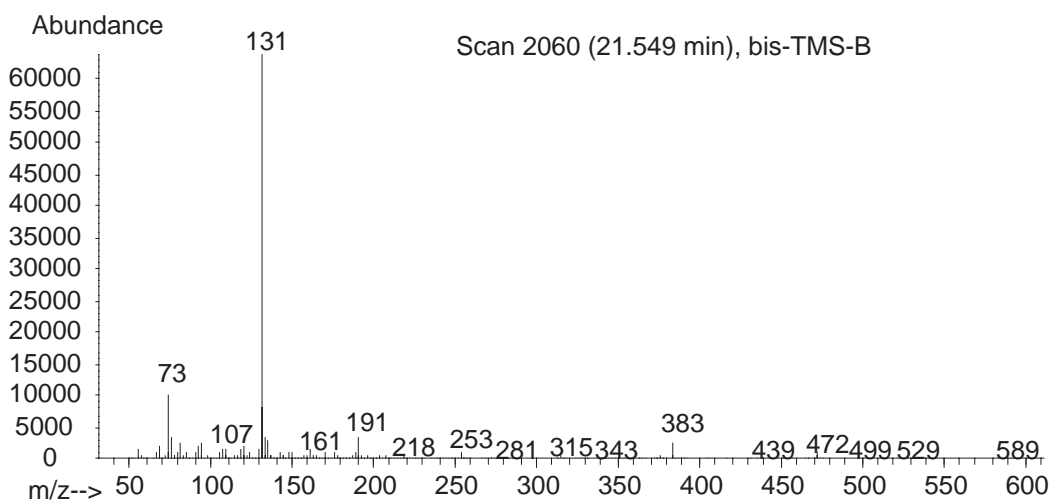
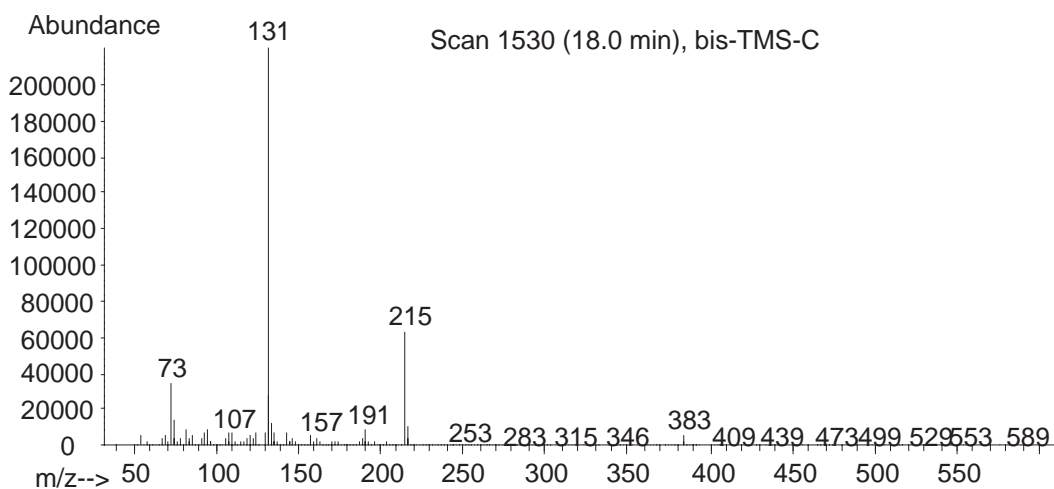
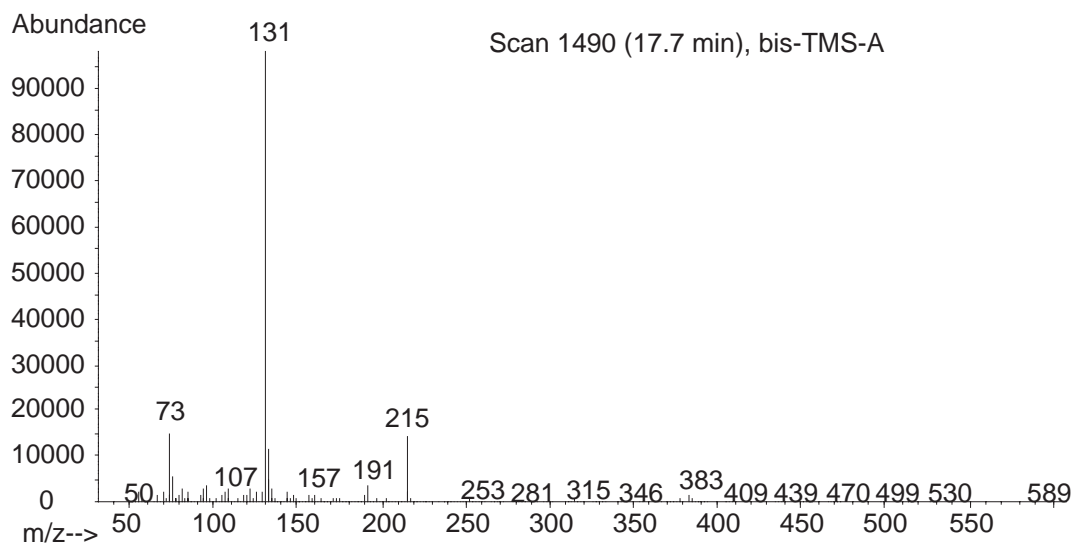


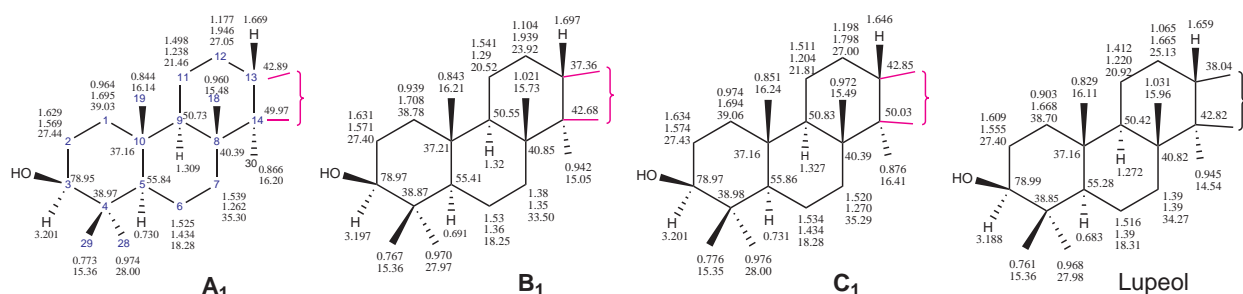
**Figure S6.** Mass spectra of the bis-TMS derivatives of compounds **A**, **C**, and **B** (**9a**, **9b**, and **8**).

### Structure Elucidation for Compounds A, B, and C (9a, 8, and 9b)

Structures of the three DOS products, designated as unknowns **A**, **B**, and **C**, were established mainly from 1D and 2D NMR analysis. The  $^{13}\text{C}$  and DEPT spectra of each unknown (Figure S3) indicated a total of 30 carbon atoms, comprising 8 methyl, 10 methylene, 6 methine, and 6 quaternary carbons. No carbons were olefinic. This pattern is consistent with pentacyclization of a  $\text{C}_{30}$  substrate to form a diol product.

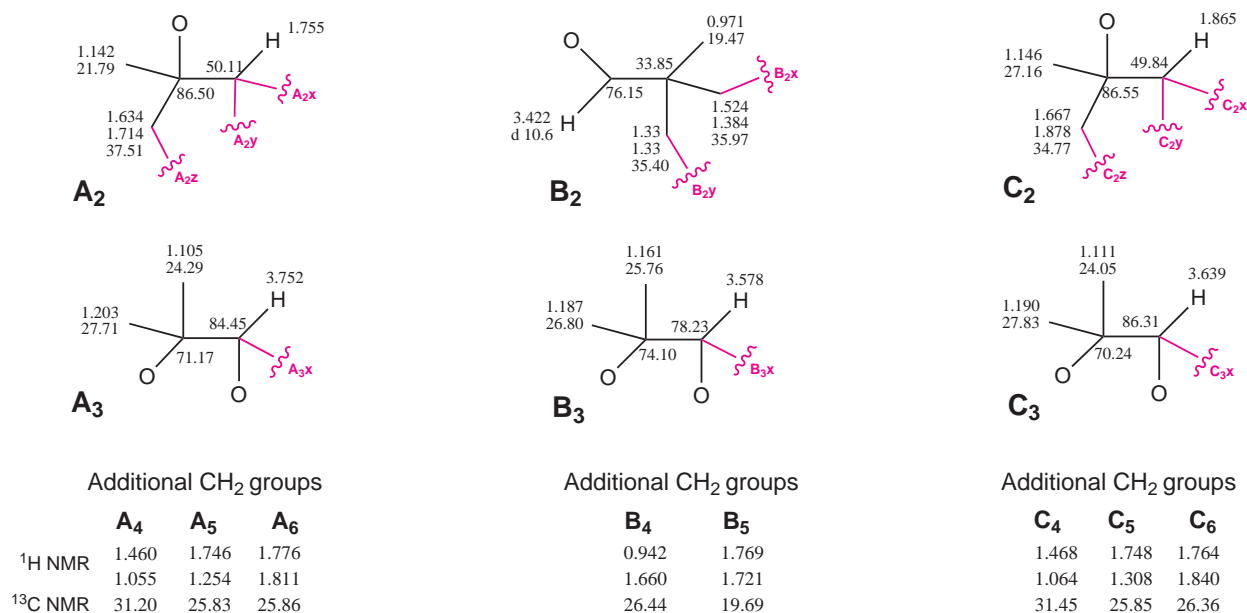
2D NMR spectra provided additional preliminary insights.  $^1\text{H}$  NMR and HMBC spectra (Figures S2 and S4) indicated that all the methyl groups are bonded to quaternary carbons. In each unknown, four carbons are attached to oxygen atoms, as judged by their downfield  $^{13}\text{C}$  chemical shifts. **A** and **C** each have two oxygenated methines and two oxygenated quaternary carbons, whereas **B** has three oxy-methines and one oxy-quaternary carbon.

The  $^1\text{H}$  and  $^{13}\text{C}$  NMR chemical shifts of lupeol<sup>16b</sup> in rings A and B could be matched closely to HSQC data for the unknowns, and the resulting signal assignments (Figure S7) were consistent with the HMBC and COSYDEC spectra. With the aid of 2D NMR correlations, these comparative signal assignments were extended to ring C. The similarity of the chemical shifts established that the unknowns all have the same carbon skeleton and stereochemistry as lupeol in rings A, B, and C.



**Figure S7.** Substructures **A**<sub>1</sub>, **B**<sub>1</sub>, and **C**<sub>3</sub> of unknowns **A**, **B**, and **C** were based on the similarity of their NMR chemical shifts with those reported for lupeol.

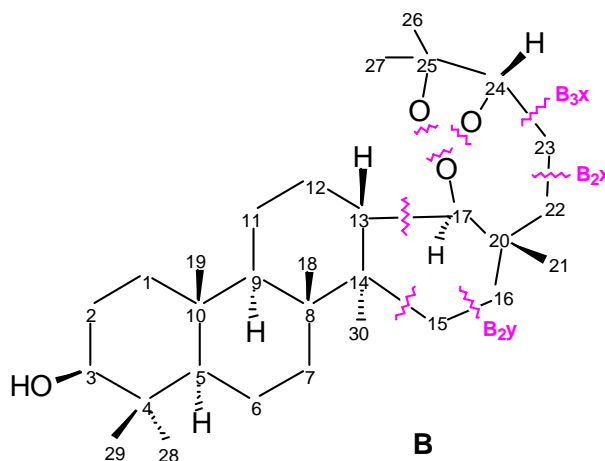
Three methyl groups remained to be allocated. HMBC spectra indicated that in all three unknowns, two of these methyls are bonded to a common oxy-quaternary carbon that is connected to an oxy-methine (substructures **A**<sub>3</sub>, **B**<sub>3</sub>, and **C**<sub>3</sub> of Figure S8). Also deduced from HMBC were the substructures **A**<sub>2</sub>, **B**<sub>2</sub>, and **C**<sub>2</sub> comprising atoms about the remaining unallocated methyl. These last substructures showed the first difference in carbon connectivity among the unknowns: In **A** and **C** the remaining methyl group is connected to an oxy-quaternary carbon, which in turn is bonded to a methylene and a methine. In contrast, the corresponding methyl group in **B** is bonded to a quaternary carbon that is connected to one oxy-methine group and two secondary carbons. The remaining unassigned methylene groups (three for **A** and **C**, two for **B**) are listed in the bottom of Figure S8.



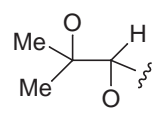
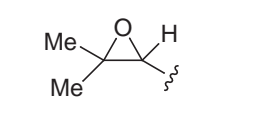
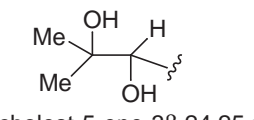
**Figure S8.** Substructures representing the remaining fragments for the unknowns.

### Structure Elucidation for Compound **B** (8)

The ABC ring system (substructure **B<sub>1</sub>**, Figure S7) was linked with fragments of Figure S8 by connectivities deduced from 2D NMR. First, the oxy-methine proton ( $\delta_C$  76.15,  $\delta_H$  3.422) of **B<sub>2</sub>** was linked by COSYDEC to the H13 methine proton. Methylene **B<sub>4</sub>** was identified as C15 by its HMBC linkage to H30 of **B<sub>1</sub>** and was also linked by COSYDEC to signals at  $\delta_H$  1.33 of **B<sub>2</sub>**. This connection of substructures **B<sub>1</sub>** and **B<sub>2</sub>** revealed a 6-membered D-ring. Methylene **B<sub>5</sub>** was linked by COSYDEC to a **B<sub>2</sub>** methylene ( $\delta_C$  35.97) and the **B<sub>3</sub>** oxy-methine (connections **B<sub>2x</sub>** and **B<sub>3x</sub>**). These correlations completed the carbon linkages for compound **B** but left undetermined oxygen connectivities (Figure S9). Note the use of sterol numbering, which is standard for epoxydammaranes, rather than triterpene numbering.



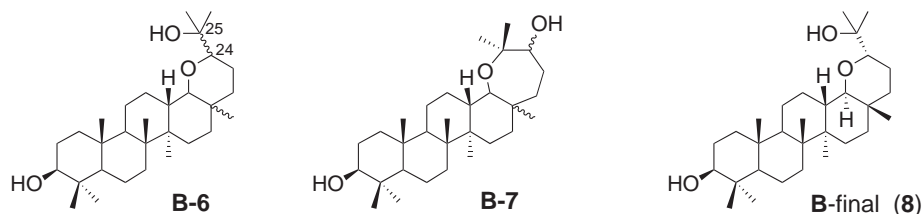
**Figure S9.** The carbon framework for compound **B**, with indication of substructure connections.

		
<b>B</b>	24,25-epoxycholesterol	cholest-5-ene-3β,24,25-triol
H-24: 3.578	H-24: 2.681 24S isomer 2.682 24R isomer	H-24: 3.282 24S isomer 3.334 24R isomer
H26/H27: 1.162, 1.187	H26/H27: 1.265, 1.305 24S isomer 1.265, 1.309 24R isomer	H26/H27: 1.164, 1.218 24S isomer 1.165, 1.216 24R isomer

**Figure S10.** Comparison of  $^1\text{H}$  NMR chemical shifts of H24, H26 and H27 of compound **B** with data for 24,25-epoxycholesterol and cholest-5-ene-3β,24,25-triol (Hui Shan and Shengrong Li, unpublished data; see also ref. 19 for earlier NMR data of 24,25-epoxycholesterol epimers).

In establishing the oxygen connectivities, we first ruled out the possibility of **B** having a 24,25-epoxy or 24,25-dihydroxy moiety by showing that  $^1\text{H}$  NMR chemical shifts for **B** differ markedly from data for 24,25-epoxycholesterol and cholest-5-ene-3β,24,25-triol (Figure S10). This result and the  $\text{C}_{30}\text{H}_{52}\text{O}_3$  formula (see above) mandate an ether linkage from C24 or C25 to form a fifth ring, with C17 as the only available terminus in the ABCD ring system. Such a fused D-E ring system was supported by NOE difference experiments suggesting limited rotational freedom for carbon atoms beyond C20. Notably, irradiation of H21 enhanced only one H22 signal, and neither the H26 nor H27 resonance was observed in the difference spectrum.

Mass spectra of **B** (Scheme S1 and Figures S5 and S6) provided evidence for a 6-membered rather than a 7-membered E ring. Ions  $m/z$  473 ( $\text{M} - \text{Me}_2\text{COH}$ ) and  $m/z$  383 ( $\text{M} - \text{TMSOH} - \text{Me}_2\text{COH}$ ) of the mono-TMS ether and ion  $m/z$  131 ( $\text{Me}_2\text{COTMS}^+$ ) of the bis-TMS ether are readily explained by the cleavage of the C24-C25 bond in structure **B-6**, whereas there appears to be no fragmentation mechanism for generating these ions from **B-7** species.



### Determination of Stereochemistry for Compound **B**

The stereochemistry of **B** was determined through NOE correlations (Table S1). The configurations at C13 and C14 (Figure S7) were confirmed by the NOE from the 8β-methyl (H18) to H13 and from the 14α-methyl (H30) to several protons on the α face. The strong NOE from H30 to H17 established the H17α stereochemistry. The β orientation of the C20 methyl (H21) was deduced from configurational transmission for the dammarenyl cation,<sup>20</sup> and this conclusion was confirmed by the NOE from H21 to H13β. Irradiation of H21 enhanced the H24 signal but not the H26/H27 signals, and irradiation of H26/H27 had no effect on H21. These results point to an α orientation of the  $\text{Me}_2\text{C}(\text{OH})$ - substituent and a β orientation of H24. As further proof of the stereochemistry of **B**, we demonstrate the good agreement of observed and predicted NMR chemical shifts (see Table S4b below). Thus, compound **B** is (17*R*,20*R*,24*S*)-17-24-epoxybaccharane-3β,25-diol (8).<sup>21,22</sup>

**Table S1.** Results of NOE difference experiments for compound **B**.<sup>a</sup>

<b>irradiate 0.942=H30 (14<math>\alpha</math>-Me)</b> 0.691 (br d, 11 Hz), weak, H5 $\alpha$ 1.103 (qd, 12.5, 5 Hz, weak, H-12 $\alpha$ 1.31-1.36 (m), strong, H7 $\alpha$ , H9 $\alpha$ , H16 $\alpha$ 1.64 (m), weak, H2 $\alpha$ 1.70 (br t, 13 Hz), medium, H13 $\beta$ 1.710 (dt, 13.5, 4 Hz), medium, H1 $\beta$ 3.200 (br d, 12 Hz), weak, H3 $\alpha$ 3.422 (d, 11 Hz), strong, H17 $\alpha$	<b>irradiate 1.021=H18 (8<math>\beta</math>-Me)</b> 0.843 (s), strong, H19 1.695 (td, 11, 3 Hz), medium, H13 $\beta$  <b>irradiate 1.161=H26/H27</b> 1.71-1.78 (m), medium, H23 1.94 (m), very weak, H12 $\beta$ 3.421 (d, 11 Hz), medium, H17 $\alpha$ 3.579 (dd, 7.3, 6.1 Hz), medium, H24
<b>irradiate 0.971= H21 + H28 (4<math>\alpha</math>-Me)</b> 0.692 (d, 12 Hz), medium, H5 $\alpha$ 0.767 (s), medium, H29 1.33 (m), medium, H16 $\beta$ 1.382 (dt, 13, 7 Hz), medium, H22 $\beta$ 1.66 (m), H15 $\beta$ 1.694 (br t, 13 Hz), strong, H13 $\beta$ 3.199 (dd, 11.5, 5 Hz), medium, H3 $\alpha$ 3.422 (d, 11 Hz), very weak, H17 $\alpha$ 3.579 (dd, 7.3, 6.1 Hz), medium, H24	<b>irradiate 1.187= H26/H27</b> 1.71-1.78 (m), medium, H23 1.94 (m), very weak, H12 $\beta$ 3.421 (d, 11 Hz), weak, H17 $\alpha$ 3.579 (dd, 7.3, 6.1 Hz), medium, H24

<sup>a</sup> Nearby signals were concomitantly irradiated in some experiments. Notably, irradiation of H30 at  $\delta$  0.942 also affected H1 $\alpha$  ( $\delta$  0.964), H28 ( $\delta$  0.970), and H21 ( $\delta$  0.971).

An NOE from H21 to H24 could not occur in a chair conformation of ring E because H24 would be equatorial and thus distant from H21. However, comparison of observed and predicted coupling constants (see Table S4a below) indicates that ring E exists as a 2:1 mixture of boat and chair conformers, at least in CDCl<sub>3</sub> solution.

### Structure Elucidation for Compounds **A** and **C** (9a and 9b)

The skeletons of **A** and **C** were established by linking substructure **A**<sub>1</sub> or **C**<sub>1</sub> (Figure S7) with substructures shown in Figure S8 (two side-chain moieties and three methylene groups). For **A**, the methine proton of **A**<sub>2</sub> ( $\delta_{\text{H}}$  1.755) was linked by COSYDEC to both H13 and methylene **A**<sub>5</sub> ( $\delta_{\text{C}}$  25.83,  $\delta_{\text{H}}$  1.746, 1.254). Methylene **A**<sub>5</sub> was also correlated to methylene **A**<sub>4</sub> ( $\delta_{\text{C}}$ : 31.19,  $\delta_{\text{H}}$ : 1.46, 1.055), which was identified as C15 from its HMBC linkage to H30. Thus, **A** has a 5-membered D ring. The remaining methylene (**A**<sub>6</sub>,  $\delta_{\text{C}}$  25.86) was linked by TOCSY and COSYDEC to the oxy-methine of **A**<sub>3</sub> ( $\delta_{\text{C}}$  84.43) and to the methylene of **A**<sub>2</sub> ( $\delta_{\text{C}}$  37.49). This completed the carbon skeleton for **A**, and the skeleton for **C** was determined similarly (Figure S11).

Oxygen connectivities were established as was described for compound **B**. The NMR chemical shifts for **A** and **C** were incompatible with data for 24,25-epoxy and 24,25-diol structures (Figure S10). This result requires a fifth ring, as does the molecular formula of C<sub>30</sub>H<sub>52</sub>O<sub>3</sub> (see above). The fifth ring must be formed by fusing two oxygens in the structure of **A** (or **C**) in Figure S11. Since a 24,25-epoxide has been excluded, two possibilities remain, a 5-membered E ring (ocotillol skeleton, e.g. **9a-c**) or a 6-membered E ring (**14**). Mass spectra of **A** and **C** show an  $m/z$

383 ion for the mono-TMS ether and base peak at  $m/z$  143 for the bis-TMS ether (Figures S5 and S6). Both ions are readily explained for the ocotillol skeleton by C24-C25 bond cleavage (Scheme S1) but are highly unlikely for **14** by usual fragmentation mechanisms. Hence, we conclude that **A** and **C** have the ocotillol skeleton.

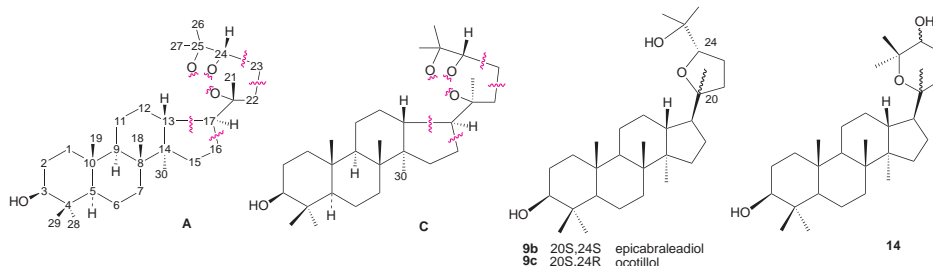


**Figure S11.** The carbon linkage for compounds **A** and **C**; structures of known epoxydammaranes, ocotillol and epicabraleadiol; and a 6-membered E-ring structure (**14**).

#### Determination of stereochemistry for compound **A** and **C** (**9a** and **9b**)

Our deduction that **A** and **C** are ocotillol stereoisomers is consistent with their identical GC mobility and EI fragmentation. The C20 and C24 configurations of **A** and **C** were established from NOE experiments and comparisons with reported NMR data. As with **B**, the stereochemistry at C13 and C14 was deduced from the NOE from the 8 $\beta$ -methyl (H18) to H13 $\beta$  and from the 14 $\alpha$ -methyl (H30) to several protons on the  $\alpha$  face, including H17 $\alpha$ . In NOE experiments for **A**, irradiation of H21 ( $\delta_H$  1.142) led to enhancement of signals at  $\delta_H$  3.752 (H24), 1.946 (H12 $\beta$ ), 1.714 (H22 $\beta$ ) and 1.669 (H13 $\beta$ ). For **C**, irradiation of H21 ( $\delta_H$  1.147) gave enhanced signals only at  $\delta_H$  2.21 (25-OH), 1.865 (H17 $\alpha$ ), and 1.668 (H22 $\alpha$ ) but not H24. Because of potentially complex conformational heterogeneity owing to multiple rotamers about the C17-C20 single bond, the NOE results cannot readily establish the C20 stereochemistry. However, the NOE results indicate that H21 and H24 are on the same face of the E ring in **A** and on opposite faces in **C**. Therefore **A** has either the 20*R*,24*S* or 20*S*,24*R* configuration and **C** has either the 20*S*,24*S* or 20*R*,24*R* configuration.

Lack of an NOE enhancement is not usually considered meaningful. However, we regard the lack of NOE from H21 to H24 to indicate that these groups are on opposite sides of ring E because of: (a) the regularity of NOE enhancements for steroid and triterpene structures, (b) the high experimental sensitivity, and (c) the ready identification of the well-resolved signals.

Comparison of  $^{13}\text{C}$  chemical shifts of **C** with data reported for epoxydammaranes (Table S3) indicated that **C** is 3-epicalabraleadiol,<sup>23</sup> whose acetate (20*S*,24*S*) has been characterized by  $^{13}\text{C}$  NMR and x-ray crystallography.<sup>24</sup> Accordingly, **C** is (20*S*,24*S*)-20,24-epoxydammarane-3 $\beta$ ,25-diol (**9b**). Compound **A** showed small but significant differences from the published NMR data for ocotillol (Table S3), whose 20*S*,24*R* configuration is also based on crystallographic evidence.<sup>25,26</sup> Thus, **A** is (20*R*,24*S*)-20,24-epoxydammarane-3 $\beta$ ,25-diol (**9b**). These assignments of configuration are consistent with the 3*S*,22*S* stereochemistry of the DOS substrate and with mechanistic and conformational analyses described below.

## <sup>1</sup>H and <sup>13</sup>C NMR Assignments for Compounds A, B, and C (9a, 8, 9b)

The completion of the structure determination for A, B, and C permitted the <sup>1</sup>H and <sup>13</sup>C NMR assignments for 8, 9a, and 9b to be presented in final form (Table S2).

**Table S2.** <sup>13</sup>C and <sup>1</sup>H NMR assignments for 8, 9a, and 9b (compounds A, B and C).<sup>a,b</sup>

	8			9a			9b		
	<sup>13</sup> C	<sup>1</sup> H (α)	<sup>1</sup> H (β)	<sup>13</sup> C	<sup>1</sup> H (α)	<sup>1</sup> H (β)	<sup>13</sup> C	<sup>1</sup> H (α)	<sup>1</sup> H (β)
C1 (CH <sub>2</sub> )	38.78	0.939	1.708	39.03	0.962	<u>1.695</u>	39.06	0.979	<u>1.693</u>
C2 (CH <sub>2</sub> )	27.40	<u>1.631</u>	<u>1.571</u>	27.44	<u>1.628</u>	<u>1.575</u>	27.43	<u>1.631</u>	<u>1.577</u>
C3 (CH)	78.97	3.197 (dd, 11.5, 4.8)		78.95	3.201 (dd, 11.7, 4.9)		78.97	3.201 (dt, 11.8, 4.8)	
C4 (qC)	38.87			38.97			38.98		
C5 (CH)	55.41	0.691		55.84	0.730		55.86	0.734	
C6 (CH <sub>2</sub> )	18.25	1.53	<u>1.36</u>	18.28	<u>1.525</u>	1.43	18.28	1.52	1.437
C7 (CH <sub>2</sub> )	33.50	<u>1.38</u>	<u>1.35</u>	35.30	<u>1.539</u>	<u>1.264</u>	35.29	1.53	1.273
C8 (qC)	40.85			40.39			40.39		
C9 (CH)	50.55	<u>1.32</u>		50.73	1.308		50.83	1.326	
C10 (qC)	37.21			37.16			37.16		
C11 (CH <sub>2</sub> )	20.52	1.541	<u>1.29</u>	21.46	1.497	1.23	21.81	1.512	1.20
C12 (CH <sub>2</sub> )	23.92	1.104	1.939	27.05	1.181	1.947	27.00	1.21	1.797
C13 (CH)	37.36	1.697		42.89	<u>1.678</u>		42.85	1.646	
C14 (qC)	42.68			49.97			50.03		
C15 (CH <sub>2</sub> )	26.44	0.943	1.659	31.20	1.054	1.463	31.45	1.065	1.469
C16 (CH <sub>2</sub> )	35.40	<u>1.33</u>	<u>1.33</u>	25.83	1.75	1.255	25.85	1.748	1.305
C17 (CH)	76.15	3.422 (d, 10.7)		50.11	1.76		49.84	1.864	
C18 (CH <sub>3</sub> )	15.73	1.021 (s)		15.48	0.960		15.49	0.972	
C19 (CH <sub>3</sub> )	16.21	0.843 (d, 0.9)		16.14	0.844		16.24	0.851	
C20 (qC)	33.85			86.50			86.55		
C21 (CH <sub>3</sub> )	19.47	0.971 (br s)		21.79	1.142		27.16	1.146	
C22 (CH <sub>2</sub> )	35.97	1.524	1.384	37.51	<u>1.638</u>	<u>1.714</u>	34.77	<u>1.669</u>	<u>1.877</u>
C23 (CH <sub>2</sub> )	19.69	<u>1.765</u>	<u>1.725</u>	25.86	<u>1.809</u>	<u>1.77</u>	26.36	<u>1.838</u>	<u>1.766</u>
C24 (CH)	78.23	3.578 (dd, 7.7, 6.0)		84.45	3.752 (dd, 7.7, 6.9)		86.31	3.639 (dd, 10.1, 5.3)	
C25 (qC)	74.10			71.11			70.24		
C26 (CH <sub>3</sub> )	<u>26.80</u>	<u>1.187</u> (d, 0.4)		<u>24.29</u>	<u>1.105</u>		<u>24.05</u>	<u>1.111</u>	
C27 (CH <sub>3</sub> )	<u>25.76</u>	<u>1.161</u> (d, 0.4)		<u>27.71</u>	<u>1.203</u>		<u>27.83</u>	<u>1.190</u>	
C28 (CH <sub>3</sub> )	27.97	0.970 (s)		28.00	0.974		28.00	0.976	
C29 (CH <sub>3</sub> )	15.36	0.767 (s)		15.36	0.773		15.35	0.776	
C30 (CH <sub>3</sub> )	15.05	0.942 (d, 0.9)		16.20	0.866		16.41	0.876	

<sup>a</sup> Data were obtained at 500 MHz in dilute CDCl<sub>3</sub> solution (<10 mM triterpene) at 25°C and referenced to Si(CH<sub>3</sub>)<sub>4</sub>. Chemical shifts were corrected for effects of strong coupling. Under the specified conditions of temperature and concentration, <sup>1</sup>H NMR values given to two (three) decimal places are reproducible to ±0.01 (±0.001) ppm except that underlined values are reproducible to about ±0.02 (±0.003) ppm. All <sup>13</sup>C values are reproducible to ca. 0.02 ppm. Colored values denote tentative assignments that may be reversed, notably C26/C27, H26/H27, and some geminal proton pairs. In the stereochemical assignments for 9a and 9b, substituents with the same orientation as the C20 methyl are designated β. <sup>b</sup> Additional couplings: compound 8: H5α, br d, 12 Hz; H12α, br qd, 12.5, 5 Hz; H13β, br d, 13 Hz; H22α, ddd, 14, 7, 7, 6 Hz; H22β, ddd, 13.4, 8.0, 7.0 Hz; H23α, ddt, 13, 8, 7 Hz; compounds 9a and 9b, H5α, dd, 11.8, 2.2 Hz; H18 and H19, d, 0.9 Hz; H21, s; H26, d, 0.4 Hz; H27, d, 0.5 Hz; H28 and H29, d, 0.3 Hz; H30, d, 1.1 Hz. Also, 9b: H15α, 11.8, 8.6, 1.6 Hz; H17α, td, 10.5, 5.7 Hz.



## Literature Review: Lack of Evidence for 20*R*-Epoxydammaranes

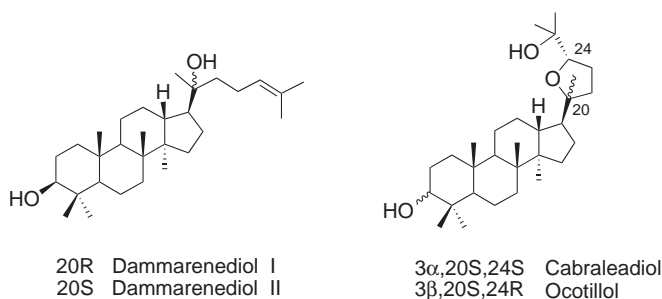
### *Errors and Confusion in the Epoxydammarane Literature*

The epoxydammarane literature has generated much confusion owing to nomenclature inconsistencies, errors in structure elucidation, and misassignments of NMR signals. Many epoxydammarane structures are possible depending on the configuration at C20 and C24 and the size of ring E. Epoxydammaranes that are stereoisomeric in ring E show only minor differences in  $^1\text{H}$  and  $^{13}\text{C}$  NMR chemical shifts, and these differences are not readily discerned unless the data were calibrated and reported with high precision. Because of conformational heterogeneity, the E-ring stereochemistry of epoxydammaranes cannot presently be deduced by NMR except by comparison with NMR data linked to crystal structures. Unfortunately, few crystallographic determinations of the E-ring stereochemistry were accompanied by NMR data.

Before 1980 epoxydammaranes isomeric in ring E were often thought to differ in configuration at C20. This belief was reinforced by the isolation of unnatural C20 isomers from acid hydrolyses, which led to epimerization. Dammarenediol had been designated as isomer I or II, according to its C20 configuration (20*R* and 20*S*, respectively).<sup>27</sup> Epoxydammaranes such as ocotillol were analogously labeled I or II, by implicit reference to the 20*R* or 20*S* configuration.<sup>28</sup>

By the middle 1980s it had become clear that natural epoxydammaranes had the 20*S* configuration and that the original assignments of ocotillols as 20*S*,24*R* (Tanaka and coworkers,<sup>25</sup> 1973) and cabraleadiols as 20*S*,24*S* (Cascon and Brown<sup>29</sup> in 1972) were correct. This situation was succinctly described in 1984 by Lavie et al.<sup>26</sup> The chemical correlations for the cabraleadiol configuration were strengthened by a 1996 NMR study by Hisham et al.<sup>23</sup> and further confirmed in 2001 by Qiu et al.,<sup>24</sup> who provided both crystallographic and NMR data for cabraleadiol acetate.

Although the E-ring stereochemistry of natural epoxydammaranes was established by 1973, the validity of the original studies was not widely recognized. Consequently, errors from other early papers proliferated, leading to many incorrect structures being reported during the past three decades. Several errors and inconsistencies have been noted by others.<sup>23,24,26,30a</sup> The abundance of errors makes the epoxydammarane literature difficult for novices to evaluate.



Our isolation of the 20*R*,24*S* and 20*S*,24*S* isomers prompted us to compare our  $^{13}\text{C}$  NMR data with values reported previously<sup>23,24,30</sup> (Table S3). The information in this table allows ready identification of the E-ring stereochemistry of epoxydammaranes for 3 of the 4 possible E-ring stereoisomers and should facilitate the search for 20*R* epoxydammaranes in nature.



**Table S3.** Comparison of reported  $^{13}\text{C}$  NMR chemical shifts for epoxydammaranes.<sup>a</sup>

	20R,24S	20S,24R						20S,24S							
structure	9a	9c	9c	3βOAc-9c	A-seco-9c	3αOH-9c	3keto-9c	9b	9b	3αOH-9b	3βOAc-9b	3αOAc-9b	A-seco-9b	3αOH-9b	3keto-9b
1 <sup>st</sup> author	this paper	Fu	Tanaka	Rouf	Roux	Fuchino	Anjaneyulu	this paper	Fu	Hisham	Rouf	Qiu	Roux	Nakamura	Anjaneyulu
year		2005	1993	2001	1998	1996	1993		2005	1996	2001	2001	1998	1997	1993
reference		ref-30a	ref-30b	ref-30c	ref-30d	ref-30e	ref-30f		ref-30a	ref-23	ref-30c	ref-24	ref-30d	ref-30g	ref-30f
C-8	40.39	40.4	40.38	40.4	39.8	40.6	40.4	40.39	40.4	40.6	40.4	40.1	39.9	40.6	40.5
C-9	50.73	50.8	50.80	50.7	40.9	50.6	50.0	50.83	50.8	50.6	50.7	50.2	41.0	50.6	50.2
C-10	37.16	37.1	37.18	37.1	38.8	37.3	36.9	37.16	37.2	37.2	37.1	36.7	38.9	37.2	37.2
C-11	21.46	21.6	21.59	21.5	22.9	21.4	22.2	21.81	21.8	21.6	21.8	21.2	22.2	21.6	22.4
C-12	27.05	25.7	25.74	27.3	27.0	27.3	26.0	27.00	25.9	27.0	26.9	26.8	26.7	27.0	26.1
C-13	42.89	43.0	42.97	42.9	42.7	42.9	43.3	42.85	42.8	42.7	42.8	42.4	42.8	42.7	43.3
C-14	49.97	50.0	50.08	50.0	50.1	50.1	50.0	50.03	50.0	50.1	50.0	49.7	50.2	50.1	50.2
C-15	31.20	26.1	31.48	31.4	31.2	31.4	31.7	31.45	27.0	31.4	31.4	31.1	32.0	31.4	31.7
C-16	25.83	31.5	27.43	25.7	25.4	25.7	27.4	25.85	31.5	25.8	25.8	25.5	25.6	25.8	27.4
C-17	50.11	49.5	49.54	49.5	49.2	49.5	50.0	49.84	49.8	49.8	49.8	49.4	49.6	49.8	50.2
C-18	15.48	15.4	15.47	15.4	16.1	16.0	16.0	15.49	15.5	15.5	15.5	15.1	16.1	15.5	16.1
C-19	16.14	16.2	16.25	16.4	19.9	15.4	15.1	16.24	16.2	16.0	16.4	15.6	20.0	16.0	15.3
C-20	86.50	86.4	86.44	86.3	86.1	86.4	86.2	86.55	86.5	86.5	86.5	86.0	86.4	86.6	86.4
C-21	21.79	23.5	23.55	23.5	23.9	23.5	23.3	27.16	27.2	27.1	24.1	26.6	27.0	27.2	26.3
C-22	37.51	35.7	35.67	35.7	35.5	35.6	36.2	34.77	34.8	34.7	34.9	34.4	34.6	34.7	35.4
C-23	25.86	27.4	26.13	26.1	25.9	26.1	26.8	26.36	26.4	26.3	26.3	26.0	26.2	26.3	26.8
C-24	84.45	83.3	83.31	83.3	83.1	83.3	84.1	86.31	86.3	86.2	86.3	85.9	86.2	86.2	87.4
C-25	71.11	71.4	71.43	71.4	71.4	71.4	71.1	70.24	70.2	70.2	70.2	69.8	70.2	70.2	70.4
C-26	24.29	27.5	24.28	24.3	27.1	27.4	26.0	24.05	27.8	27.8	27.1	27.2	27.6	24.0	26.8
C-27	27.71	24.2	27.43	27.4	24.3	24.2	26.8	27.83	24.1	24.0	27.8	23.9	23.9	27.9	26.8
C-30	16.20	16.5	16.47	16.4	15.0	16.5	16.4	16.41	16.4	16.5	16.5	16.2	15.2	16.5	16.5

<sup>a</sup> Assignment corrections are suggested by color coding: values in blue, reddish brown, dark green, orange, pale green, tan, and pink denote shieldings that should probably be assigned to C12, C15, C16, C18, C19, C23, and C30, respectively.

The  $^{13}\text{C}$  NMR comparisons revealed many apparent errors in signal assignments. Structure elucidation is commonly based on NMR assignments, and misassignments can lead to a faulty interpretation of NOE experiments. Thus, simple assignment errors can lead to an incorrect structure. It should be noted that, despite some assignment problems, the reference data in [Table S3](#) are of relatively high quality. Many papers that were not cited have more serious deficiencies, such as erroneous structures. Two references cited in the table contain confusing or incorrect structures. Tanaka et al.<sup>30b</sup> shows a structure with 20*R*,24*S* instead of the apparently intended 20*S*,24*R* stereochemistry, which is evident from the references cited. Rouf et al.<sup>30c</sup> propose structures of epoxydammaranes with 6-membered rings (**14**). However, NMR data for the proposed 3 $\beta$ -acetyoxy-20,25-epoxydammarane-24 $\alpha$ -ol structure is almost identical with that for ocotillol (**9c**), and NMR data for the proposed 3 $\beta$ -acetyoxy-20,25-epoxydammarane-24 $\beta$ -ol structure matches closely to our data for **9b** (after correction of signal assignments).

### **Lack of Evidence for 20*R*-Epoxydammaranes in Nature**

As indicated in [Table S3](#), many 20*S* isomers with either 24*R* or 24*S* configuration have been characterized by NMR, and this reflects the prevalence of 20*S* epoxydammaranes in nature. NMR data for 20*R* isomers is scarce, and we could not locate  $^{13}\text{C}$  NMR data that corresponded to our 20*R*,24*S* isomer **9a**.

Many 20*R* isomers were obtained by acid hydrolysis of natural epoxydammaranes or dammarenediols, but this work was mainly done before 1980, when NMR characterization was either not done or limited to low-field proton shieldings. In 1995, Tanaka and coworkers<sup>31</sup> reported  $^{13}\text{C}$  NMR data for 12 $\beta$ -hydroxy derivatives of **9a** and its 20*R*,24*R* isomer, which were obtained by acidic treatment of dammarenediol I. Unfortunately, the effects of the 12 $\beta$ -hydroxyl on E-ring resonances prevented a useful comparison with our NMR data for **9a**.

The few reports<sup>32,33</sup> of the parent 20*R* epoxydammarane 3,25-diols in nature appeared mainly before 1980, when the 20*S* configuration of epoxydammaranes was not widely known. In a 1974 study of trevoagenins, the 20*R*,24*S* epoxydammarane structure of **9a** was reported under the name kapurol.<sup>32a,b</sup> The structural evidence was based on chemical transformation, and a mixture melting point with an authentic standard; no NMR data were given. Since kapurol was correlated with an ocotillone isomer (now known to have 20*S* configuration), we suspect that kapurol also has the 20*S* configuration. A subsequent study of trevoagenins by some of the same authors<sup>34</sup> did not mention the kapurol work; this study describes a crystal structure of a 20*R*,24*R* isomer, which the authors suggest may be of artefactual origin since the 20*R*,24*R* and 20*S*,24*R* isomers were equilibrated under their glycoside hydrolysis conditions (2 M HCl in ethanol). After a long hiatus without further mention of 20*R*,24*S* isomers (other than products obtained from chemical reactions<sup>31,35</sup>), Akihisa et al.<sup>33</sup> recently reported the 20*R*,24*S* kapurol structure but without NMR data. In an apparent reversal of citations, Fuchino et al.<sup>30e</sup> (describing only 20*S* epoxydammaranes) was referenced for the 20*R*,24*S* isomer and Gonzalez et al.<sup>32a</sup> for the 20*S*,24*R* isomer. Another historical account of ocotillol stereoisomers is given by Fu et al.<sup>30a</sup>

In summary, we cannot find any documented evidence for 20*R* epoxydammaranes in nature. Natural epoxydammaranes are associated with dammarenediols, whose cyclases (as yet uncharacterized) seem to make only 20*S* isomers. In addition to the DOS metabolites we describe, 20*R* epoxydammaranes may yet be uncovered in nature.

## Evidence for Traces of Diol **8** in a Published Lupanediol Spectrum

The isolation of diols **8**, **9a**, and **9b** from SMY8[JR1.16] cultures indicated that these diols have similar silica gel chromatographic behavior with lupane-3 $\beta$ ,20-diol. We suspected that traces of **8**, **9a**, and/or **9b** might be present in a  $^1\text{H}$  NMR spectrum of lupanediol that was published in Supporting Information of a paper on non-lupeol products of LUP1.<sup>15</sup> As shown in Figure S12A, the C26 and C27 methyl signals of **8** were found as trace components of this spectrum. Signals downfield of 3.3 ppm were not shown in the published spectrum, but the original spectrum was located and examined. Figure S12B shows the presence of signals for H17 and H24 in the lupanediol spectrum. The four resonances (H17, H24, H26, and H27) in the lupanediol spectrum showed identical chemical shifts ( $\pm 0.001$  ppm) and coupling constants ( $\pm 0.1$  Hz) with data in Table S2 for **8**. This result provides strong evidence that **8** was present in the LUP1 incubation from which lupanediol was isolated, and this further supports the hypothesis that oxacycles are formed in vivo from DOS during secondary metabolism.

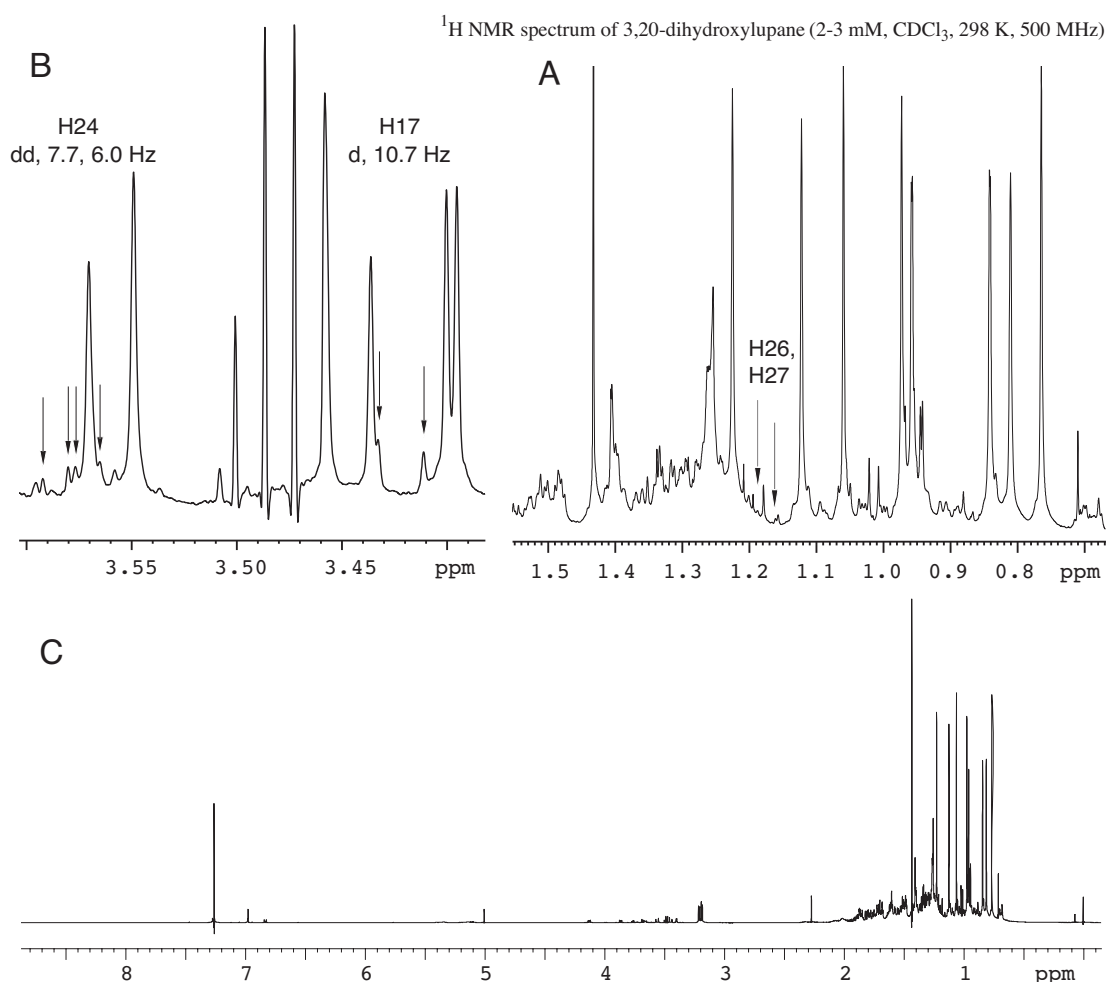


**Figure S12.** Detection of **8** in the published  $^1\text{H}$  NMR spectrum of lupane-3 $\beta$ ,20-diol. A. Methyl signals of **8** are indicated by arrows on the NMR spectrum in ref. 15. B. Downfield methine signals of **8** in an unpublished region of the same NMR spectrum. (The major signals are impurities, not lupanediol resonances.) C. Full spectrum of the lupanediol sample.

## Comparison of Observed and Predicted NMR Data for **8**

The structure of **8** was further confirmed by comparing the observed  $^1\text{H}$  and  $^{13}\text{C}$  NMR chemical shifts with shieldings predicted by quantum mechanical calculations using the GIAO method. First, B3P91/6-311G(2d,p)//B3LYP/6-31G\* shieldings were calculated for the full  $\text{C}_{30}\text{H}_{52}\text{O}_3$  structure. To compensate for conformational heterogeneity in the E ring, we calculated shieldings for 18 conformers of a  $\text{C}_{18}\text{H}_{32}\text{O}_2$  model structure comprising rings C, D, and E. Ring E was a boat or twist in half the conformers and a chair in the other half. Each set of 9 conformers comprised the 3 rotamers about the C25-O bond (hydroxyl rotamers) paired with the 3 rotamers about the C24-C25 bond (hydroxyl *anti* to C24, H24, or the ether oxygen). Boltzmann distributions of the 18 conformers were calculated from the mPW1PW91/6-311+G(2d,p)/B3LYP/6-31G\* energies and used to weight the shielding corrections from the 18 conformers. The shieldings calculated for the full  $\text{C}_{30}\text{H}_{52}\text{O}_3$  structure were then corrected based on the difference between the weighted  $\text{C}_{18}\text{H}_{32}\text{O}_2$  shieldings and the shieldings of  $\text{C}_{18}\text{H}_{32}\text{O}_2$  conformer corresponding to the full structure. Shielding corrections for the multiplicity of C3-O rotamers were made similarly using  $\text{C}_{15}\text{H}_{28}\text{O}$  model structures comprising rings A and B. The corrected shieldings were converted to chemical shifts using empirical adjustments derived from comparisons between thousands of predicted and calculated chemical shifts in  $\text{CDCl}_3$  in over 200 hydrophobic compounds.<sup>36</sup>

These predicted chemical shifts are compared with observed values in Table S4b. The rms deviations of 0.080 and 0.55 ppm for  $^1\text{H}$  and  $^{13}\text{C}$  data were in the range typically found for the set hydrophobic compounds, i.e. 0.03-0.08 ppm for  $^1\text{H}$  and 0.3-1.0 ppm for  $^{13}\text{C}$ . The good agreement between theory and experiment further confirms the structural assignment for **8**.

The rather high  $^1\text{H}$  rms value suffered from positive deviations for sterically hindered hydrogens at ring junctions; the same trend is observed for lupeol and other triterpenes.<sup>36</sup>

Coupling constants observed for ring E were also compared with predicted values (Table S4a). These predictions were based on an extended Karplus relationship implemented in PCMODEL (Serena Software, Inc.; Bloomington, IN). Couplings were calculated for each of the 18 B3LYP/6-31G\* conformers and weighted according to the mPW1PW91/6-311+G(2d,p) Boltzmann distribution, either from gas-phase or the polarized continuum model (PCM). The superior agreement for the gas-phase model relative to the PCM validates the use of gas-phase calculations for Table S4b and supports the structural assignment for **8**.

**Table S4a.** Comparison of observed and predicted vicinal coupling constants in ring E of **8**.<sup>a,b</sup>

	22 $\alpha$ -23 $\alpha$	22 $\alpha$ -23 $\beta$	22 $\beta$ -23 $\alpha$	22 $\beta$ -23 $\beta$	23 $\alpha$ -24	23 $\beta$ -24
observed	7.0	6.0	8.0	7.0	7.7	6.9
gas-phase	6.6	4.8	8.0	6.9	8.0	4.4
PCM	5.8	8.7	5.1	6.1	4.7	6.1

<sup>a</sup> Couplings are in Hz. Observed couplings are shown in reddish brown. Couplings between the C22 and C23 protons were all roughly 7 Hz (estimated accuracy, ca.  $\pm 0.5$  Hz). <sup>b</sup> The percentage of chair conformers differed markedly depending on the method used to calculate energies for the Boltzmann distribution: 34% for gas-phase; 65% for the PCM. Without diffuse functions, i.e. B3PW91/6-311G(2d,p), these values were 44% for gas-phase and 81% for the PCM.

**Table S4b.** Comparison of observed and predicted NMR chemical shifts for **8**.<sup>a</sup>

<sup>1</sup> H NMR chemical shift, $\delta_{\text{H}}$				<sup>13</sup> C NMR chemical shift, $\delta_{\text{C}}$			
	observed	predicted	difference		observed	predicted	difference
H1 $\alpha$	0.94	0.95	0.01	C1	38.8	38.9	0.2
H1 $\beta$	1.71	1.75	0.04	C2	27.4	28.2	0.8
H2 $\alpha$	1.63	1.61	-0.02	C3	79.0	78.2	-0.8
H2 $\beta$	1.57	1.53	-0.04	C4	38.9	38.6	-0.3
H3 $\alpha$	3.20	3.19	-0.01	C5	56.4	56.0	-0.4
H5 $\alpha$	0.69	0.77	0.08	C6	18.3	18.6	0.3
H6 $\alpha$	1.53	1.50	-0.03	C7	33.5	33.6	0.1
H6 $\beta$	1.36	1.40	0.04	C8	40.9	41.3	0.5
H7 $\alpha$	1.38	1.45	0.07	C9	50.6	51.4	0.9
H7 $\beta$	1.35	1.35	0.00	C10	37.2	37.1	-0.1
H9 $\alpha$	1.32	1.46	0.14	C11	20.5	21.1	0.6
H11 $\alpha$	1.54	1.54	0.00	C12	23.9	24.4	0.4
H11 $\beta$	1.29	1.25	-0.04	C13	37.4	38.0	0.6
H12 $\alpha$	1.10	1.10	0.00	C14	42.7	43.2	0.5
H12 $\beta$	1.94	2.00	0.06	C15	26.4	26.6	0.2
H13 $\beta$	1.70	1.94	0.24	C16	35.4	35.2	-0.2
H15 $\alpha$	0.94	0.92	-0.02	C17	76.2	75.9	-0.2
H15 $\beta$	1.66	1.71	0.06	C18	15.7	15.0	-0.7
H16 $\alpha$	1.33	1.29	-0.04	C19	16.2	17.4	1.2
H16 $\beta$	1.33	1.29	-0.04	C20	33.9	33.6	-0.2
H17 $\alpha$	3.42	3.67	0.25	C21	19.5	19.7	0.3
H18	1.02	1.04	0.02	C22	36.0	35.8	-0.2
H19	0.84	0.85	0.01	C23	19.7	19.8	0.1
H21	0.97	0.95	-0.02	C24	78.2	78.6	0.4
H22 $\alpha$	1.52	1.45	-0.08	C25	74.1	73.2	-0.9
H22 $\beta$	1.38	1.30	-0.09	C26	26.8	27.0	0.2
H23 $\alpha$	1.77	1.89	0.13	C27	25.8	25.1	-0.7
H23 $\beta$	1.73	1.66	-0.07	C28	28.0	27.3	-0.7
H24	3.58	3.66	0.08	C29	15.4	15.2	-0.1
H26	1.19	1.20	0.01	C30	15.1	14.3	-0.8
H27	1.16	1.14	-0.02				
H28	0.97	0.96	-0.01				
H29	0.77	0.70	-0.07				
H30	0.94	0.97	0.03				
average error			0.02				0.03
rms error <sup>b</sup>			0.080				0.53

<sup>a</sup> Predicted chemical shifts were calculated by the GIAO method at the B3PW91/6-311G(2d,p)//B3LYP/6-31G\* level and reflect the Boltzmann distribution of gas-phase mPW1PW91/6-311+G(2d,p) energies, as described in the text. Assignments of the C26/C27 and H26/H27 pairs may be reversed. <sup>b</sup> Root-mean-square (rms) error. The <sup>1</sup>H and <sup>13</sup>C rms errors for NMR calculations using the PCM for CHCl<sub>3</sub> were 0.096 and 0.79 with the PCM Boltzmann distribution and 0.088 and 0.55 with the gas-phase Boltzmann distribution.

## Molecular Modeling: Formation of Oxonium Ions **10-12** from **5**

Quantum mechanical calculations were done with Gaussian 03 (Linux and Windows versions B.02, B.05, C.01, or C.02). Geometry optimizations and vibrational frequency calculations were performed with B3LYP/6-31G\*. Single-point energies were calculated with mPW1PW91/6-311+G(2d,p) and HF/3-21G. All models were considered as closed-shell systems (restricted calculations) with the frozen-core approximation. Zero-point energies and thermal energies at the B3LYP/6-31G\* level were scaled by 0.96. Only the thermal energy contribution to enthalpies and free energies was scaled. All energy calculations were done with SCF=tight.

Conversion of the oxidodammarenyl cation **5** to oxonium ions **10-12** can proceed by a variety of pathways (Scheme S2). The mobile side chain can rotate until the epoxide can attack the *si* face of the C20 cation to form **12** (Path A) or attack the *re* face to form **11** (Path B). Alternatively, D-ring expansion can precede oxonium ion formation, via a transition state with an extended side chain (**15**, Path C) or partially folded side chain (**17**, Path D). Finally, **11** might undergo ring expansion to form **10** (Path F). We used quantum mechanical methods to study the energetics of these pathways, which is summarized in Table S5a.

We modeled Path A by a relaxed potential energy surface (PES) scan of the C20-C22-C23-C24 dihedral angle (Table S6). Rotation about this dihedral, together with other geometry changes, converts the extended side-chain conformer **5A** into oxonium ion **12**. The PES scan suggests two activation energies of about 3-4 kcal/mol, a typical range for single-bond rotations. This result indicates that there is a low-barrier pathway from **5** to **12**. Like Path A, Path B consists of single-bond rotations and should also involve small energy barriers in the gas-phase model. The active site cavity of triterpene synthases sterically restricts side-chain rotation. This could fully block Path A, Path B, or both pathways. LUP1 allows both pathways but favors Path B. The active site probably has little effect on the strong exothermicity of these pathways.

The PES scan does not correspond to a minimum energy path (MEP). However, determining transition states and following a MEP with intrinsic reaction coordinate (IRC) calculations would provide little additional mechanistic insight, considering the many possible rotational pathways from **5A** to **12** and the modifications to the PES by enzyme residues of the active site.

We studied the ring expansion of **11** to **10** (Path E) by a relaxed PES scan of the C16-C20 bond. The results (Table S7) suggested a large energy barrier caused by disruption of the oxonium ion structure. We optimized the transition state (**17**) and showed that this saddle point represents D-ring expansion as judged by IRC calculations (Table S8) and examination of normal mode displacements for the vibration corresponding to the imaginary frequency. The high activation enthalpy of 16 kcal/mol indicates that this pathway is inoperative in cyclases. Enzymatic effects are unlikely to alter this barrier significantly. Thus, **10** (the precursor of **8**) is produced only if D-ring expansion is faster than oxonium ion formation.

Because **10** cannot arise via path E, we considered D-ring expansion for an extended side chain (Path C). The secondary cation **16** and the preceding transition state **15** represent a dual barrier of 7-8 kcal/mol (depending on whether B3LYP or mPW1PW91 enthalpies or electron energies are calculated). Conversion of **16** to **10** should entail energy barriers of about 3-4 kcal/mol, similar to those in the PES scan of Table S6. In path D, the best route to **10**, the overall barrier can be as low as 4-5 kcal/mol due to modest epoxide stabilization of the transition state.

**Scheme S2.** Pathways for the formation of oxonium ions **10-12** from the oxidodammarenyl cation (**5**). Major pathways are shown in magenta. Boxed red numbers represent relative mPW1PW91/6-311+G(2d,p)//B3LYP/6-31G\* enthalpies.

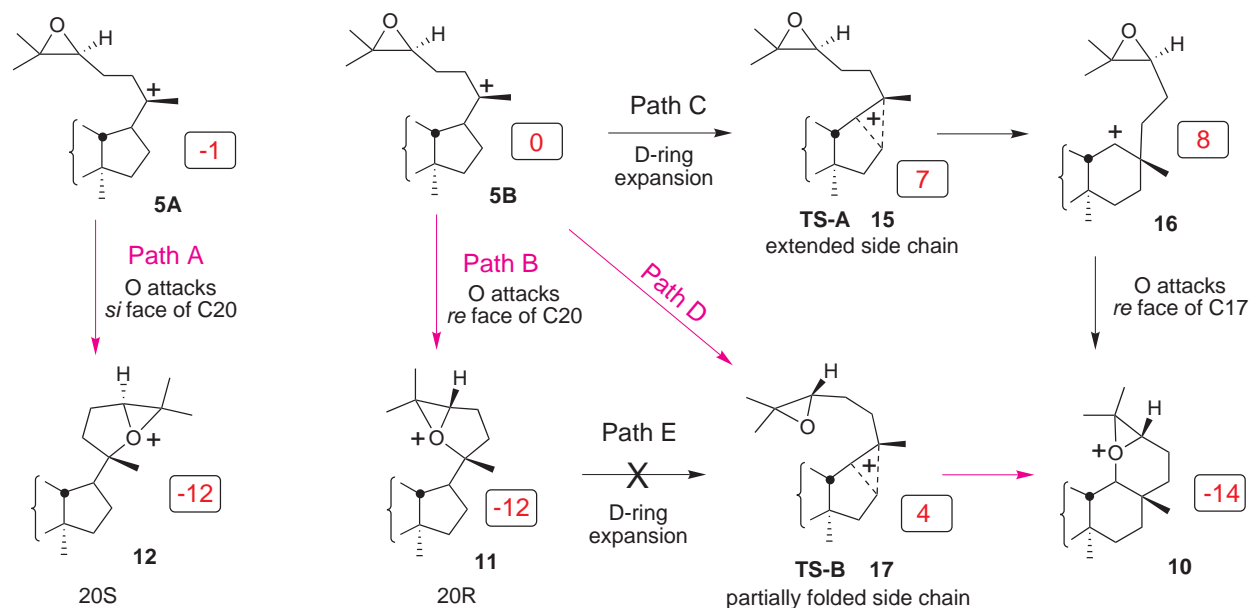


**Table S5a.** Relative energies (kcal/mol) of species involved in the formation of **10-12** from **5**.<sup>a</sup>

	20R extended SC <b>5B</b>	20R oxonium ion <b>11</b>	20R TS-B fused <b>17</b>	20R oxonium ion, fused <b>10</b>	20R TS-A <b>15</b>	20R D-ring expanded <b>16</b>	20S extended SC <b>5A</b>	20S oxonium ion <b>12</b>
$\Delta E$ , B3LYP/6-31G*	0.0	-13.6	4.5	-16.1	7.5	7.2	-1.8	-12.9
$\Delta E$ , HF/3-21G	0.0	-32.3	1.9	-36.8	8.4	7.9	-0.9	-31.1
$\Delta E$ , mPW1PW91	0.0	-13.8	4.2	-16.2	7.2	7.9	-1.4	-13.0
$\Delta H$ , mPW1PW91	0.0	-12.4	3.9	-14.4	6.7	7.7	-1.3	-11.9
$\Delta G$ , mPW1PW91	0.0	-8.2	6.0	-9.0	8.6	8.5	-1.8	-8.5
ZPE correction	0.0	2.2	0.2	2.9	0.0	-0.1	0.0	1.9
$\Delta H$ correction	0.0	1.3	-0.3	1.8	-0.5	-0.2	0.1	1.1
$\Delta G$ correction	0.0	5.6	1.8	7.1	1.4	0.7	-0.4	4.5
$\Delta S$ , cal/mol-K	0.0	-14.0	-7.1	-17.5	-6.7	-2.8	1.6	-11.4

<sup>a</sup> Geometries and thermochemical predictions are from B3LYP/6-31G\* calculations for C<sub>25</sub>H<sub>43</sub>O models (incorporating rings BCD). The 6-311+G(2d,p) basis set was used for mPW1PW91 single point energies; the enthalpy data shown in Scheme S2 above are shaded. Relative enthalpies ( $\Delta H$ ) and free energies ( $\Delta G$ ) were scaled only for thermal energy corrections. Notation: SC, side chain; fused, fused D-E ring system.



**Table S5b.** Dihedral angles and bond lengths for stationary points of Table S5a.<sup>a</sup>

	Dihedral angle (degrees)				Bond length (Å)								
	17-20-22-23	20-22-23-24	22-23-24-25	H-17-20-21	O-C20	O-C17	O-C24	O-C25	C13-C17	C16-C17	C16-C20	C17-C20	C20-C21
<b>5A</b>	-87.7	175.1	-130.9	-165.8	4.301	4.788	1.429	1.454	1.646	1.560	2.594	1.441	1.483
<b>5B</b>	103.5	177.6	-129.0	161.9	4.294	5.459	1.428	1.454	1.545	1.640	2.399	1.450	1.485
<b>10</b>	64.6	-32.2	-74.0	170.7	2.484	1.536	1.517	1.571	1.525	2.457	1.552	1.534	1.545
<b>11</b>	141.8	-22.7	-60.5	169.2	1.585	2.525	1.496	1.592	1.547	1.576	2.558	1.530	1.525
<b>12</b>	-84.1	-22.4	-61.1	173.1	1.590	2.419	1.492	1.594	1.560	1.567	2.617	1.540	1.517
<b>16</b>	72.9	-179.1	-133.9	149.4	4.478	5.433	1.435	1.450	1.424	2.328	1.637	1.456	1.544
<b>15</b>	84.0	179.1	132.2	161.2	4.433	5.467	1.435	1.451	1.460	2.144	1.759	1.420	1.528
<b>17</b>	82.9	-59.4	-111.2	162.6	3.375	2.997	1.445	1.455	1.476	2.049	1.822	1.409	1.520

<sup>a</sup> Values are from B3LYP/6-31G\* geometries. Compounds **15** and **17** correspond to **TS-A** and **TS-B**.

Path D may give a mixture of **10** and **11**, as the transition state **17** could collapse in different directions. Evaluating the relative importance of path C versus path D and the two fates of path D would probably require a molecular dynamics study.

We assert that the side chain of **5** adopts an extended conformation in the LUP1 active site. If the side chain of **5** were prefolded (e.g. for facile E-ring formation in lupeol synthesis), the epoxide would immediately attack the C20 cation to form an oxonium ion by a strongly exothermic process. A prefolded side-chain conformation could not generate **10** because oxonium ion formation cannot precede ring expansion, and constraints of cyclase active-site cavities indicate that prefolding is unlikely in the formation of **11** and **12**.

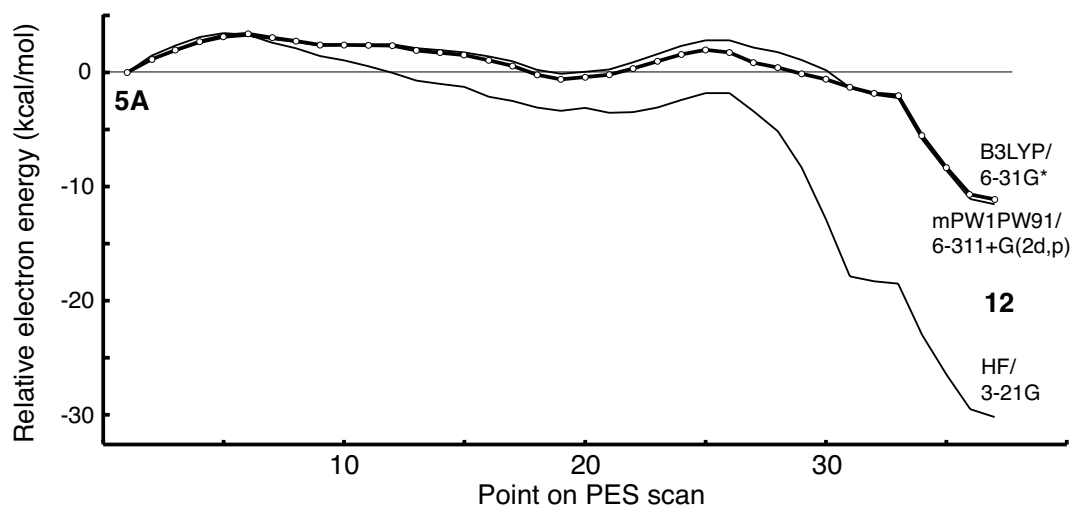
Ions **11** and **12** cannot both arise from prefolded conformers, as this would require an active site cavity so spacious that the substrate could not be preorganized for regio- and stereoselective cyclization. At most, prefolding might occur for **11**. However, because the substrate contracts toward C3 during cyclization, prefolding would require a large open space at the *re* face of C20 and extending distally. This open space would strongly favor formation of **11** over **12** from any extended side chain conformation. Considering that the ratio of **9a:9b** (i.e. **11:12**) is 2:1, most of **11** must also arise from an extended conformation. Given the 3:4:2 ratio of **8:9a:9b**, more than 75% of the side chain must be in an extended conformation. Instead of such a multiplicity of side-chain conformations, a single substrate (intermediate) conformation is more plausible in a cyclase active site. A single linear conformation permits the tail of the substrate to slide through the active site tunnel readily as contraction toward C3 occurs.

An extended side-chain conformation is also expected for the dammarenyl cation in OS cyclization by LUP1 because the 24,25-epoxide should not perturb enzyme-substrate interactions relative to those of the native olefin. Model calculations indicate the similarity of epoxide, ether, and olefin binding energies with representative residues of the active site.<sup>20</sup> DOS should be a useful probe for studying the side-chain conformation of dammarenyl cations in other cyclases.

Oxonium ion formation is effectively irreversible because the reverse activation energies for each pathway are 15-20 kcal/mol. Thus, oxonium ions represent energy sinks in the cascade of cationic intermediates. Unlike carbocations, the oxonium ions show little hyperconjugation. Hence, the usual processes of 1,2-shifts and ring expansion are unavailable to oxonium ions, which can only wait for quenching by water acting as a nucleophile or a base.



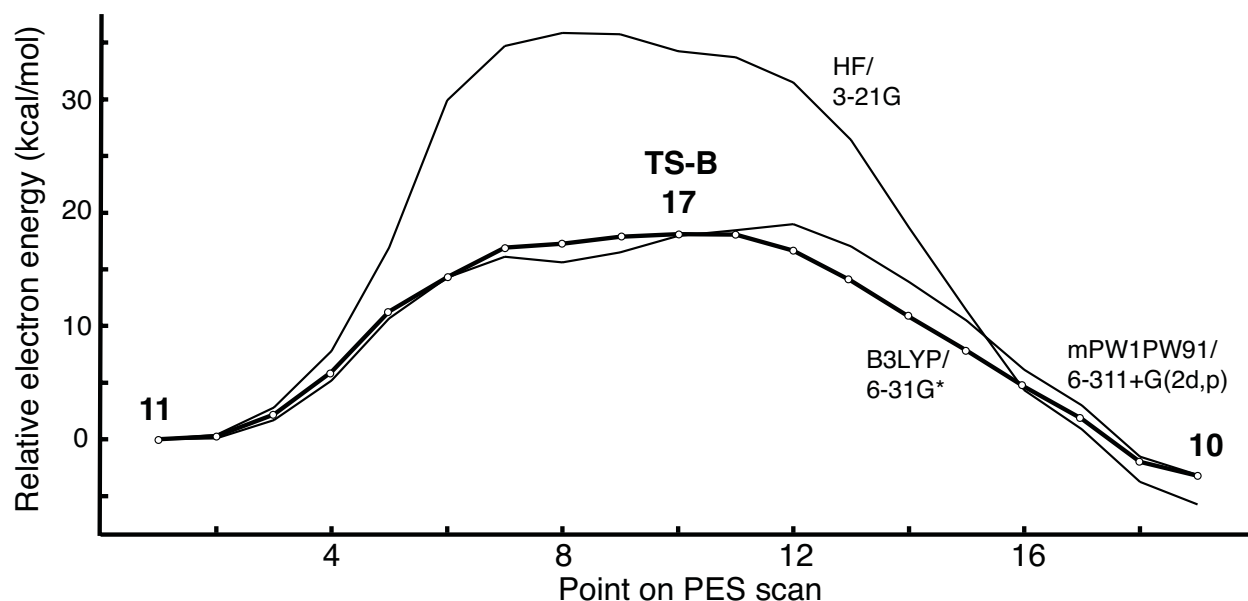
**Table S6.** Relative energies and geometries for a PES scan that models the conversion of **5A** to **12** by rotation of the C20-C22-C23-C24 dihedral angle.<sup>a</sup>



Point	Dihedral angle (degrees)				Bond length (Å)								
	17-20- 22-23	20-22- 23-24	22-23- 24-25	H-17- 20-21	O-C20	O-C17	O-C24	O-C25	C13-C17	C16-C17	C16-C20	C17-C20	C20-C21
1	-87.7	175.1	-130.9	-165.8	4.301	4.788	1.429	1.454	1.646	1.560	2.594	1.441	1.483
2	-84.9	<b>-160</b>	-128.1	-168.2	4.396	5.176	1.429	1.452	1.642	1.562	2.597	1.443	1.483
3	-86.1	<b>-150</b>	-127.4	-167.9	4.400	5.293	1.429	1.452	1.643	1.561	2.596	1.443	1.484
4	-87.7	<b>-140</b>	-125.3	-168.1	4.367	5.366	1.428	1.452	1.643	1.561	2.599	1.443	1.484
5	-89.1	<b>-130</b>	-122.4	-167.8	4.302	5.400	1.428	1.452	1.641	1.561	2.599	1.443	1.484
6	-92.1	<b>-120</b>	-119.5	-167.3	4.212	5.402	1.428	1.451	1.641	1.561	2.600	1.443	1.484
7	-95.0	<b>-110</b>	-114.4	-166.4	4.080	5.354	1.429	1.451	1.643	1.560	2.598	1.443	1.484
8	-96.1	<b>-105</b>	-111.2	-166.0	3.996	5.307	1.429	1.451	1.643	1.560	2.598	1.443	1.484
9	<b>-96</b>	<b>-100</b>	-106.7	-165.5	3.890	5.231	1.431	1.451	1.643	1.560	2.598	1.443	1.483
10	<b>-96</b>	<b>-100</b>	<b>-100</b>	-165.4	3.819	5.176	1.432	1.451	1.643	1.560	2.598	1.442	1.483
11	<b>-96</b>	<b>-100</b>	<b>-90</b>	-165.9	3.717	5.092	1.434	1.452	1.642	1.560	2.598	1.442	1.483
12	<b>-96</b>	<b>-100</b>	-78.8	-166.4	3.607	4.997	1.437	1.455	1.642	1.560	2.599	1.442	1.482
13	-96.8	<b>-95</b>	-81.9	-167.9	3.561	4.957	1.437	1.454	1.641	1.560	2.602	1.443	1.481
14	-95.4	<b>-92.5</b>	-84.6	-168.1	3.548	4.940	1.438	1.454	1.642	1.560	2.602	1.443	1.480
15	-94.0	<b>-90</b>	-87.7	-168.5	3.541	4.927	1.438	1.454	1.641	1.561	2.602	1.443	1.480
16	-89.5	<b>-85</b>	-90.5	-169.1	3.487	4.852	1.439	1.454	1.639	1.563	2.595	1.444	1.479
17	-88.0	<b>-80</b>	-97.3	-169.7	3.478	4.831	1.439	1.454	1.638	1.564	2.593	1.444	1.479
18	-84.1	<b>-70</b>	-106.7	-169.3	3.430	4.739	1.439	1.455	1.638	1.564	2.594	1.444	1.477
19	-81.6	<b>-60</b>	-112.5	-168.9	3.351	4.606	1.439	1.456	1.639	1.564	2.594	1.443	1.475
20	-80.0	<b>-50</b>	-119.3	-168.0	3.296	4.483	1.439	1.457	1.640	1.564	2.593	1.443	1.474
21	<b>-75</b>	<b>-50</b>	<b>-110</b>	-167.6	3.177	4.307	1.443	1.452	1.637	1.565	2.589	1.444	1.472
22	<b>-75</b>	<b>-50</b>	<b>-100</b>	-168.2	3.069	4.195	1.444	1.448	1.637	1.565	2.589	1.445	1.471
23	<b>-75</b>	<b>-50</b>	<b>-90</b>	-169.2	3.021	4.085	1.443	1.448	1.637	1.565	2.587	1.445	1.472
24	<b>-75</b>	<b>-50</b>	<b>-80</b>	-169.9	2.962	3.969	1.441	1.452	1.637	1.565	2.584	1.446	1.474
25	<b>-75</b>	<b>-50</b>	<b>-70</b>	-171.0	2.887	3.828	1.437	1.460	1.637	1.566	2.581	1.446	1.478
26	<b>-75</b>	<b>-50</b>	<b>-60</b>	-179.5	2.659	3.552	1.432	1.484	1.620	1.572	2.579	1.453	1.485
27	<b>-75</b>	<b>-50</b>	<b>-50</b>	177.8	2.457	3.305	1.439	1.500	1.607	1.572	2.581	1.461	1.488
28	<b>-75</b>	<b>-50</b>	<b>-45</b>	175.9	2.297	3.139	1.448	1.514	1.597	1.571	2.587	1.470	1.492
29	<b>-75</b>	<b>-50</b>	<b>-40</b>	174.0	<b>2.100</b>	2.949	1.465	1.536	1.585	1.569	2.593	1.484	1.499
30	<b>-75</b>	<b>-50</b>	<b>-40</b>	171.1	<b>1.900</b>	2.788	1.478	1.593	1.571	1.568	2.598	1.502	1.509
31	<b>-75</b>	<b>-50</b>	<b>-40</b>	168.0	1.680	2.616	1.503	1.676	1.559	1.567	2.604	1.524	1.521
32	<b>-75</b>	<b>-50</b>	<b>-35</b>	168.5	1.690	2.607	1.517	1.623	1.560	1.567	2.604	1.524	1.520
33	<b>-75</b>	<b>-50</b>	-30.4	168.8	1.683	2.585	1.534	1.586	1.560	1.567	2.606	1.525	1.519
34	<b>-75</b>	<b>-45</b>	-37.3	170.3	1.648	2.528	1.523	1.594	1.560	1.567	2.607	1.529	1.519
35	-71.5	<b>-40</b>	-45.9	173.7	1.641	2.467	1.507	1.591	1.561	1.568	2.609	1.531	1.515
36	-78.4	<b>-30</b>	-54.9	172.5	1.603	2.435	1.497	1.596	1.560	1.567	2.615	1.537	1.516
37	-84.1	-22.4	-61.1	173.1	1.590	2.419	1.492	1.594	1.560	1.567	2.617	1.540	1.517

<sup>a</sup> Boldface type denotes dihedral angles or bond lengths that were fixed during geometry optimization. Point 1 and 37, **5A** and **12**.

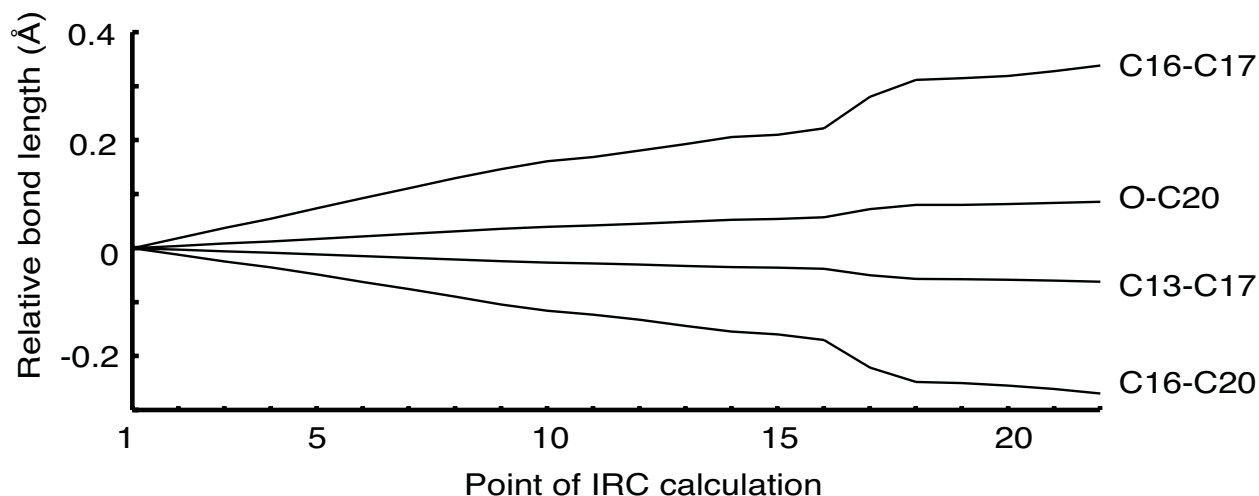
**Table S7.** D-ring expansion of oxonium ion **11**. Relative energies and geometries for a PES scan that models the conversion of **11** to **10** by decreasing the C16-C20 bond length.<sup>a</sup>



Point	Dihedral angle (degrees)				Bond length (Å)								
	17-20- 22-23	20-22- 23-24	22-23- 24-25	H-17- 20-21	O-C20	O-C17	O-C24	O-C25	C13-C17	C16-C17	C16-C20	C17-C20	C20-C21
1	141.8	-22.7	-60.5	169.2	1.585	2.525	1.496	1.592	1.547	1.576	2.558	1.530	1.525
2	141.5	-22.8	-60.3	169.2	1.596	2.525	1.495	1.589	1.546	1.563	<b>2.500</b>	1.517	1.525
3	140.7	-23.0	-60.0	169.0	1.623	2.524	1.491	1.580	1.543	1.545	<b>2.400</b>	1.496	1.526
4	139.4	-23.3	-59.7	168.8	1.673	2.539	1.485	1.565	1.541	1.535	<b>2.300</b>	1.477	1.527
5	137.4	-25.2	-59.4	167.8	1.822	2.624	1.472	1.534	1.538	1.542	<b>2.200</b>	1.455	1.522
6	134.0	-42.4	-62.9	163.9	2.502	3.040	1.446	1.471	1.531	1.627	<b>2.100</b>	1.423	1.496
7	129.5	-45.1	-67.2	163.1	2.638	3.052	1.444	1.465	1.525	1.661	<b>2.000</b>	1.411	1.499
8	87.9	-61.7	-112.5	163.1	3.403	3.113	1.441	1.456	1.513	1.772	<b>1.900</b>	1.404	1.507
9	85.6	-61.3	-111.8	163.6	3.396	3.075	1.442	1.455	1.501	1.859	<b>1.860</b>	1.402	1.512
10	82.9	-59.4	-111.2	162.6	3.375	2.997	1.445	1.455	1.476	2.049	1.822	1.409	1.520
11	84.9	-55.4	-110.7	161.1	3.312	2.905	1.447	1.455	1.466	2.129	<b>1.800</b>	1.416	1.524
12	92.3	-49.6	-72.4	159.0	2.966	<b>2.600</b>	1.451	1.465	1.447	2.285	<b>1.750</b>	1.436	1.532
13	83.9	-43.9	69.2	161.2	2.821	<b>2.300</b>	1.460	1.477	1.454	2.352	<b>1.750</b>	1.448	1.534
14	76.2	-38.9	-69.7	165.2	2.680	<b>2.000</b>	1.476	1.500	1.475	2.426	<b>1.750</b>	1.469	1.535
15	71.4	-35.7	-71.1	168.4	2.587	<b>1.800</b>	1.493	1.524	1.497	2.485	<b>1.750</b>	1.489	1.535
16	66.0	-31.9	-74.3	172.6	2.471	1.557	1.515	1.584	1.525	2.559	<b>1.750</b>	1.518	1.535
17	65.7	-32.0	-74.2	172.1	2.473	1.551	1.516	1.566	1.525	2.534	<b>1.700</b>	1.522	1.537
18	64.9	-32.1	-74.1	171.1	2.480	1.541	1.517	1.569	1.525	2.482	<b>1.600</b>	1.530	1.542
19	64.6	-32.2	-74.0	170.7	2.484	1.536	1.517	1.571	1.525	2.457	1.552	1.534	1.545

<sup>a</sup> Boldface type denotes bond lengths that were held fixed during geometry optimization. Points 1, 10, and 19 correspond to **11**, **17**, and **10**. The shaded values represent the transition state (**17**). In the PES plots of this table and Table S6, the thick curve with individual points corresponds to B3LYP/6-31G\* energies. Both curves and data in Table S5a suggest that HF/3-21G energies strongly overestimate the energetics of oxonium ion formation.

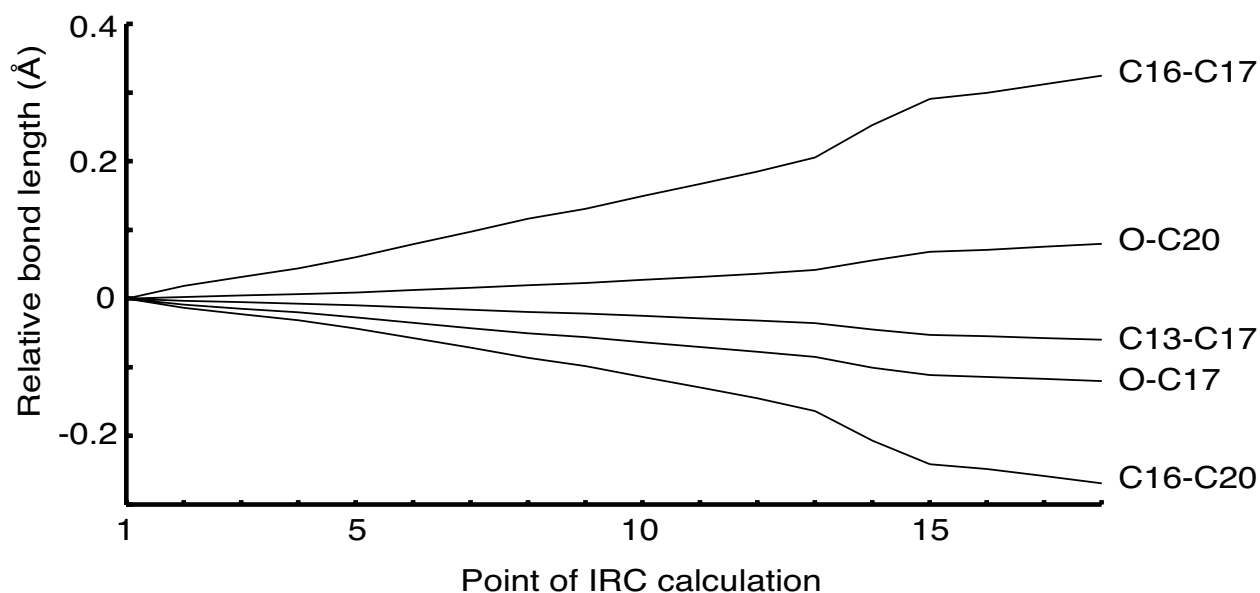
**Table S8a.** Bond lengths (Å) and relative energies (kcal/mol) for points of an IRC calculation related to transition state A (**15**).<sup>a-c</sup>



Point	O-C20	O-C17	O-C24	O-C25	C13-C17	C16-C17	C16-C20	C17-C20	ΔE	Coord.
1	4.360	5.445	1.434	1.453	1.510	1.863	1.981	1.404	-1.90	-2.72
2	4.364	5.446	1.434	1.453	1.507	1.882	1.969	1.403	-1.68	-2.52
3	4.369	5.448	1.434	1.453	1.505	1.901	1.956	1.402	-1.46	-2.33
4	4.373	5.449	1.434	1.453	1.502	1.918	1.945	1.401	-1.28	-2.14
5	4.378	5.451	1.434	1.453	1.499	1.938	1.932	1.401	-1.08	-1.95
6	4.382	5.453	1.434	1.453	1.496	1.956	1.918	1.401	-0.90	-1.75
7	4.387	5.454	1.434	1.452	1.493	1.974	1.905	1.402	-0.74	-1.56
8	4.391	5.456	1.435	1.452	1.489	1.993	1.891	1.402	-0.58	-1.36
9	4.396	5.457	1.435	1.452	1.486	2.010	1.876	1.403	-0.45	-1.17
10	4.400	5.459	1.435	1.452	1.484	2.025	1.864	1.405	-0.36	-1.01
11	4.402	5.460	1.435	1.452	1.482	2.032	1.858	1.404	-0.31	-0.89
12	4.406	5.461	1.435	1.452	1.480	2.044	1.848	1.406	-0.25	-0.74
13	4.409	5.462	1.435	1.452	1.478	2.056	1.836	1.407	-0.19	-0.58
14	4.413	5.463	1.435	1.452	1.475	2.069	1.826	1.409	-0.13	-0.43
15	4.414	5.463	1.435	1.452	1.474	2.074	1.821	1.409	-0.12	-0.34
16	4.418	5.464	1.435	1.451	1.472	2.086	1.810	1.411	-0.08	-0.19
17	4.433	5.467	1.435	1.451	1.460	2.144	1.759	1.420	0.00	0.00
18	4.440	5.467	1.435	1.451	1.453	2.175	1.733	1.425	-0.01	0.19
19	4.441	5.467	1.435	1.451	1.453	2.178	1.731	1.426	-0.02	0.28
20	4.442	5.467	1.435	1.451	1.452	2.183	1.726	1.427	-0.03	0.36
21	4.444	5.467	1.435	1.451	1.450	2.191	1.719	1.429	-0.04	0.50
22	4.446	5.467	1.435	1.451	1.448	2.202	1.711	1.431	-0.06	0.67

<sup>a</sup> Geometries and energies are from B3LYP/6-31G\* calculations. The shaded values represent the transition state. Coord., reaction coordinate. <sup>b</sup> The accompanying graph shows the relative changes in bond length as the reaction progresses. The data represent a small portion of the reaction path for the conversion of **5B** to **16** (D-ring expansion with an extended side chain).

**Table S8b.** Bond lengths (Å) and relative energies (kcal/mol) for points of an IRC calculation related to transition state B (**17**).<sup>a-c</sup>



Point	O-C20	O-C17	O-C24	O-C25	C13-C17	C16-C17	C16-C20	C17-C20	$\Delta E$	Coord.
1	3.333	3.082	1.442	1.455	1.513	1.844	1.985	1.405	-1.09	-2.23
2	3.336	3.073	1.442	1.455	1.510	1.862	1.972	1.404	-0.93	-2.04
3	3.338	3.067	1.442	1.455	1.508	1.875	1.963	1.403	-0.82	-1.88
4	3.340	3.062	1.442	1.455	1.506	1.888	1.954	1.403	-0.72	-1.73
5	3.343	3.054	1.442	1.455	1.504	1.904	1.942	1.402	-0.59	-1.55
6	3.346	3.046	1.443	1.455	1.500	1.923	1.928	1.402	-0.46	-1.35
7	3.349	3.039	1.443	1.455	1.497	1.941	1.914	1.402	-0.34	-1.16
8	3.353	3.031	1.443	1.455	1.494	1.960	1.899	1.403	-0.24	-0.96
9	3.356	3.025	1.444	1.455	1.492	1.974	1.887	1.403	-0.17	-0.79
10	3.361	3.018	1.444	1.455	1.488	1.993	1.871	1.404	-0.10	-0.59
11	3.365	3.011	1.444	1.455	1.485	2.011	1.856	1.406	-0.04	-0.39
12	3.370	3.004	1.444	1.455	1.482	2.029	1.840	1.407	-0.01	-0.19
13	3.375	2.997	1.445	1.455	1.478	2.049	1.822	1.409	0.00	0.00
14	3.389	2.981	1.446	1.454	1.468	2.096	1.778	1.416	-0.07	0.20
15	3.402	2.970	1.446	1.454	1.460	2.134	1.744	1.423	-0.20	0.37
16	3.405	2.968	1.446	1.454	1.459	2.144	1.737	1.424	-0.24	0.50
17	3.409	2.965	1.447	1.453	1.456	2.156	1.727	1.427	-0.30	0.68
18	3.414	2.962	1.447	1.453	1.454	2.169	1.716	1.430	-0.36	0.86

<sup>a</sup> Geometries and energies are from B3LYP/6-31G\* calculations. The shaded values represent the transition state. Coord., reaction coordinate. <sup>b</sup> The accompanying graph shows the relative changes in bond length as the reaction progresses. The points represent a small portion of the reaction path for D-ring expansion en route to **10**. The substantial changes in C16-C17 and C16-C20 bond length correspond to modest energy changes. Differences in transition-state geometries for similar ring expansions (other data herein and in ref. 10) are sensitive to DFT method and basis set and are probably not meaningful. The O-C20 and O-C17 bond lengths show little change; this path might begin from either **5B** or **11**.

## Lack of C17 Epimerization in Oxacycle Formation from DOS

Our NMR structure determinations indicated that no epimerization occurs at C17 during DOS cyclization by LUP1. This outcome was expected because LUP1 cyclizes OS to lupeol without any epimerization at C17. However, C17 epimerization does evidently occur in the biosynthesis of certain pentacyclic triterpenes, such as nepehinol.<sup>37</sup> A cyclase active site that permits or favors C17 epimerization in OS cyclization might produce the C17 epimer of **8** from DOS. The C17 epimerization entails a moderately higher activation energy than usual E-ring formation, and the active site of LUP1 apparently prevents any formation of byproducts via this alternative pathway.

Whereas some cyclases might allow C17 epimerization en route to epoxybaccharanes, no such epimerization is expected for epoxydammaranes, as this would require the side chain of the dammarenyl cation to rotate 180°. Experiment and theory indicate that such a large rotation in the cyclase active site is highly unlikely.<sup>20</sup> Any epoxydammaranes with a 17 $\alpha$  side chain presumably originate from cyclases that access the 17 $\alpha$ -dammarenyl cation, as described below (Predicted DOS Metabolites from Other Cyclases).

## Formation of Unsaturated Oxacyclic Triterpenes by LUP1

### *Evidence for Unsaturated Oxacyclic Triterpenes from LUP1 and in Nature*

Most triterpene synthases generate olefinic products from OS. Olefins are formed when a carbocationic intermediate undergoes deprotonation. Alternatively, carbocations can be quenched by water to form diols. Diol formation is usually negligible but represents roughly 40% of the LUP1 products from OS. Although we isolated only diols from DOS cyclization with LUP1, olefinic products would also be anticipated.

We examined early fractions of the LUP1 incubation for signs of olefinic analogs **18**, **19a**, and **19b** (Figure S13). The <sup>1</sup>H NMR spectrum of the ergosterol-containing fraction showed minor signals characteristic for terminal olefins, notably broad singlets at 4.65, 4.76 (weak), 4.83, 4.87, and 5.01 ppm. This fraction also contained the H3 $\alpha$  doublet-doublet (a marker for triterpenes) and several methyl singlets at 0.75-0.8 ppm (expected shielding for 4 $\beta$ -methyl protons) and 0.9-1.2 ppm. Some fractions eluting after ergosterol contained similar signals. The triterpene components in these fractions totaled roughly 20% of the amount of oxacyclic diols (**8**, **9a**, and **9b**). The spectral and chromatographic properties, together with mechanistic expectations, provide substantial indirect evidence for unsaturated products in DOS metabolism.

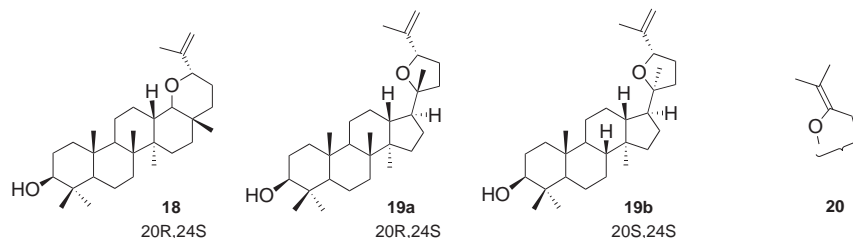


**Figure S13.** Possible unsaturated analogs of **8**, **9a**, and **9b** that may be formed from DOS as minor products accompanying oxacyclic triterpene diols. Labile internal olefins like **20** are less likely as enzymatic products.

Unsaturated epoxydammaranes or epoxybaccharanes have rarely been reported. However, Aalbersberg and Singh isolated several unsaturated epoxydammaranes from the fruits of *Dysoxylum richii*, a large tree endemic to Fiji.<sup>38</sup> The unsaturated epoxydammaranes, which included **19b**, were characterized by <sup>1</sup>H and <sup>13</sup>C NMR. Olefinic singlets reported for **19b** ( $\delta$  4.77 and 5.00) matched minor olefinic signals observed in our LUP1 products. The authors did not report any 20*R* isomers, which would correspond to the major olefinic DOS products anticipated from LUP1.

This isolation of epoxydammarane diols together with smaller amounts of olefinic epoxydammaranes<sup>38</sup> suggests an origin from DOS cyclization. The alternative pathway, involving post-cyclization oxidation by P450s and other oxidases, seems less likely to produce olefinic epoxydammarane byproducts. We suggest that DOS cyclization is probably responsible for epoxydammarane synthesis in organisms that also produce olefinic epoxydammaranes and that olefinic epoxydammaranes might find use as reporter molecules for the DOS pathway. Post-cyclization oxidation would be likely when olefinic epoxydammaranes are not detected.

Olefinic epoxydammaranes have rarely been reported in nature. To the extent that literature reports can be relied on to estimate the distribution of natural products, it might be concluded that epoxydammaranes are less commonly derived from DOS than OS (with later oxidation).

It is noteworthy that olefinic epoxydammaranes (from *Dysoxylum richii*)<sup>38</sup> and epoxybaccharane derivatives of **8** (from *Aglaia foveolata*)<sup>22</sup> were both isolated from fruits of trees in the Meliaceae family. Unlike epoxydammaranes **9a** and **9b**, epoxybaccharanes like **8** are almost certainly derived from DOS cyclization rather than from post-cyclization oxidation by P450s. This markedly strengthens our hypothesis that some saponins are derived from DOS.

### ***Molecular Modeling of Olefin Formation in Epoxydammarane Synthesis from DOS***

We attempted to understand why the proportion of LUP1 diol products is much higher in DOS cyclization (80%) than OS cyclization (40%). We considered that, relative to carbocations, oxonium ion intermediates might disfavor elimination to olefins. Indeed, certain C-H bonds of terminal methyls adjacent to carbocations are elongated by hyperconjugation, whereas the corresponding C-H bonds in oxonium ions **10-12** showed little elongation, at least in the absence of a nearby base. However, a study of oxonium ion deprotonation at a terminal methyl by a base comprising water-histidine-water (Figure S14) indicated almost no energy barrier. Moreover, bringing water into proximity of the methyl resulted in C-H bond elongation and modest lengthening of the C25-O bond (Table S9). As the reaction progressed, the C25-O bond lengthened rapidly, converting the oxonium ion into a C25 carbocation prior to proton transfer.

This reaction was studied as a series of PES scans, in which B3LYP/6-31G\* geometry optimizations were done with the O-H bond length fixed at 1.1, 1.2, 1.3, 1.4, 1.5, 1.6, and 1.7 Å. This bond length optimized to 0.98 and 2.1 Å at the beginning and end of the deprotonation process. Some geometries required freezing certain parameters to prevent unwanted attractions, such as hydrogen bonding of water to oxygen of the oxonium ion.

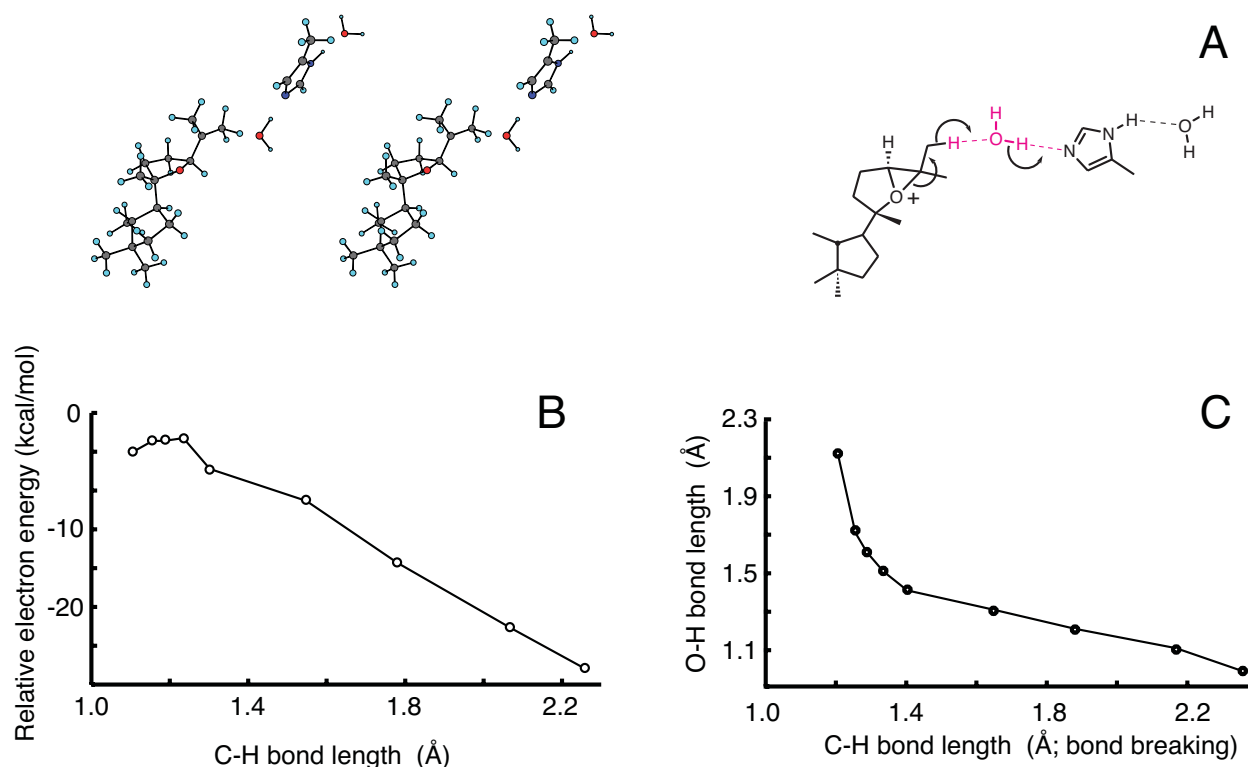


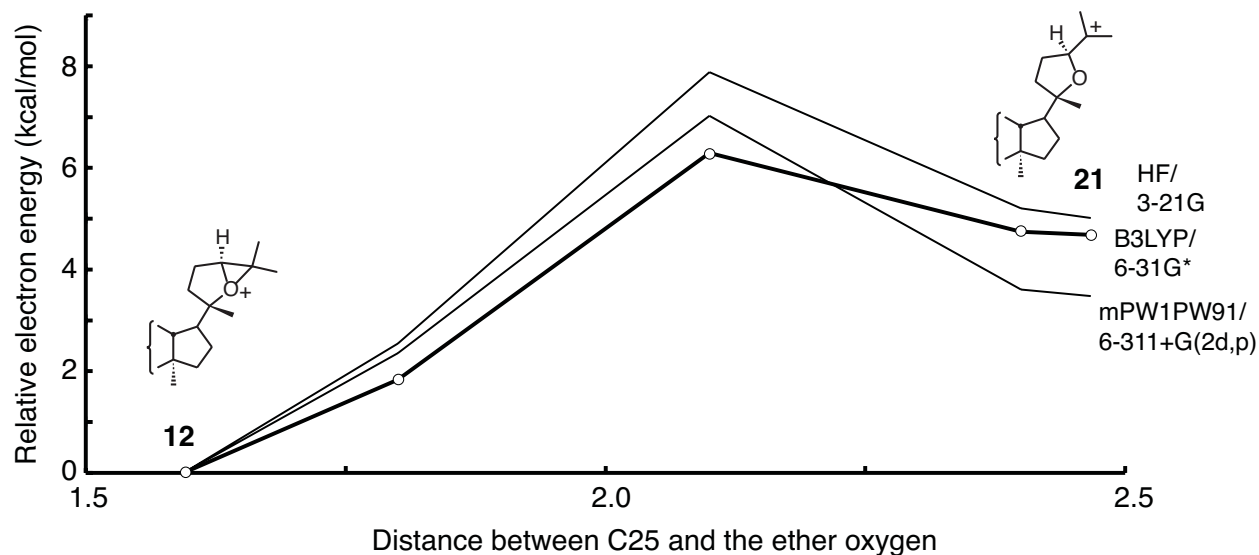
**Figure S14.** Olefin formation by deprotonation of the oxonium ion at a terminal methyl. As shown in the stereoview (A), the base is a water molecule hydrogen-bonded to histidine, which is stabilized by a distal water molecule. B3LYP/6-31G\*/B3LYP/6-31G\* calculations predict the energy barrier to be negligible (B). Panel C illustrates the formation of the O-H bond as the C-H bond is broken. The stereoview shows the structure with a 1.4 Å O-H bond distance.

**Table S9.** Geometries and relative energies for the PES scan of Figure S14.<sup>a</sup>

Point	C26-H	H-O	O-H	H-N	C25-O	C24-O	C20-O	C24-C25	C25-C26	C26-H	B3LYP	HF
<b>12</b>	<b>1.097</b>				<b>1.594</b>	<b>1.492</b>	<b>1.590</b>	<b>1.475</b>	<b>1.507</b>	<b>1.093</b>		
1	1.106	2.099	1.002	1.769	1.712	1.483	1.541	1.475	1.489	1.088	0.0	0.0
2	1.155	<b>1.700</b>	1.014	1.702	2.005	1.454	1.503	1.492	1.446	1.088	1.4	2.3
3	1.187	<b>1.600</b>	1.012	1.714	2.119	1.445	1.492	1.502	1.427	1.089	1.4	2.8
4	1.234	<b>1.500</b>	1.028	1.638	2.194	1.440	1.485	1.511	1.408	1.089	1.8	3.0
5	1.302	<b>1.400</b>	1.068	1.517	2.405	1.409	1.472	1.500	1.394	1.092	-2.2	-1.5
6	1.548	<b>1.300</b>	1.494	1.095	2.420	1.422	1.468	1.514	1.363	1.089	-6.3	-9.6
7	1.780	<b>1.200</b>	1.577	1.069	2.412	1.427	1.466	1.517	1.352	1.088	-14.3	-21.4
8	2.067	<b>1.100</b>	1.631	1.057	2.418	1.435	1.466	1.516	1.345	1.087	-22.7	-33.0
9	2.257	0.981	1.664	1.050	2.417	1.437	1.464	1.517	1.343	1.087	-27.9	-40.5

<sup>a</sup> Bond lengths (Å) for proton transfer (first 4 values), oxonium ion geometry changes (next 3 values), and olefin formation (last 3 values). Relative B3LYP/6-31G\* and HF/3-21G\* energies are given at right. Boldface type denotes bond lengths that were held fixed during geometry optimization. Relevant bond lengths of the 20S oxonium ion **12** are given in magenta for comparison.

**Table S10.** Relative energies and geometries for a PES scan that models the conversion of oxonium ion **12** to carbocation **21** by increasing the C25-O bond length.<sup>a</sup>



	Dihedral angle (degrees)				Bond length (Å)								
	17-20-22-23	20-22-23-24	22-23-24-25	H-17-20-21	O-C20	O-C17	O-C24	O-C25	C13-C17	C16-C17	C16-C20	C17-C20	C20-C21
1	-84.1	-22.4	-61.1	173.1	1.590	2.419	1.492	1.594	1.560	1.567	2.617	1.540	1.517
2	-85.6	-23.5	-70.5	171.5	1.549	2.410	1.475	<b>1.800</b>	1.558	1.566	2.619	1.545	1.520
3	-85.7	-27.0	-83.5	170.2	1.509	2.408	1.455	<b>2.100</b>	1.556	1.565	2.618	1.552	1.523
4	-81.2	-17.8	-128.2	168.1	1.487	2.467	1.385	<b>2.400</b>	1.552	1.564	2.603	1.550	1.523
5	-81.4	-17.5	-127.7	168.1	1.487	2.467	1.381	2.467	1.552	1.564	2.603	1.550	1.523

<sup>a</sup> Boldface type denotes bond lengths that were held fixed during geometry optimization.

We also studied the conversion of oxonium ion **12** to carbocation **21** by a relaxed PES scan in which the C25-O bond length was increased. As shown in Table S10, the oxonium ion was predicted to be about 5 kcal/mol more stable than the carbocation in the gas-phase model. However, nearby enzyme residues and ordered water molecules could increase the carbocation character of the intermediate, as was observed above when a polarized water molecule was in proximity to a terminal methyl (Table S9).

In summary, molecular modeling did not indicate any energy barrier to deprotonation via an ordered water molecule, whose proximity to a terminal methyl led to some C-H hyperconjugation and C25 carbocation character. The prevalence of LUP1 diol products from DOS might be explained by the presence of an ordered water molecule that cannot readily transfer a proton to a basic residue. It is not clear which factors predominate in determining the diol-olefin ratio: the reactivity of oxonium ions versus carbocations; the precise positioning of ordered water near C25; or the accessibility of a basic residue.

## Possible Factors Affecting the Availability of DOS to LUP1

Our LUP1 cultures of SMY8[JR1.16] produced oxacyclic triterpenes at remarkably high levels. Relative to lupeol and lupanediol, **8**, **9a**, and **9b** were present at levels of about 7%, 2%,



and 2%, respectively. Wong et al.<sup>39</sup> reported similar ratios for cultured human macrophages (THP-1; almost 1% 24,25-epoxycholesterol relative to cholesterol for de novo synthesis), and they observed much higher ratios in the presence of a cyclase inhibitor.<sup>40</sup> However, the ratio of these sterols extracted from blood or tissue is markedly lower (levels of roughly 10-50 ng/g for the epoxysterol versus about 1 mg/g for cholesterol).<sup>41</sup> NMR analysis of wild-type yeast<sup>42</sup> (JBY575) similarly indicated at most low levels of 24,25-oxidolanosterol and other 24,25-epoxysterols ( $\leq 0.1\%$  of ergosterol). As with the human cells, treatment of yeast with a cyclase inhibitor (Ro48-8071) resulted in elevated levels of DOS and a substance believed to be 24,25-epoxycholesta-5,7,22-trien-3 $\beta$ -ol.<sup>5</sup>

We initially anticipated low levels of DOS metabolites in the SMY8[JR1.16] system, which should be strongly biased against DOS cyclization. This system should have normal squalene epoxidase (Erg1p) levels<sup>43</sup> but expresses lupeol synthase from the strongest known yeast promoter. Because lupeol synthase can consume OS prior to further oxidation, the high cyclase levels, together with presumably normal epoxidase activity,<sup>43</sup> should minimize oxacycle formation. To rationalize the unexpectedly high levels of epoxydammaranes observed in the in vivo experiment, we considered the subcellular organization of yeast sterol synthesis.

The later enzymes of sterol synthesis, beginning with Erg1p, are variously distributed between the endoplasmic reticulum (ER) and lipid particles (LP). Lipid particles contain lanosterol synthase (Erg7p), sterol 24-methyl transferase (Erg6p), Erg1p, and Erg26p.<sup>45</sup> All the later sterol synthesis enzymes (except perhaps Erg7p) are found in the ER, where they appear to be tethered, probably in large complexes that function as a single catalytic unit.<sup>46</sup> Current evidence suggests that Erg28p and perhaps other proteins are involved in organizing these biosynthetic complexes of the ER.<sup>46</sup>

If the enzymes of sterol synthesis in the ER are well organized, the product of one enzyme will be poised to enter the active site of a suitable following enzyme, and intermediates will rarely drift off from the biosynthetic complex. This picture is consistent with the known path-multiplicity of sterol synthesis<sup>47</sup> and with the low levels of sterol intermediates observed in wild-type yeast.<sup>42</sup> Even lower concentrations of intermediates are found in mammals,<sup>48</sup> suggesting that enzyme complexes became better organized as mammals evolved, perhaps to avoid the adverse effects of aberrant hormones derived from sterol intermediates, as occurs in Smith-Lemli-Opitz syndrome.<sup>49</sup> If the cluster of sterol biosynthesis enzymes in the yeast ER includes Erg1p and Erg7p (this is not certain<sup>50</sup>), then very little DOS should accumulate. Such low accumulation of DOS would be consistent with the lack of 24,25-epoxysterols in JBY575.

LP are thought to be formed by budding from the ER.<sup>45b,51</sup> Along with neutral lipids, proteins selectively depart from the ER, including Erg1p, Erg7p, and Erg6p. Notably, these enzymes lack transmembrane spanning domains.<sup>45c</sup> LUP1 would presumably not be recognized as sterol biosynthesis enzyme by Erg28p. Excluded from the proximity of Erg1p in the ER, LUP1 would have little available substrate. We suggest that LUP1, like Erg7p, may join the neutral lipids as they bud off to form an LP. It is relevant that cycloartenol synthase from *A. thaliana* also segregates to LP, where it was found as the major protein component.<sup>45c</sup>

In our in vivo experiments with SMY8[JR1.16], Erg7p is absent and could not cyclize OS. In such an unorganized environment, the OS produced by Erg1p could return to be epoxidized a second time. The resulting DOS would be available to LUP1 in the LP for cyclization to

oxacyclic triterpenes. Despite some uncertainty,<sup>52</sup> this appears to be the currently most plausible explanation for the substantial amounts of oxacyclic triterpenes in our in vivo experiments.

Sterol biosynthesis enzymes also appear to be tethered in plants and animals, among which Erg28 is broadly conserved.<sup>46</sup> Triterpenoid synthesis probably also occurs in a large complex including a cyclase and several oxidases. In the conventional biosynthetic pathway to saponin aglycones,<sup>53</sup> several enzymes would be required to convert the 24,25-olefin of dammarenediol to an epoxydammarane. Evolution of the catalytic enzymes and chaperones to form the large enzyme complexes appears improbable because most biosynthetic intermediates would lack biological activity. DOS metabolism to epoxydammaranes requires no organization of enzymes and can produce aglycones of saponins with biological activity. Such a simple route to epoxydammaranes could be later refined as P450 enzymes (perhaps oxidizing at C6 or C12) in the crude complex of saponin biosynthetic enzymes were recruited to perform oxidations at C24 and C25. Some vestigial DOS cyclization systems may still exist, as suggested by the isolation of olefinic epoxydammaranes from the fruits of *Dysoxylum richii*.<sup>38</sup>

## Predicted DOS Metabolites from Other Cyclases

DOS metabolism is predicted to vary according to the type of cyclase:

1. Cyclases that generate tetracycles (e.g. lanosterol, euphol, tirucallol, dammarenediol). The distal epoxide remains intact during cyclization, and no oxacycles are formed. Apparently, these cyclases block side-chain folding sufficiently that rearrangement/deprotonation/quenching occurs first. However, if this block is not absolute, some epoxydammarane product would form. In dammarenediol synthesis, incomplete blockage of side-chain folding could lead to reaction between the 20-hydroxyl and the 24,25-epoxide by a post-cationic mechanism (a remote possibility). Cyclases that generate 6/6/6/6 tetracycles also probably block side-chain folding and are in this category, as are cyclases that make monocycles, bicycles, and tricycles.

2. Cyclases that make pentacyclic triterpenes via the 17 $\beta$ -dammarenyl cation (5). The dammarenyl cation is the usual tetracyclic intermediate en route to triterpene precursors of secondary metabolites in plants and has a 17 $\beta$  side chain (17 $\alpha$  hydrogen).<sup>20</sup> These cyclases should convert DOS to **8**, **9a**, and **9b**. Cyclases that promote epimerization at C17, e.g. to form nepehinal,<sup>37</sup> might cyclize DOS to the C17 epimer of **8**.

3. Cyclases that make pentacyclic triterpenes via the 17 $\alpha$ -dammarenyl cation (22). The epidammarenyl cation (17 $\alpha$  side chain) is the putative intermediate in some oxidosqualene cyclases that produce hopene-type skeletons.<sup>37</sup> These cyclases should convert DOS to **24a** and **24b**, the C17 epimers of **9a** and **9b** (Figure S15). Because D-ring expansion with C13 migration is observed for these cyclases,<sup>20,37</sup> the *si* face of C20 should be more favored for attack than the *re* face. (This situation is opposite to that in LUP1.) When D-ring expansion from **22** occurs faster than oxonium ion formation, **23** (the analog of **8**) should be formed. The angular methyl at the D-E ring junction should have an  $\alpha$  orientation because the C20 methyl initially points down in the epidammarenyl cation and the active site cavity maintains this orientation during E-ring formation.<sup>20</sup>

4. Cyclases that make pentacyclic triterpenes via the protosteryl cation. A few pentacyclic triterpenes are synthesized via the protosteryl cation.<sup>37</sup> Both C13 and C17 migration are observed in D-ring expansions. These cyclases should convert the epoxypotosteryl cation (**25**) to pentacycles **26** or **27** and to epoxypotostanes **28a** and **28b**.

5. Cyclases that make multiple products spanning different categories. These cyclases should generate DOS metabolites corresponding to each category, although not necessarily in the same proportion as for the OS metabolites.

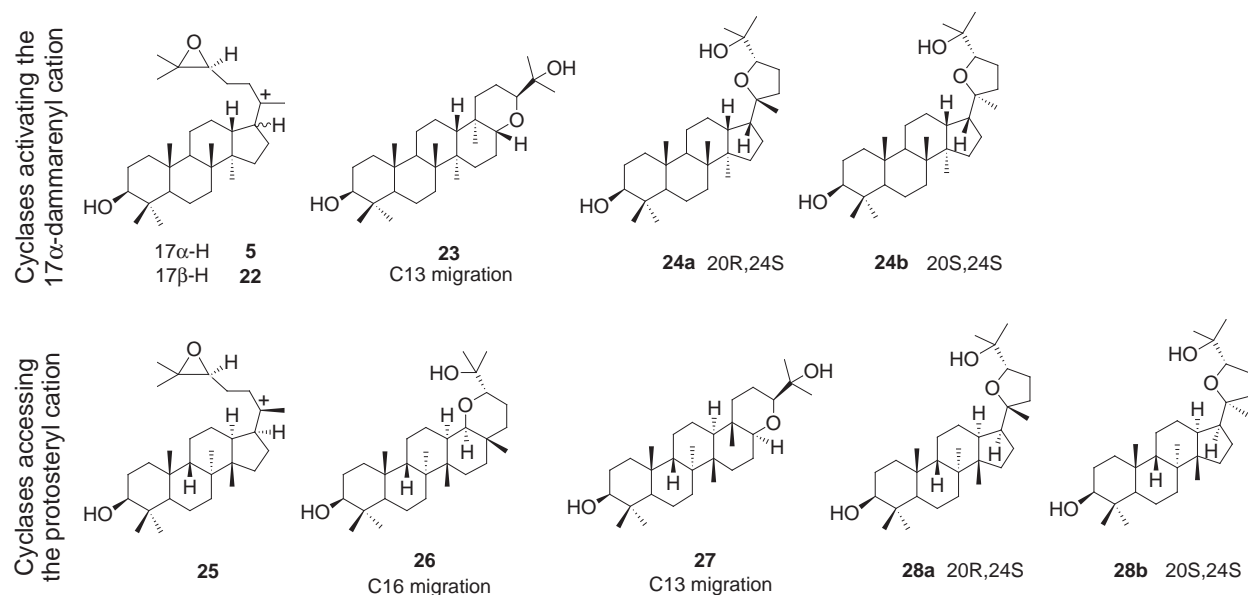


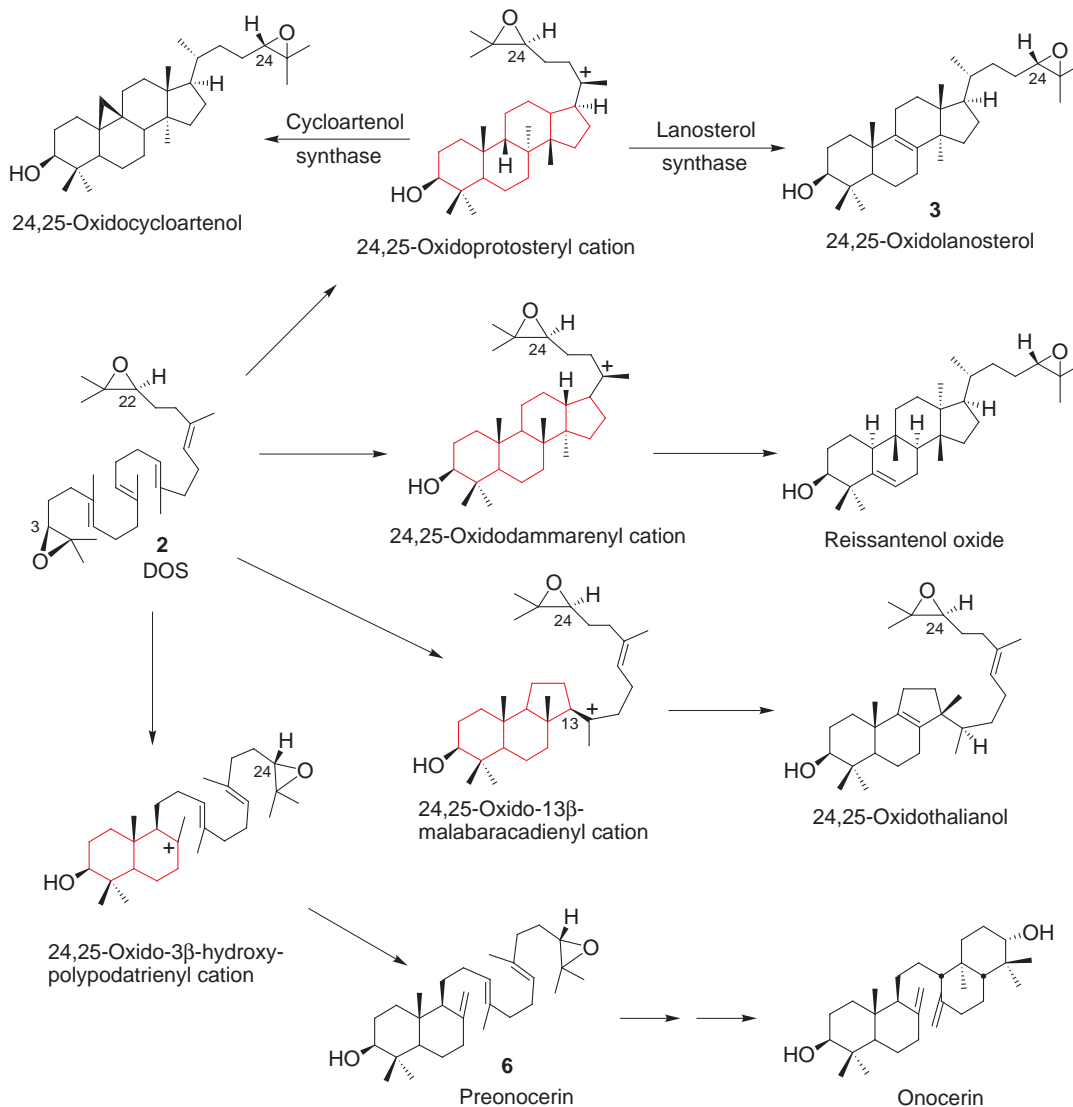
**Figure S15.** Predicted analogs of **8**, **9a**, and **9b** that may be formed from DOS by cyclases that access the oxido-17 $\alpha$ -dammarenyl cation (**22**) or oxido-protosteryl cation (**25**).

In addition to the diols that would be produced when oxonium ions are quenched by attack of water at C25, terminally unsaturated oxacycles (analogs of **18**, **19a**, and **19b**) should be formed by deprotonation at C26 or C27.

## Reported DOS Metabolites

DOS cyclization was reviewed recently by Xu et al.<sup>37</sup> In all known cyclizations of 2,3:22,23-DOS (**2**), one epoxide is protonated to initiate cationic cyclization, and the distal epoxide either remains intact or initiates a second cyclization in a separate reaction (cf. **6**). As illustrated in [Scheme S3](#), the key cationic intermediates shown can have 2, 3, or 4 rings. In the bi- and tricyclic intermediates, the distal epoxide is too far from the cationic center to react with the cation. In cyclases that generate tetracyclic triterpenes like lanosterol, the epoxide also does not react, apparently because the active site cavity prevents side-chain rotation that would allow the epoxide to approach the C20 cation and because the 1,2-shift of H17 to C20 is relatively fast.

**Scheme S3.** Known or inferred cyclization of DOS by triterpene synthases. References to the DOS products are given in Xu et al.<sup>37</sup> except for 24,25-oxidothalianol.<sup>11</sup> Reissantenol oxide and 24,25-oxidothalianol are presumed to originate from DOS. The ring skeletons of the key cationic intermediates are highlighted in red.



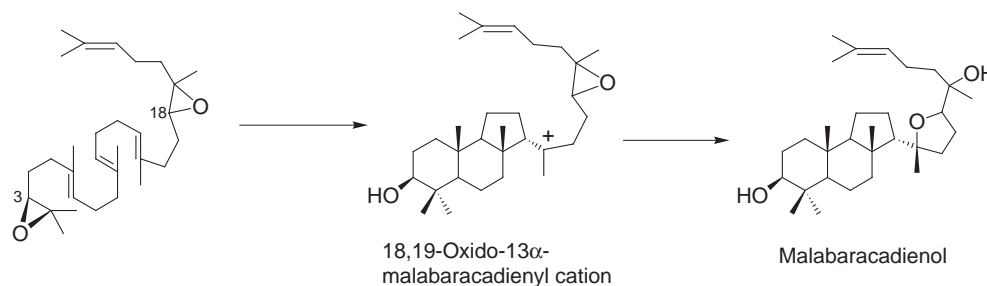
not react, apparently because the active site cavity prevents side-chain rotation that would allow the epoxide to approach the C20 cation and because the 1,2-migration of H17 to C20 may be relatively fast.

24,25-Oxidolanosterol is generally accepted by enzymes of sterol biosynthesis and can be metabolized to 24,25-epoxycholesterol in mammals<sup>39</sup> and apparently to 24,25-epoxycholesta-5,7,22-trien-3β-ol in yeast.<sup>5</sup> A biosynthetic intermediate, 4α-methyl-24,25-epoxy-cholest-7-en-3-one was isolated from an *erg27* mutant and identified by <sup>1</sup>H NMR.<sup>2c,54</sup>

Although the distal epoxide in 2,3:22,23-DOS was not previously known to react with carbocationic intermediates to form oxacycles,<sup>55</sup> non-terminal epoxides can apparently quench cationic intermediates in triterpene synthesis to generate oxacyclic rings. A possible example

related to epoxydammarane formation is shown in [Scheme S4](#), and more exotic examples are suggested by marine natural products and biomimetic syntheses.<sup>56</sup> Oxacyclic rings are also formed by incubation of triterpene synthases with (oxido)squalene analogs containing ether or hydroxyl groups.<sup>57</sup>

**Scheme S4.** Malabaricadienol could originate by cyclization of 2,3:18,19-DOS as shown or the corresponding 18,19-diol. See Xu et al.<sup>37</sup> for discussion and references.



## Atomic Coordinates from B3LYP/6-31G\* Geometry Optimizations

For economy of space, coordinates are given in condensed format. These data are easily converted to tabular form by global find-and-replace routines available in most word processors. First, replace the paragraph mark with nothing; spaces might also need to be deleted; then replace “|” with the paragraph mark. If desired, commas can be replaced by the tab mark.

Compound **8**, neutral structure for NMR calculations. In this conformer, the 3-hydroxyl hydrogen is *anti* to H3α, ring E is a chair, the oxygen on C25 is *anti* to H24, and its hydroxyl hydrogen is *anti* to C24. Although this structure was optimized with Gaussian 98, all NMR calculations were (re)done with Gaussian 03.

```
1\1\GINC-DFTB\FOpt\RB3LYP\6-31G(d)\C30H52O3\BILLW\22-Apr-2003\0\#\ B3L
YP/6-31G(D) OPT=READFC GUESS=READ GEOM=ALLCHECK\C30H52O3 Mike-fused D
OS product 24S\0,1\C,-3.5312962056,1.7983486247,-0.0669706273\C,-5.04
19377531,1.9578005425,-0.2859378317\C,-5.5936696701,0.9661080403,-1.30
96208755\C,-5.2776738374,-0.5203201482,-0.9643426645\C,-3.7336154921,-
0.6285607238,-0.7029915284\C,-3.223389373,-2.0613902955,-0.4765027182\
C,-1.7019277606,-2.1363833763,-0.6737936368\C,-0.8920536131,-1.1863718
783,0.2476833959\C,-1.5303778257,0.2553927448,0.1756540512\C,-3.104717
4662,0.3595372845,0.3428342581\C,-0.7361759511,1.2566914758,1.04048675
63\C,0.7484157046,1.3146574548,0.6513163837\C,1.4028438165,-0.07325941
45,0.681456159\C,0.6444346194,-1.0944752334,-0.2412747363\C,1.36147504
37,-2.4745051899,-0.145575482\C,2.882344721,-2.4102492626,-0.389752010
2\C,3.6014032569,-1.4035233959,0.5337108445\C,-0.9685684689,-1.7740266
947,1.6811549796\C,-3.5744053429,0.1267522879,1.8045046359\C,2.9086987
624,-0.029887688,0.367702356\C,3.5690208845,-1.8957529165,1.9974926642
\C,5.0657494668,-1.1962655897,0.0874320595\C,5.7460961281,-0.059412809
1,0.8697137828\C,4.9020072929,1.2352312897,0.958779919\C,5.1056776888,
2.245784622,-0.2096546859\C,4.0596076492,3.3670765229,-0.1451605222\C,
6.5191138208,2.8531333144,-0.1478931705\C,-5.6525999084,-1.3566820701,
-2.210619398\C,-6.1604653422,-1.0173912297,0.2014125718\C,0.7342269099
,-0.6539011273,-1.7298686228\O,3.5237801007,0.948238544,1.2268936372\O
```

, -6.9857221907, 1.1941295753, -1.5472814777\O, 4.9630486716, 1.5180922172, -1.4458009533\H, -7.4354712189, 1.1418935526, -0.6891458842\H, 5.0476027973, 2.1594879109, -2.169876907\H, -3.2084024293, 2.5226141826, 0.6893892153\H, -3.0137506511, 2.0722974582, -0.9981327989\H, -5.5821709458, 1.8387880939, 0.6643162551\H, -5.2633508389, 2.9743431378, -0.6329984346\H, -5.1225745919, 1.1790332934, -2.2789041303\H, -3.2921719774, -0.3119554326, -1.664049622\H, -3.6916765546, -2.7476460486, -1.1899573526\H, -3.5072661237, -2.4260382626, 0.5178243843\H, -1.36489051, -3.1701688378, -0.5258783782\H, -1.5062379268, -1.8962318847, -1.7246378946\H, -1.383303446, 0.5825311536, -0.861547938\H, -1.1618405058, 2.2612228582, 0.9439642142\H, -0.8121335051, 0.9983839503, 2.1043446702\H, 1.2857441064, 1.9768166258, 1.3370648768\H, 0.8501921744, 1.7568217944, -0.3501567495\H, 1.3214350303, -0.4346456538, 1.7132454054\H, 0.9177473498, -3.1714865122, -0.8674530246\H, 1.1975462746, -2.9173793982, 0.8399704023\H, 3.3115271396, -3.4115841176, -0.2434520425\H, 3.0875098874, -2.1463314057, -1.435666573\H, -2.0014725814, -1.8665610409, 2.0141177669\H, -0.545750953, -2.7817654001, 1.7169555372\H, -0.4480379492, -1.1725089627, 2.4298825782\H, -4.4917001876, 0.67997565, 2.0245596667\H, -3.7801959048, -0.9209194252, 2.0352492786\H, -2.8241130133, 0.4769042318, 2.5193534215\H, 3.0558118007, 0.2967259783, -0.6678939522\H, 2.5658414618, -2.1850374896, 2.3233282773\H, 3.9183686944, -1.122401043, 2.6864404705\H, 4.215215744, -2.7753031016, 2.1113481917\H, 5.6385419805, -2.1244162969, 0.2236852921\H, 5.0832308118, -0.9583739615, -0.9817210519\H, 6.7230104758, 0.1583550836, 0.4263725273\H, 5.9432818305, -0.3952436329, 1.8943777019\H, 5.217456757, 1.7833878527, 1.8551314392\H, 4.1153755113, 3.9095760078, 0.8053891763\H, 4.2359450814, 4.0918421047, -0.9514016379\H, 3.0504991466, 2.9660103102, -0.2481494312\H, 6.6867876716, 3.3926728681, 0.7912857836\H, 7.2916899049, 2.0863390537, -0.2517955569\H, 6.6506932071, 3.5714982993, -0.9672274408\H, -4.9571546359, -1.1728711357, -3.0394156807\H, -5.6538002658, -2.4320669632, -2.0045141755\H, -6.6562675482, -1.0781843887, -2.5458985879\H, -6.1015506215, -0.3899705163, 1.0946715789\H, -7.2099540867, -1.0565380936, -0.113681632\H, -5.8805403206, -2.0337363661, 0.4978632621\H, 0.1933057229, 0.2686832464, -1.9493842975\H, 1.7700028844, -0.4855121887, -2.0316343135\H, 0.3431126635, -1.4299407941, -2.3943033784\Version=x86-Linux-G98RevA.9\HF=-1400.1672112\RMSD=6.315e-09\RMSF=4.415e-06\PG=C01 [X(C30H52O3)]\ \@

# Compound 5A, oxidodammarenyl cation, extended side chain, for 20S intermediate.

1|1|UNPC-UNK|SP|RB3LYP|6-31G(d)|C25H43O1(1+)|PCUSER|07-May-2005|0||# B3LYP/6-31G\* SP SCF=TIGHT GEOM=CHECK|Hui epoxy dammarane, extended side chain for 20S, nothing frozen|1,1|C,0,-1.6660561818,-0.159840798,-1.7951646666|C,0,-0.2810264824,-0.2894006589,-1.1145743745|C,0,-0.2825029006,0.5757126566,0.1346066804|C,0,-1.3896801179,0.1973504273,1.173186905|C,0,-2.8048681773,0.4382508138,0.4531290098|C,0,-2.8392866485,-0.4683387612,-0.8403642171|C,0,-1.2199036529,-1.2587509459,1.6770072035|C,0,1.0607648097,0.5995952217,1.0861111298|C,0,-1.0314674878,1.1315827868,2.3512848971|C,0,0.5098453082,1.0498054988,2.474882711|C,0,1.9646547183,1.462132424,0.3675602716|C,0,1.8790517432,2.9407238588,0.4518279687|C,0,3.0098599545,0.8729180341,-0.4873079167|C,0,-3.0016365615,1.9409701337,0.1350755881|C,0,-4.2295477428,-0.612430204,-1.5707862551|C,0,-3.9570625236,0.0058286851,1.4016806338|C,0,-5.326679115,-0.0174403497,0.706995887|C,0,-5.3084101581,-0.9497498278,-0.5083967127|C,0,-4.6667734969,0.6077239973,-2.4130909263|C,0,-4.1558004118,-1.8190345252,-2.5378879937|C,0,4.2958151331,0.5945283231,0.3876478715|C,0,5.303359362,-0.1206872326,-0.4896291324|C,0,6.032882237,-1.3597111741,-0.1213744354|C,0,7.3517800903,-1.6407380155,-0.8109859923|C,0,5.8431758743,-2.0555245443,1.2094097361|H,0,-1.6859795406,-0.8449169498,-2.6473701461|H,0,-1.7591215899,0.8494292796,-2.2138290052|H,0,-0.0805700307,-1.3369627924,-0.8592871956|H,0,0.4954422327,0.0188587691,-1.8253544866|H,0,-0.45

96356116,1.6142166129,-0.1594202442|H,0,-2.6641912575,-1.4879847299,-0.4750885878|H,0,-1.4431294562,-2.0169459848,0.9256217202|H,0,-0.2022615602,-1.4538641412,2.0289350577|H,0,-1.8760326899,-1.4408613324,2.5314202786|H,0,1.4403138515,-0.4255813639,1.0928110837|H,0,-1.3224663953,2.1635494109,2.1394447863|H,0,-1.5223704026,0.8441271824,3.2854706821|H,0,0.9425736575,1.9977372842,2.8067957543|H,0,0.8186781001,0.3016354326,3.2104321805|H,0,1.0064769811,3.306565996,0.9935039122|H,0,2.7808321119,3.3025809946,0.9732242389|H,0,1.922565394,3.3893175273,-0.5481427213|H,0,3.2846477561,1.5341612109,-1.3149660192|H,0,2.7016129189,-0.1042965535,-0.8755861025|H,0,-2.288792711,2.3430339436,-0.5905963291|H,0,-2.940502605,2.5512114766,1.0408908554|H,0,-3.9903368671,2.1221306646,-0.2811364147|H,0,-3.7687747663,-1.0049431764,1.7798049336|H,0,-3.9842232998,0.6691488569,2.2762600247|H,0,-5.6393639827,0.992708134,0.4177356515|H,0,-6.0795954314,-0.3673639075,1.4235728592|H,0,-6.2931681141,-0.9579725815,-0.9927078415|H,0,-5.1355521892,-1.9763500376,-0.1525873102|H,0,-4.982320692,1.4652223416,-1.8147965763|H,0,-3.874924546,0.9455967229,-3.0908926082|H,0,-5.5228672962,0.327205153,-3.0372991832|H,0,-3.7532108974,-2.7118509404,-2.0435539913|H,0,-5.1603118641,-2.0673778289,-2.8986204703|H,0,-3.5421257472,-1.612719522,-3.4214403896|H,0,4.0196831187,-0.0138545976,1.2518383264|H,0,4.7160694765,1.5385218415,0.7519141137|H,0,5.7695862219,0.5299067593,-1.2347779224|H,0,7.4191473767,-1.1154717183,-1.7677165945|H,0,7.4531794881,-2.7146121194,-1.003173652|H,0,8.1923936823,-1.3307222571,-0.1801211714|H,0,4.8383534937,-1.9153094435,1.6148778354|H,0,5.9996884768,-3.1325217242,1.0845646454|H,0,6.5742619352,-1.6962052228,1.9424575193|O,0,4.8816747302,-1.3838789515,-1.0085218398||Version=IA32W-G03RevC.02|State=1-A|HF=-1053.4962648|RMSD=9.120e-009|PG=C01 [X(C25H43O1)]||@

## Compound **5B**, oxidodammarenyl cation, extended side chain, for 20R intermediate.

1\1\GINC-DFTC\FOpt\RB3LYP\6-31G(d)\C25H43O1(1+)\BILLW\14-May-2005\0\#\B3LYP/6-31G\* OPT GEOM=ALLCHECK\Hui epoxy dammarane open angles like SHC, not frozen\1,1\C,-1.8494211455,-1.2380368824,1.3706232533\C,-0.4792799721,-0.550824363,1.18899583\C,-0.4479679977,0.1405425928,-0.1720999378\C,-1.5934536782,1.1781117938,-0.3697947268\C,-2.9949928085,0.4204623091,-0.2692341809\C,-3.0414657508,-0.2783535685,1.1506676374\C,-1.4811171868,2.3497614233,0.6434214099\C,0.8435436144,0.8987042993,-0.5531993813\C,-1.1962679557,1.7475674166,-1.7545987662\C,0.3417722148,1.9349023117,-1.721522119\C,1.9380211706,0.2169050949,-1.2154723706\C,1.7068649293,-0.958198894,-2.0928572052\C,3.3181023889,0.6736054468,-1.0098356716\C,-3.1434698916,-0.5911225341,-1.4332337664\C,-4.4281730722,-0.8810396702,1.5984347764\C,-4.1733290213,1.4252011032,-0.372235369\C,-5.5354238645,0.7956488253,-0.0465629465\C,-5.5299620225,0.1838713995,1.3577296899\C,-4.8189483848,-2.2180134216,0.9279318178\C,-4.3842864827,-1.1441440339,3.1237759656\C,4.0325320244,-0.3277764837,-0.010551647\C,5.4700455193,0.1292766562,0.1382025379\C,6.6623716977,-0.7420891301,-0.0249403972\C,7.944456743,-0.3277928117,0.6665453256\C,6.5607090572,-2.2138360055,-0.3628403428\H,-1.8933527252,-1.6586260155,2.3792955449\H,-1.9096222707,-2.0913057336,0.6835266128\H,-0.3098257475,0.1783974442,1.9920553981\H,0.3226816589,-1.2978269444,1.272578797\H,-0.5971472348,-0.6330546555,-0.9329815416\H,-2.9007777353,0.5387809335,1.8694874273\H,-1.7186739852,2.0651492261,1.6694581384\H,-0.4747472107,2.7809033738,0.6647282893\H,-2.1553682415,3.1631306105,0.3643746266\H,1.2270097518,1.5044708251,0.2717189421\H,-1.4529049509,1.0572836589,-2.5611751794\H,-1.6723615474,2.7072419345,-1.9846152153\H,0.7950227537,1.7475408633,-2.7003386442\H,0.6638220852,2.9297365259,-1.4087653155\H,0.7951481956,-0.8534585792,-2.6893280773\H,2.5591283605,-1.1771214304,-2.73901349\H,1.5317452229,-1.83121569,-1.4424596871\H,3.3544078557,1.6797556377,-0.5820712302\H,3.9051121025,0.6341132784,-1.9343734074\H,-2.4056

490219,-1.39877063,-1.4206416845\H,-3.0788321972,-0.0915391232,-2.4051098322\H,-4.1191610981,-1.0721772422,-1.4105589908\H,-4.0224311923,2.2496277151,0.3335903905\H,-4.1910321118,1.8719017359,-1.3759575332\H,-5.8121213007,0.0453813914,-0.7965650413\H,-6.3089197484,1.5709931461,-0.1033267874\H,-6.5083764087,-0.2601712778,1.5812781373\H,-5.3908673997,0.9969364115,2.0858926737\H,-5.1145711769,-2.1147875124,-0.1183401143\H,-4.0096529381,-2.9549428215,0.9758685662\H,-5.6767099214,-2.6500331379,1.4561298528\H,-4.0185024936,-0.2699193514,3.6764879596\H,-5.3923423063,-1.3670838399,3.4914421212\H,-3.7533579215,-2.000500074,3.3853706552\H,3.9783882637,-1.3402053378,-0.4154398426\H,3.5276496323,-0.3156075758,0.9615184574\H,5.5818742478,1.019342065,0.7633561194\H,7.9570344537,0.746880903,0.8680591325\H,8.8061635867,-0.5663750495,0.0333487196\H,8.0644176319,-0.8646771441,1.6142337135\H,5.6683462211,-2.4497076706,-0.9475782024\H,7.4306245899,-2.5122546502,-0.9578836796\H,6.5575920751,-2.8211976936,0.5492503846\O,6.2294974312,0.1706242824,-1.0700779572\\Version=x86-Linux-G03RevB.02\HF=-1053.4934383\RMSD=3.594e-09\RMSF=3.319e-06\Dipole=2.6828856,0.4911346,0.3937468\PG=C01 [X(C25H43O1)]\\@

### Compound 10, oxonium ion for fused system.

1|1|UNPC-UNK|FOpt|RB3LYP|6-31G(d)|C25H43O1(1+)|PCUSER|17-May-2005|0||#B3LYP/6-31G\* OPT GEOM=ALLCHECK|Hui epoxy dammarane, fused oxonium ion intermediate, nothing frozen, opt ||1,1|C,-1.9970520546,1.0015021462,-0.7413370414|C,-0.5281811779,0.8347964067,-1.1555169362|C,0.3254540618,0.3378086946,0.0218695196|C,-0.2195006032,-1.0165399781,0.6296547167|C,-1.7442741192,-0.7755865633,1.1008381817|C,-2.5827112413,-0.2924706206,-0.1458843355|C,-0.1249003071,-2.1662325863,-0.4116141553|C,1.8037106002,0.1810167344,-0.3171143982|C,0.7051265221,-1.4049203491,1.8216780183|C,2.201659104,-1.467775958,1.4609299147|C,2.7413209419,-0.1454992654,0.852203987|C,2.7755148796,0.958571036,1.9326297443|C,4.1512208083,-0.3608430642,0.2614946896|C,-1.7859226582,0.2495300288,2.2628069185|C,-4.1543874682,-0.2651911264,-0.0014138981|C,-2.3640213513,-2.0991406318,1.6303196963|C,-3.8724093853,-1.9968809242,1.8994950375|C,-4.6227083801,-1.6026135326,0.6252183143|C,-4.731874171,0.9260877273,0.7985250043|C,-4.7727630092,-0.1895034579,-1.4190804218|C,4.7455805201,0.9151167889,-0.3866419521|C,3.7374003651,1.8562027085,-1.0282339685|C,3.021983109,1.6448313156,-2.3034240794|C,2.4797958947,2.8406656355,-3.0407884499|C,3.1940274357,0.3880166164,-3.1107601822|H,-2.5727673035,1.3091419451,-1.619718095|H,-2.0738761342,1.8270473393,-0.023126405|H,-0.4575439512,0.1327484955,-1.9987307965|H,-0.1427271071,1.7970839234,-1.5137146423|H,0.2669063703,1.0964211432,0.8084794786|H,-2.4339746777,-1.0691845231,-0.9069005449|H,-0.7897554635,-2.0395430527,-1.2672591659|H,0.8859723103,-2.2808303855,-0.8136542468|H,-0.3709974952,-3.1238286068,0.0532432753|H,1.9411731466,-0.5434831746,-1.1199206888|H,0.5780637931,-0.6988259387,2.6460292241|H,0.4069148363,-2.3828692579,2.2137315719|H,2.7859678846,-1.6939582149,2.3613274026|H,2.3928923985,-2.2918128621,0.7626589671|H,1.8113332821,1.0878814848,2.4284970354|H,3.504447063,0.68699703,2.7038946563|H,3.0650927158,1.9381387936,1.5383133242|H,4.1073950974,-1.1767854167,-0.4701968521|H,4.8387272693,-0.6930770683,1.0462861191|H,-1.3025130839,1.2035469282,2.0344017456|H,-1.3152888797,-0.1546779199,3.1637000197|H,-2.8118844148,0.4869790511,2.5348180752|H,-2.2232146974,-2.9002313916,0.8957233944|H,-1.8451612691,-2.4155340505,2.5438539665|H,-4.0785296485,-1.2860954387,2.7084285781|H,-4.2371441458,-2.9683511143,2.2545755393|H,-5.7017818607,-1.5476658195,0.8187132088|H,-4.4858874038,-2.403748845,-0.1166937856|H,-4.577251775,0.846411953,1.877290732|H,-4.3156648908,1.8846925974,0.4698338732|H,-5.8153788135,0.9754817854,0.640035473|H,-4.3501655947,-0.951149796,-2.0861661804|H,-5.853252371,-0.3642129251,-1.3632432302|H,-4.6316865331,0.79030887



52,-1.8881655781|H,5.4968588161,0.6450996936,-1.1381437315|H,5.2709605  
327,1.4951954548,0.3762771078|H,3.82829289,2.8962971231,-0.7227934784|  
H,2.2647497373,3.6701080623,-2.3629375539|H,1.5692180784,2.5815567407,  
-3.5890641885|H,3.2292654752,3.1746237091,-3.7681165181|H,3.6437972207  
, -0.4374153663, -2.5587627956|H,2.2412460792,0.0653248503, -3.5421901896  
|H,3.8617946897,0.6301743059, -3.9460678021|O,2.2628559915,1.5120416498  
, -0.9349587306||Version=IA32W-G03RevC.02|HF=-1053.5191133|RMSD=4.941e-  
009|RMSF=6.938e-006|Dipole=-4.6423868,1.2083869,0.8400213|PG=C01 [X(C2  
5H43O1)]||@

## Compound 11, 20R-oxonium ion.

1\1\GINC-DFTB\FOpt\RB3LYP\6-31G(d)\C25H43O1(1+)\BILLW\14-May-2005\0\#\n  
B3LYP/6-31G\* OPT GEOM=ALLCHECK\Hui epoxy dammarane, 20R oxonium ion,  
, nothing frozen \\1,1\C,0.3815587757,-0.5200850127,2.053591608\  
C,-0.6454680409,-0.1773347067,0.9556627585\C,0.0810544594,0.3201038979  
, -0.2938692988\C,1.1393698735,-0.6974180549,-0.8277607826\C,2.23487783  
61,-0.9656493796,0.2994775228\C,1.4706982415,-1.5058191851,1.574446221  
9\C,0.4650194283,-2.0092830932,-1.3145374365\C,-0.7338553865,0.7168141  
835,-1.5474179955\C,1.612293866,0.0519394068,-2.1015917782\C,0.3241148  
649,0.6672901875,-2.7138830268\C,-1.4697001473,2.0581631679,-1.5338441  
279\C,-0.6740697426,3.2578397868,-1.0317037381\C,-2.2589662819,2.36900  
32019,-2.8186871598\C,3.0313680169,0.3305821873,0.5920894529\C,2.35066  
90782,-2.0925804636,2.7457077177\C,3.2557910344,-2.041330611,-0.157615  
5353\C,4.1995335656,-2.4926051076,0.965809684\C,3.4023819509,-3.061558  
2911,2.1440408609\C,3.0456212312,-1.0437204507,3.6443942043\C,1.439485  
7123,-2.936917954,3.6697051907\C,-3.5784742211,3.0670707427,-2.4043359  
981\C,-3.8401371162,2.6694262932,-0.9638580653\C,-4.0273943086,1.26956  
78889,-0.5378080295\C,-4.496683423,1.0231951343,0.8730140194\C,-4.2121  
490195,0.1190188113,-1.4880592634\H,-0.1507133549,-0.9417731503,2.9119  
550223\H,0.8384702455,0.4117055771,2.4103415816\H,-1.2489574889,-1.065  
8098843,0.7173682847\H,-1.3398224294,0.5836939494,1.3353918665\H,0.647  
2570533,1.2109744113,0.0020711027\H,0.9319280537,-2.3948317794,1.22071  
76275\H,0.024298745,-2.6045956492,-0.5124838386\H,-0.3338059298,-1.808  
305139,-2.0357094138\H,1.1871458747,-2.643597439,-1.8342938552\H,-1.49  
29050695,-0.048051569,-1.7415497851\H,2.3057962911,0.856899063,-1.8471  
165521\H,2.1239051329,-0.5999611324,-2.8162983966\H,0.5287673886,1.659  
0626419,-3.1307170852\H,-0.059005185,0.062286428,-3.5407319995\H,0.229  
8372256,3.3671984539,-1.6391325237\H,-1.2476537148,4.1857998259,-1.119  
6212792\H,-0.3714847265,3.1337749786,0.0096538827\H,-2.4498112467,1.45  
32230403,-3.3820045437\H,-1.6674053253,3.0195959938,-3.4682696281\H,2.  
4110509981,1.1698232399,0.918825919\H,3.5928406609,0.6543687655,-0.289  
6743513\H,3.7655234931,0.1702848584,1.3785679651\H,2.7257929028,-2.933  
8021192,-0.5091730699\H,3.8329031365,-1.6635009462,-1.0123343513\H,4.8  
448006933,-1.6686371383,1.2928449015\H,4.8758873841,-3.2643645197,0.57  
82735731\H,4.0820889101,-3.3880993255,2.9419450229\H,2.8817197122,-3.9  
674111442,1.7987079217\H,3.8860509215,-0.540351125,3.1609206065\H,2.34  
83592998,-0.2728440869,3.9906946976\H,3.4456050155,-1.5396729053,4.536  
5603114\H,0.8338090748,-3.6498211267,3.0964519007\H,2.0521701114,-3.51  
46349522,4.3713684366\H,0.7617352647,-2.3203154212,4.2703295515\H,-4.4  
125464453,2.7815672385,-3.0530780571\H,-3.4888638442,4.1548938507,-2.4  
583338255\H,-4.1784612036,3.4468305958,-0.2822697712\H,-4.2438050555,1.  
.8514662877,1.5386617883\H,-4.0676060155,0.0994514181,1.2711276389\H,-  
5.5877644203,0.9120098705,0.858768986\H,-3.8953343422,0.3145191882,-2.  
5103811001\H,-3.7119112211,-0.7785959145,-1.1149275753\H,-5.2879945229  
, -0.0957284613,-1.5088901866\O,-2.6129416915,1.9938749718,-0.437794928  
8\\Version=x86-Linux-G03RevB.02|HF=-1053.515086\RMSD=6.931e-09\RMSF=5.  
147e-06|Dipole=1.371018,-4.5334646,3.3272448\PG=C01 [X(C25H43O1)]\\@

## Compound 12, 20S-oxonium ion.

```
1|1|UNPC-UNK|FOPT|RB3LYP|6-31G(d)|C25H43O1(1+)|PCUSER|07-May-2005|0||#
B3LYP/6-31G* OPT|Hui epoxy dammarane intermediate, 20S-oxonium ion,
nothing frozen,opt||1,1|C,2.0071636709,-1.7454248562,0.1435077201|C,0.
5578446545,-1.5554146968,-0.351782021|C,0.0272423608,-0.1874398489,0.0
815949793|C,0.9435600271,0.9914560705,-0.3838942385|C,2.4018671386,0.8
0549883,0.2344790989|C,2.9466558207,-0.5908087379,-0.2662326154|C,0.97
06704116,1.1021931106,-1.9330101139|C,-1.4041624295,0.2713686608,-0.33
62473309|C,0.1201397161,2.201710508,0.1273170424|C,-1.3640379433,1.823
7745339,-0.1285862429|C,-2.5569212355,-0.4468392568,0.3887155367|C,-2.
4947831479,-0.4289649063,1.9038645825|C,-2.9327137956,-1.8056952336,-0
.2287184807|C,2.3468312368,0.8980692809,1.7808636304|C,4.4734670487,-0
.8984327541,-0.0161564135|C,3.3600216688,1.9233648981,-0.2570949472|C,
4.8270515085,1.669216311,0.1175187229|C,5.3071253067,0.3327956276,-0.4
571067048|C,4.8418393981,-1.3017764679,1.4300849158|C,4.8950718811,-2.
0773950837,-0.9265982593|C,-3.90836042,-1.543837028,-1.4036086041|C,-4
.5373675871,-0.187486911,-1.1455875693|C,-5.3485122445,0.1046318524,0.
051289079|C,-6.0943771135,1.4132186932,0.0940163093|C,-5.82838059,-0.9
460246509,1.0138667722|H,2.3845955716,-2.6938435863,-0.2511559585|H,1.
9932301645,-1.856733062,1.2349976406|H,0.5171372875,-1.6527758421,-1.4
456041642|H,-0.0531487029,-2.3717497937,0.0572379211|H,0.046575208,-0.
1660962334,1.1775769781|H,2.8950601217,-0.5361249063,-1.3614172626|H,1
.4367252643,0.250061916,-2.4317079817|H,-0.0380761341,1.198724932,-2.3
471431868|H,1.5089498694,1.9997398651,-2.2462239593|H,-1.5346649265,0.
0564922464,-1.4042909678|H,0.2704900901,2.3557861462,1.1984253083|H,0.
3908975205,3.1373042341,-0.3715695174|H,-1.9959685332,2.1395702253,0.7
069719531|H,-1.7627064585,2.3275912412,-1.0141173775|H,-2.2628547663,0
.5650851025,2.2934941651|H,-3.4274247319,-0.7774094992,2.3529787428|H,
-1.7032363938,-1.1119135522,2.2278942178|H,-3.3812457085,-2.4576847119
,0.5248256515|H,-2.0339516261,-2.309582492,-0.5875031752|H,1.707394002
7,0.1455247999,2.2502140958|H,1.9943800057,1.8825219904,2.1028763526|H
,3.3354231927,0.7720204039,2.2176586492|H,3.3166699331,1.9990190314,-1
.3493377479|H,3.0282517181,2.893564656,0.1369229237|H,4.9667702626,1.6
977983163,1.2047743007|H,5.4455499318,2.4814944382,-0.2836369516|H,6.3
595769125,0.1618918916,-0.1956063328|H,5.2731840368,0.3994508448,-1.55
49399847|H,4.8103869645,-0.4714142374,2.1390375452|H,4.1901879424,-2.0
945658352,1.8138461085|H,5.8661195782,-1.6921780254,1.4469038399|H,4.5
843828052,-1.9168523252,-1.9664817587|H,5.986284161,-2.1812188055,-0.9
211126589|H,4.4817149017,-3.0349757529,-0.5918415943|H,-4.6686622355,-
2.3270802958,-1.4850009205|H,-3.3795445219,-1.5092517036,-2.3592406325
|H,-4.6341605419,0.4899352748,-1.9913262074|H,-5.6321096632,2.16730205
94,-0.5467078411|H,-6.1512851891,1.7976477213,1.1165617534|H,-7.118548
9897,1.2401227483,-0.2585065827|H,-5.2896785854,-1.8900408908,0.964260
5005|H,-5.8208516844,-0.5707777041,2.0409717101|H,-6.8754756643,-1.148
187242,0.7552671958|O,-3.7959943053,0.4601573427,-0.0242742346|Versio
n=IA32W-G03RevC.02|HF=-1053.5139875|RMSD=8.132e-009|RMSF=2.534e-006|Di
pole=-6.3728102,-0.5952619,-0.1145809|PG=C01 [X(C25H43O1)]|@
```

Compound 14 (TS-A), transition state structure for ring expansion (anti-Markovnikov), not oxygen stabilized, from QST3 optimization. The frequency calculation showed one imaginary frequency ( $97.6\text{ cm}^{-1}$ ), with IR intensity 108.9 (unscaled values). Normal mode displacements for the vibration of imaginary frequency were largest for C16, C17, C20, H17, and H16 $\beta$ . Animation of the normal-mode displacements in Gaussview showed D-ring expansion/contraction, with C16 moving between C17 and C20.

```
1\1\GINC-DFTB\FTS\RB3LYP\6-31G(d)\C25H43O1(1+)\BILW\21-Jul-2005\0\#\#
B3LYP/6-31G* OPT=QST3 FREQ\\transition state guess--from oxonium ion T
```

S by straightening SC, then doing opt\\1,1\\C,-2.5301190599,1.957109805  
3,0.0107238082\\C,-1.0959831094,1.810531644,-0.5214481513\\C,-0.47161336  
65,0.5098858047,0.0223441513\\C,-1.348574727,-0.7861801964,-0.409974144  
1\\C,-2.8019290694,-0.6060471988,0.2292766304\\C,-3.4217203155,0.7419946  
077,-0.3188086882\\C,-1.3940132566,-0.9356240241,-1.9525610083\\C,0.8891  
003311,0.2186087555,-0.4193699915\\C,-0.5257927304,-1.973927739,0.15749  
46679\\C,0.9356594539,-1.9189455353,-0.2632513329\\C,1.85564325,-0.53004  
72051,0.302151787\\C,1.852057065,-0.5381408403,1.829660688\\C,3.24904365  
77,-0.6456272549,-0.3245586578\\C,-2.7193913378,-0.6340078674,1.7755206  
011\\C,-4.9552595634,0.9876819668,-0.0422812812\\C,-3.7143006425,-1.7880  
672195,-0.2117917326\\C,-5.1853695272,-1.5862355688,0.1797154349\\C,-5.7  
382826504,-0.2938294425,-0.4280210139\\C,-5.3131905837,1.4232274185,1.3  
973410628\\C,-5.4440596624,2.1162994603,-0.9828262783\\C,4.1767679878,0.  
5507202497,-0.0233529075\\C,5.5264380359,0.315366445,-0.6716050699\\C,6.  
8464065506,0.4817330546,-0.0216059962\\C,8.0527791481,0.7336921265,-0.9  
03954133\\C,7.0004499164,0.9380322452,1.4142269637\\H,-2.9584012293,2.86  
34516043,-0.4269635263\\H,-2.4927029261,2.132742744,1.0925465283\\H,-1.0  
876019172,1.8062461581,-1.6181350448\\H,-0.4925278476,2.6684927137,-0.2  
03694574\\H,-0.4968411858,0.5369784296,1.1127367228\\H,-3.397520702,0.64  
10449791,-1.4112197276\\H,-1.9854760863,-0.1642152512,-2.4453159897\\H,-  
0.4017005917,-0.9047117358,-2.4113753489\\H,-1.8291779031,-1.9004690963  
,-2.2236978055\\H,1.1328973593,0.4374053784,-1.4610661422\\H,-0.58385610  
79,-2.0185929887,1.2462917636\\H,-0.9333492422,-2.9231791522,-0.2126977  
052\\H,1.5576452713,-2.6537904754,0.2584767729\\H,1.0995784599,-2.044658  
0412,-1.3337800595\\H,0.8616806561,-0.6712047142,2.2665694779\\H,2.49870  
6273,-1.3405464168,2.1967318436\\H,2.2551778836,0.4093759229,2.20001900  
46\\H,3.1524162373,-0.7618522173,-1.4123065073\\H,3.7367051719,-1.552845  
5978,0.048685911\\H,-2.1101361253,0.1653588392,2.206837203\\H,-2.3295356  
625,-1.5897400884,2.1389310167\\H,-3.7077310715,-0.5273137997,2.2160928  
92\\H,-3.6819794988,-1.9000818468,-1.3010515298\\H,-3.3364134534,-2.7270  
38895,0.2146360195\\H,-5.3051555575,-1.5889166803,1.269232098\\H,-5.7667  
047429,-2.440805695,-0.1863895011\\H,-6.7914830316,-0.1649977882,-0.148  
8458644\\H,-5.7236587572,-0.3947173695,-1.5234421423\\H,-5.2589948086,0.  
6148741123,2.1300937135\\H,-4.6769217915,2.241519366,1.751762024\\H,-6.3  
45169209,1.791271482,1.4150633584\\H,-5.1425822163,1.9391031633,-2.0226  
380145\\H,-6.5383629141,2.1668873634,-0.9624177142\\H,-5.0742834293,3.10  
2755272,-0.6834357392\\H,4.2919099682,0.6727935066,1.0566264745\\H,3.741  
8482726,1.4810399845,-0.4153178473\\H,5.5066299713,0.3961146064,-1.7630  
935941\\H,7.8847187648,0.3584355663,-1.9174138826\\H,8.933206395,0.22623  
91601,-0.4942210718\\H,8.2774177295,1.8050771079,-0.9594484467\\H,6.1473  
510945,0.6551517866,2.0353902656\\H,7.8932600096,0.4777964272,1.8519082  
193\\H,7.1285076071,2.0255052184,1.4646643753\\O,6.2500170145,-0.8294004  
989,-0.1967000446\\Version=x86-Linux-G03RevB.02\\HF=-1053.4814076\\RMSD=  
7.427e-09\\RMSF=2.625e-06\\Dipole=0.6356836,-0.0528148,-0.1183299\\PG=C01  
[X(C25H43O1)]\\@

### Compound 15, ring expansion (anti-Markovnikov), not oxygen stabilized.

1\\1\\GINC-DFTC\\FOpt\\RB3LYP\\6-31G(d)\\C25H43O1(1+)\\BILLW\\16-Jul-2005\\0\\#  
B3LYP/6-31G\* OPT\\Hui epoxy dammarane baccharenyl-type ring expansion  
,not frozen\\1,1\\C,-2.6142111671,1.7562934491,-0.7455646377\\C,-1.23485  
42398,1.3226935812,-1.2549207863\\C,-0.4065673043,0.6467820658,-0.15443  
48416\\C,-1.2562339694,-0.7002098561,0.4988347189\\C,-2.6294925181,-0.08  
4622664,1.0512792056\\C,-3.4198184597,0.593635365,-0.1353939294\\C,-1.46  
08217738,-1.7727788036,-0.5946366042\\C,0.8154745533,0.0166257151,-0.52  
49752178\\C,-0.3232255039,-1.2535405809,1.5988053687\\C,1.0758786523,-1.  
6171095307,1.1122837594\\C,1.8680587957,-0.3723210804,0.4032786277\\C,2.  
2260428768,0.6680522076,1.4867193999\\C,3.1181276391,-0.9491645563,-0.2  
966305698\\C,-2.3640876933,0.8948250177,2.2193296551\\C,-4.9370250821,0.

```

9509055851,0.1179226216\C,-3.4868916305,-1.2633647919,1.6198292524\C,-
4.9144029689,-0.8353168529,1.9881215576\C,-5.6402461444,-0.2674304123,
0.7672101603\C,-5.1905183905,2.2218402375,0.9616029837\C,-5.6125344084
,1.1848147511,-1.2555824705\C,3.990430199,0.081598409,-1.0371516939\C,
5.1624881277,-0.6185373723,-1.6943854284\C,6.5767619009,-0.18235353,-1
.6549113372\C,7.5031804545,-0.6512382603,-2.7594604858\C,7.0260671917,
1.0726161648,-0.9361387417\H,-3.1609970759,2.1876044875,-1.5889221217\
H,-2.4913501297,2.5682984575,-0.0194644063\H,-1.3358314342,0.648769297
3,-2.1145593457\H,-0.6818982555,2.2001436182,-1.6105764085\H,-0.282272
3644,1.2924735984,0.7145375371\H,-3.4864507804,-0.177885326,-0.9129524
181\H,-2.0293510084,-1.4145625336,-1.4529962969\H,-0.5163098707,-2.165
1267621,-0.9780415514\H,-2.0018025744,-2.6257519541,-0.1794349188\H,0.
8788812123,-0.3909602762,-1.5374017185\H,-0.2457511889,-0.5505337741,2
.4296235774\H,-0.7808068263,-2.1629269695,2.0090254508\H,1.7315027625,
-1.8905582472,1.9467801051\H,1.065801952,-2.4625490848,0.4205229127\H,
1.3820211469,0.9299626889,2.1281153461\H,3.0155582876,0.2581240427,2.1
237877709\H,2.6038726953,1.5892108663,1.0347348166\H,2.8002651208,-1.7
287246625,-1.0030947353\H,3.7410548244,-1.4489291353,0.4533849667\H,-1
.732918726,1.7482487682,1.9563758245\H,-1.90848325,0.3893728165,3.0753
73188\H,-3.3000233992,1.316212399,2.5782012239\H,-3.5761230317,-2.0613
162578,0.8760459106\H,-2.9853021062,-1.6952766432,2.4944462961\H,-4.90
8436866,-0.1156712169,2.8145502735\H,-5.4522411625,-1.7153817865,2.360
6867365\H,-6.666719406,0.0138727456,1.0329084196\H,-5.7274967224,-1.06
56074485,0.0150194036\H,-4.979059867,2.0959199663,2.0263601842\H,-4.61
14445571,3.079559116,0.6036605082\H,-6.2483346915,2.4968737382,0.88482
76827\H,-5.4067437077,0.3654849313,-1.9553506582\H,-6.69912355,1.24247
25836,-1.1282199689\H,-5.2977563767,2.1224011277,-1.7257769719\H,4.347
8477849,0.8428282605,-0.3389889266\H,3.4018163516,0.5993782766,-1.8102
791713\H,4.8730690839,-1.2536517596,-2.5379303969\H,7.1330712442,-1.57
21644295,-3.2191559039\H,8.502406161,-0.8496555069,-2.3559494189\H,7.6
008196592,0.1145210558,-3.5376732551\H,6.3747491956,1.3272307265,-0.09
67535955\H,8.0359254463,0.9260885782,-0.5369314099\H,7.061671672,1.923
4626166,-1.626367152\O,6.0916524381,-1.2484308166,-0.7997913481\\Versi
on=x86-Linux-G03RevB.02\HF=-1053.4819567\RMSD=4.546e-09\RMSF=2.919e-06
\Dipole=-0.1754363,0.0324523,-0.1040305\PG=C01 [X(C25H43O1)]\@

```

Compound **16** (TS-B), transition state structure, oxygen stabilized, from QST3 optimization. The frequency calculation showed one imaginary frequency ( $140.0\text{ cm}^{-1}$ ), with IR intensity 87.8 (unscaled values). Normal mode displacements for the vibration of imaginary frequency were largest for C16, C17, C20, H17, and H16 $\beta$ . Animation of the normal-mode displacements in Gaussview showed D-ring expansion/contraction, with C16 moving between C17 and C20.

```

1|1|UNPC-UNK|FTS|RB3LYP|6-31G(d)|C25H43O1(1+)|PCUSER|05-Jul-2005|0||#
B3LYP/6-31G* OPT=QST3 FREQ||TS from PES-186 ||1,1|C,-1.6719172734,1.8
373597781,-0.2924800129|C,-0.285671397,1.2712767284,-0.6478441454|C,0.
0738850505,0.1551194012,0.3503247841|C,-1.0042908217,-1.0212775442,0.3
337538865|C,-2.40982243,-0.4058147204,0.7737560446|C,-2.7693047858,0.7
52726519,-0.24249193|C,-1.0706714547,-1.7042617601,-1.0587507114|C,1.3
870968655,-0.4881516712,0.1370309215|C,-0.3850907145,-2.0466688537,1.3
239350298|C,1.0709183272,-2.3290890926,0.979168141|C,2.258939761,-0.95
75753275,1.1401342119|C,2.2141907367,-0.4390250673,2.5679291839|C,3.61
5758638,-1.5083727885,0.6980211577|C,-2.345275366,0.0914890844,2.23877
31188|C,-4.234327631,1.3321300699,-0.1714348521|C,-3.5151670046,-1.495
909093,0.6954269869|C,-4.9300461475,-0.9323234175,0.8889041745|C,-5.23
45392852,0.1468964256,-0.1546073459|C,-4.5177002769,2.2913371603,1.007
9744459|C,-4.505666226,2.1320925529,-1.469119095|C,4.6909648471,-0.420

```

2744448,0.4655322003|C,4.2858006481,0.5869735053,-0.5990512534|C,4.9074530219,0.7343305337,-1.9370251586|C,4.8075622596,2.0717376097,-2.6405718095|C,6.048869065,-0.1495994005,-2.390566145|H,-1.9298611928,2.5935651959,-1.0392761063|H,-1.6050668551,2.3681572644,0.6654261947|H,-0.2744985901,0.8831224671,-1.6732695217|H,0.4653253379,2.0686478308,-0.6054782307|H,0.0510258722,0.5835946044,1.3540438666|H,-2.7591597337,0.2743134669,-1.2296939131|H,-1.5643837185,-1.0950721632,-1.8157812682|H,-0.081718136,-1.9462531355,-1.4587547973|H,-1.6194202461,-2.6472732669,-0.9924299279|H,1.6888074144,-0.6984090553,-0.8886346219|H,-0.4471373167,-1.7000917895,2.3574245759|H,-0.9190510797,-3.004353717,1.2838024119|H,1.5971683058,-2.886185344,1.7599720424|H,1.2311469152,-2.8480579742,0.0345015927|H,1.2112026719,-0.1999468068,2.921809555|H,2.6584923945,-1.1681547732,3.2520368123|H,2.8144130298,0.4755001514,2.629167979|H,3.4963974967,-2.0624459992,-0.238523883|H,3.9779945193,-2.2123134878,1.4557895881|H,-1.6160366548,0.88858984,2.4096147689|H,-2.1202892881,-0.7270219897,2.9297821678|H,-3.3064994498,0.4910820078,2.5530706298|H,-3.4915539016,-1.9813168681,-0.2865943253|H,-3.3168239623,-2.2793452783,1.4395615469|H,-5.0614972048,-0.5412581752,1.9045841255|H,-5.6532638434,-1.750573727,0.7896510783|H,-6.2489079748,0.5389532564,-0.0085964224|H,-5.2303901704,-0.3249903288,-1.1486351103|H,-4.6150924797,1.7882888963,1.9728921296|H,-3.7450057834,3.0613972295,1.1080639613|H,-5.4658398914,2.8110434234,0.8294735653|H,-4.2347801026,1.5593224529,-2.3647044107|H,-5.5729165232,2.3695053295,-1.5417496352|H,-3.9651334138,3.0842988989,-1.49717658|H,5.6111924337,-0.9414451052,0.1861352401|H,4.9117788712,0.1155552035,1.3959470069|H,3.7877237427,1.4791625464,-0.2081919138|H,3.9479129625,2.6454335704,-2.2819964379|H,4.6962337653,1.9251619217,-3.7205548187|H,5.714846397,2.6631379295,-2.4740265006|H,6.0163716362,-1.1383082253,-1.9269066357|H,5.9990521951,-0.2890981295,-3.4759223695|H,7.0130534114,0.3167829631,-2.1585062248|O,3.6328122128,0.053317721,-1.7722097693| |Version=IA32W-G03RevC.02|HF=-1053.4862025|RMSD=6.450e-009|RMSF=3.817e-006|Dipole=2.5197145,-0.2319108,1.0905337|PG=C01 [X(C25H43O1)]|@

## References and Notes

- (1) Moss, G.P. *Pure Appl. Chem.* **1989**, *61*, 1783-1822.
- (2) (a) DOS formation using a cyclase inhibitor: Field, R. B.; Holmlund, C. E. *Arch. Biochem. Biophys.* **1977**, *180*, 465-471. (b) DOS formation using a cyclase mutant: Lorenz R. T.; Parks L. W. *J. Bacteriol.* **1987**, *169*, 3707-3711. (c) Gachotte, D.; Sen, S. E.; Eckstein, J.; Barbuch, R.; Krieger, M.; Ray, B. D.; Bard, M. *Proc. Natl. Acad. Sci. USA* **1999**, *96*, 12655-12660.
- (3) Pogliani, L.; Ceruti, M.; Ricchiardi, G.; Viterbo, D. *Chem. Phys. Lipids* **1994**, *70*, 21-34.
- (4) Corey, E. J.; Yi, K. Y.; Matsuda, S. P. T. *Tetrahedron Lett.* **1992**, *33*, 2319-2322.
- (5) Gardner, R. G.; Shan, H.; Matsuda, S. P. T.; Hampton, R. Y. *J. Biol. Chem.* **2001**, *276*, 8681-8694.
- (6) Nadeau, R. G.; Hanzlik, R. P. *Methods Enzymol.* **1968**, *15*, 346-351.
- (7) Barton, D. H. R.; Jarman, T. R.; Watson, K. G.; Widdowson, D. A.; Boar, R. B.; Damps, K. *J. Chem. Soc., Chem. Commun.* **1974**, 861-862.
- (8) Nagumo, A.; Kamei, T.; Sakakibara, J.; Ono, T. *J. Lipid Res.* **1995**, *36*, 1489-1497.

- 
- (9) Dean, P. D. G. *Steroidologia* **1971**, 2, 143-157.
- (10) Nelson, J. A.; Steckbeck, S. R.; Spencer, T. A. *J. Biol. Chem.* **1981**, 256, 1067-1068.
- (11) Fazio, G. C.; Xu, R.; Matsuda S. P. T. *J. Am. Chem. Soc.* **2004**, 126, 5678-5679.
- (12) Schiestl, R. H.; Gietz, R. D. *Curr. Genet.* **1989**, 16, 339-346.
- (13) Ausubel, F. M.; Brent, R.; Kingston, R. E., Moore, D. D.; Seidman, J. G.; Smith, J. A.; Struhl, K., Eds. *Current Protocols in Molecular Biology*; Wiley-Interscience: New York, 1999.
- (14) Gollub, E. G.; Liu, K.; Dayan, J.; Adlersberg, M.; Sprinson, D. B. *J. Biol. Chem.* **1977**, 252, 2846-2854
- (15) Segura, M. J. R.; Meyer, M. M.; Matsuda, S. P. T. *Org. Lett.* **2000**, 2, 2257-2259.
- (16) (a) SMY8: Corey, E. J.; Matsuda, S. P. T.; Baker, C. H.; Ting, A. Y.; Cheng, H. *Biochem. Biophys. Res. Commun.* **1996**, 219, 327-331. (b) SMY8[JR1.16]: Herrera, J. B. R.; Bartel, B.; Wilson, W. K.; Matsuda, S. P. T. *Phytochemistry* **1998**, 49, 1905-1911.
- (17) The effect of derivatizing conditions on the extent of TMS derivatization has been noted previously: (a) St. Pyrek, J.; Wilson, W. K.; Numazawa, S.; Schroepfer, G. J., Jr. *J. Lipid Res.* **1991**, 32, 1371-1380. (b) Shan, H.; Pang, J.; Li, S.; Chiang, T. B.; Wilson, W. K.; Schroepfer, G. J., Jr. *Steroids* **2003**, 68, 221-233.
- (18) Many of the ions discussed here have been noted previously in the epoxydammarane literature. See, for example: (a) Dominguez, X. A.; Gonzalez, R.; Carrero, R. *Rev. Soc. Quim. Mex.* **1969**, 13, 266A-268A. (b) Ohmoto, T.; Nikaido, T.; Ikuse, M. *Chem. Pharm. Bull.* **1978**, 26, 1437-1442.
- (19) Emmons, G. T.; Wilson, W. K.; Schroepfer, G. J., Jr. *J. Lipid Res.* **1989**, 30, 133-138.
- (20) Xiong, Q.; Rocco, F.; Wilson, W. K.; Xu, R.; Ceruti, M.; Matsuda, S. P. T. *J. Org. Chem.* **2005**, 70, 5362-5375.
- (21) After completion of this work, we became aware of a report of the 3-keto derivative of **8**.<sup>22</sup> The <sup>1</sup>H and <sup>13</sup>C NMR data for rings C, D, and E reported for this 3-keto derivative were essentially identical to data for **8** (except for an apparent error in the shielding for one of the C23 protons).
- (22) Hwang, B. Y.; Su, B. N.; Chai, H.; Mi, Q.; Kardono, L. B.; Afriastini, J. J.; Riswan, S.; Santarsiero, B. D.; Mesecar, A. D.; Wild, R.; Fairchild, C. R.; Vite, G. D.; Rose, W. C.; Farnsworth, N. R.; Cordell, G. A.; Pezzuto, J. M.; Swanson, S. M.; Kinghorn, A. D. *J. Org. Chem.* **2004**, 69, 3350-3358.
- (23) Hisham, A.; Ajitha Bai, M. D.; Fumimoto, Y.; Hara, N.; Shimada, H. *Magn. Reson. Chem.* **1996**, 34, 146-150.
- (24) Qiu, S.-X.; van Hung, N.; Xuan, L. T.; Gu, J.-Q.; Lobkovsky, E.; Khanh, T. C.; Soejarto, D. D.; Clardy, J.; Pezzuto, J. M.; Dong, Y.; Tri, M. V.; Huong, L. M.; Fong, H. H. S. *Phytochemistry* **2001**, 56, 775-780.
- (25) A crystal structure was obtained for an epoxydammarane derivative synthesized chemically from 3-deoxydammarenediol II: (a) Tanaka, O.; Tanaka, N.; Ohsawa, T.; Iitaka, Y.;

- 
- Shibata, S. *Tetrahedron Lett.* **1968**, 4235-4238. in 1968, Chemical correlations linked the crystal structure to ocotillol: (b) Nagai, M.; Tanaka, N.; Tanaka, O.; Ichikawa, S. *Chem. Pharm. Bull.* **1973**, *21*, 2061-2065.
- (26) An X-ray structure of methyl shoreate (a ring A-*seco* ocotillol metabolite) resolved contradictory findings about the E-ring stereochemistry of epoxydammaranes: Lavie, D.; Frolow, F.; Meshulam, H. *Tetrahedron* **1984**, *40*, 419-420.
- (27) Mills, J. S. *J. Chem. Soc.* **1956**, 2196-2202.
- (28) Ocotillol was first described by Warnhoff and Halls: (a) Warnhoff, E. W.; Halls, C. M. M. *Can. J. Chem.* **1965**, *43*, 3311-3321. (b) Halls, C. M. M.; Warnhoff, E. W. *Chem Ind.* **1963**, 1986. Later ocotillol-I was reported by Dominguez et al.<sup>9a</sup>
- (29) Cascon, S. C.; Brown, K. S. *Tetrahedron* **1972**, *28*, 315-323.
- (30) (a) Fu, L.; Zhang, S.; Li, N.; Wang, J.; Zhao, M.; Sakai, J.; Hasegawa, T.; Mitsui, T.; Kataoka, T.; Oka, S.; Kiuchi, M.; Hirose, K.; Ando, M. *J. Nat. Prod.* **2005**, *68*, 198-206. (b) Tanaka, R.; Masuda, K.; Matsunaga, S. *Phytochemistry* **1993**, *32*, 472-474. (c) Rouf, A. S. S.; Ozaki, Y.; Rashid, M. A.; Rui, J. *Phytochemistry* **2001**, *56*, 815-818 (d) Roux, D.; Martin, M.-T.; Adeline, M.-T.; Hevenet, T.; Hadi, A. H. A.; Pais, M. *Phytochemistry* **1998**, *49*, 1745-1748. (e) Fuchino, H.; Satoh, T.; Tanaka, N. *Chem. Pharm. Bull.* **1996**, *44*, 1748-1753. (f) Anjaneyulu, V.; Babu, J. Suresh; Krishna, M. Murali; Connolly, J. D. *Phytochemistry* **1993**, *32*, 469-471. (g) Nakamura, N.; Kojima, S.; Lim, Y. A.; Meselhy, M. R.; Hattori, M.; Gupta, M. P.; Correa, M. *Phytochemistry* **1997**, *46*, 1139-1141.
- (31) Fujita, S.; Kasai, R.; Ohtani, K.; Yamasaki, K.; Chiu, M.-H.; Nie, R.-L.; Tanaka, O. *Phytochemistry* **1995**, *39*, 591-602.
- (32) (a) Gonzalez, A. G.; Cortes, M.; Suarez, E. *Tetrahedron Lett.* **1974**, *33*, 2791-2792. Original report of kapurol: (b) Hirose, Y.; Yanagawa, T.; Nakatsuka, T. *Mokuzai Gakkaishi* **1968**, *14*, 59. (c) Dominguez, X. A.; Gonzalez, R.; Carrero, R. *Rev. Soc. Quim. Mex.* **1969**, *13*, 266A-268A. (d) Wahlberg I.; Enzell C. R. *Acta Chem. Scand.* **1971**, *25*, 352-354.
- (33) Akihisa, T.; Tokuda, H.; Ukiya, M.; Suzuki, T.; Enjo, F.; Koike, K.; Nikaido, T.; Nishino, H. *Chem. Pharm. Bull.* **2004**, *52*, 153-156.
- (34) Betancor, C.; Freire, R.; Hernandez, R.; Suarez, E.; Cortes, M.; Prange, T.; Pascard, C. *J. Chem. Soc., Perkin Trans. I* **1983**, 1119-1126.
- (35) Brandt, C. A.; Comasseto, J. V.; Ferraz, H. M. C.; Gaeta, K. K.; Pinto, A. C. *Quim. Nova* **1987**, *10*, 151-152.
- (36) Guo, L.-W.; Wilson, W. K.; Shackleton, C. H. L., unpublished results
- (37) Xu, R.; Fazio, G. C.; Matsuda, S. P. T. *Phytochemistry* **2004**, *65*, 261-291.
- (38) Aalbersberg, W.; Singh, Y. *Phytochemistry* **1991**, *30*, 921-926.
- (39) Wong, J.; Quinn, C. M.; Brown, A. J. *Arterioscler. Thromb. Vasc. Biol.* **2004**, *24*, 2365-2371. These results are in line with previous work indicating a regulatory role for 24,25-epoxycholesterol in mammals: (b) Review: Spencer, T. A. *Acc. Chem. Res.* **1994**, *27*, 83-90. (c) Rowe, A. H.; Argmann, C. A.; Edwards, J. Y.; Sawyez, C. G.; Morand, O. H.;

- 
- Hegele, R. A.; Huff, M. W. *Circ. Res.* **2003**, *93*, 717-725. (d) Review: Huff, M. W.; Telford, D. E. *Trends Pharmacol. Sci.* **2005**, *26*, 335-340.
- (40) Enzyme kinetic studies of cycloartenol synthase indicated how cyclase inhibitors can increase the levels of DOS and epoxysterols: Boutaud, O.; Dolis, D.; Schuber, F. *Biochem. and Biophys. Res. Commun.* **1992**, *188*, 898-904.
- (41) (a) Zhang, Z.; Li D.; Blanchard, D. E.; Lear, S. R.; Erickson, S. K.; Spencer, T. A. *J. Lipid Res.* **2001**, *42*, 649-658. See also discussion and further references in: (b) Schroepfer, G. J., Jr. *Physiol. Rev.* **2000**, *80*, 361-554. (c) Bjorkhem, I.; Diczfalusy, U. *Arterioscler. Thromb. Vasc. Biol.* **2004**, *24*, 2209-2210.
- (42) Ruan, B.; Lai, P. S.; Yeh, C. W.; Wilson, W. K.; Pang, J.; Xu, R.; Matsuda, S. P. T.; Schroepfer, G. J., Jr. *Steroids* **2002**, *67*, 1109-1119.
- (43) Erg1p catalyzes a rate-limiting step of sterol synthesis, and its transcription is enhanced by low levels of ergosterol. Although the SMY8[JR1.16] strain is a sterol auxotroph, a *hem1* deletion allows import of exogenous ergosterol, which was supplemented in the medium. This strain had growth rates comparable to wild-type yeast and thus should have normal levels of ergosterol and Erg1p. Recent work suggests that transcription of ERG1 and ERG7 is coordinately regulated.<sup>44</sup>
- (44) Germann, M.; Gallo, C.; Donahue, T.; Shirzadi, R.; Stukey, J.; Lang, S.; Ruckenstuhl, C.; Oliaro-Bosso, S.; McDonough, V.; Turnowsky, F.; Balliano, G.; Nickels, J. T. Jr. *J. Biol. Chem.* **2005**, *280*, 35904-35913.
- (45) Erg1p, Erg6p, Erg7p: (a) Zweytick, D.; Athenstaedt, K.; Daum, G. *Biochim. Biophys. Acta* **2000**, *1469*, 101-120. (b) Müllner, H.; Zweytick, D.; Leber, R.; Turnowsky, F.; Daum, G. *Biochim. Biophys. Acta* **2004**, *1663*, 9-13. Erg7p: (c) Milla, P.; Viola, F.; Oliaro Bosso, S.; Rocco, F.; Cattell, L.; Joubert, B. M.; LeClair, R. J.; Matsuda, S. P.; Balliano, G. *Lipids* **2002**, *37*, 1171-1176. Erg26p (NSDHL) was found in lipid particles of mammalian cells (COS7 or CHO cells): (d) Caldas, H.; Herman, G. E. *Hum. Mol. Genet.* **2003**, *12*, 2981-2991. (e) Ohashi, M.; Mizushima, N.; Kabeya, Y.; Yoshimori, T. *J. Biol. Chem.* **2003**, *278*, 36819-36829.
- (46) Mo, C.; Bard, M. *J. Lipid Res.* **2005**, *46*, 1991-1998.
- (47) The steps of sterol synthesis can be carried out in many different orders. For example, in cholesterol synthesis, the  $\Delta^{24}$  bond can be reduced at almost any stage of the pathway. Organization of a sterol biosynthesis complex may be sufficiently loose that the product released from one enzyme could diffuse within the complex to become the substrate for any of several different enzymes.
- (48) Ruan, B.; Wilson, W. K.; Pang, J.; Gerst, N.; Pinkerton, F. D.; Tsai, J.; Kelley, R. I.; Whitby, F. G.; Milewicz, D. M.; Garbern, J.; Schroepfer, G. J., Jr. *J. Lipid Res.* **2001**, *42*, 799-812 and references therein.
- (49) Marcos, J.; Guo, L.-W.; Wilson, W. K.; Porter, F. D.; Shackleton, C. *Steroids* **2004**, *69*, 51-60 and references therein.



- 
- (50) Erg7p appears to be almost absent from the ER in some studies (see ref. 45b), but Erg1p and Erg7p are retained in the ER in a yeast strain devoid of LP: Sorger, D.; Athenstaedt, K.; Hrastnik, C.; Daum, G. *J. Biol. Chem.* **2004**, 279, 31190-31196. In another study<sup>46</sup> Erg7p is localized with Erg11p, an enzyme found only in the ER.
- (51) Review: Müllner, H.; Daum, G. *Acta Biochim. Pol.* **2004**, 51, 323-347.
- (52) One study found that Erg1 in LP is catalytically inactive: Leber, R.; Landl, K.; Zinser, E.; Ahorn, H.; Spok, A.; Kohlwein, S. D.; Turnowsky, F.; Daum, G. *Mol. Biol. Cell* **1998**, 9, 375-386.
- (53) (a) Harrison D. M. *Nat. Prod. Rep.* **1990**, 7, 459-484. (b) Jung, J. D.; Park, H.-W.; Hahn, Y.; Hur, C.-G.; In, D. S.; Chung, H.-J.; Liu, J. R.; Choi, D.-W. *Plant Cell Rep.* **2003**, 22, 224-230. (c) Duc, N. M.; Kasai, R.; Ohtani, K.; Ito, A.; Yamasaki, K.; Nham, N. T.; Tanaka, O. In *Saponins Used in Traditional and Modern Medicine*; Waller, G. R.; Yamasaki, K., Eds.; Plenum Press: New York, 1996; pp 129-149.
- (54) If the assignments for H9 and H24 are reversed and a 0.01 ppm referencing correction is applied, the NMR data for H24 match our values for 24,25-epoxysterols in ref. 11 and [Figure S10](#).
- (55) The recently described 17,24-epoxybaccharanes<sup>27</sup> are the first examples of triterpenoids that appear to be derived from attack of a cationic intermediate by the distal epoxide of DOS.
- (56) (a) Valentine, J. C.; McDonald, F. E.; Neiwert, W. A.; Hardcastle, K. I. *J. Am. Chem. Soc.* **2005**, 127, 4586-4587. (b) Carter-Franklin, J. N.; Butler, A. *J. Am. Chem. Soc.* **2005**, 127, 15060-15061. (c) Connolly, J. D.; Hill, R. A. *Nat. Prod. Rep.* **2003**, 20, 640-659. (d) Bravo, F.; McDonald, F. E.; Neiwert, W. A.; Hardcastle, K. I. *Org. Lett.* **2004**, 6, 4487-4489.
- (57) (a) Wendt, K. U.; Schulz, G. E.; Corey, E. J.; Liu, D. R. *Angew. Chem. Int. Ed.* **2000**, 39, 2812-2833. (b) Abe, T.; Hoshino, T. *Org. Biomol. Chem.* **2005**, 3, 3127-3139.